REVIEW OF THE VARIOUS SPHERE DECODER APPROACHES FOR MIMO-OFDM SYSTEM

Jaskirat Kaur[1], Harmandar Kaur[2]

[1]Student, M.Tech, [2]Asst. Professor, Department of Electronics and Communication,
Guru Nanak Dev University Regional Campus, Ladhewali, Jalandhar, (India)

ABSTRACT

Sphere decoding algorithms for Multiple Input Multiple Output (MIMO) - Orthogonal Frequency Division Multiplexing (OFDM) linear channels are considered. The principle of the sphere decoding algorithm is to search the closest lattice point to the received signal within a sphere radius, where every codeword is represented by a lattice point in a lattice field. In this paper, a comprehensive survey of existing sphere decoding algorithms is presented. The existing search strategies are described in a unified framework and their pros and cons have been described.

Keywords: Lattice theory, MIMO system, MIMO detection, OFDM, Wireless Channel

I. INTRODUCTION

The pursuit of high speed wireless data services has made the communication researchers relatively active. The limitations of wireless medium are a challenge to the researchers as demand is continuously increasing for available limited bandwidth. This has led to the search for a reliable and high data rate communication system. To fulfill these requirements, MIMO systems are preferred because they provide high data rate transmission over wireless channels and theoretically show considerably improved spectral efficiencies. In multi-antenna system, space-time (along with traditional error-correcting) codes are often employed at the transmitter to induce diversity. Moreover to secure the highly reliable data transmission, special attention should be given to the design of receiver antenna. The received signal is the combination of the transmitted signals affected by noise, Inter Symbol Interference (ISI) & Inter User Interference (IUI).

MIMO systems have attracted much attention for more than a decade because they provide high data rate transmission over wireless channels and theoretically show considerably improved spectral efficiencies. Optimal detection of signals or the Maximum Likelihood (ML) transmitted over MIMO channels is well-known to be an *NP-complete problem (NP-Complete (Non-deterministic polynomial-time complete) problem is a class of decision problems where a given solution can be verified, but there is no efficient way of locating that solution. Computational time increases rapidly with the problem size).* An optimal performance can be obtained by implementing the ML decoder but its exponential complexity makes it unrealizable in practical systems when a large number of antennas and higher order modulation schemes are used.

In order to attain ML performance at reduced complexity, a multichannel equalizer is used to suppress ISI and IUI. By using nonlinear different equalizers like Vertical Bell Layered Space-Time (V-BLAST) [1] or linear equalizers like Zero-Forcing (ZF) equalizer [2]-[3] and Minimum Mean Squared Error Detector (MMSE) [4], better performance in terms of high signal to noise ratio (SNR) can be realized.

But a feasible option to obtain optimal performance in case of larger number of transmit antennas and/or higher modulation schemes is the application of Sphere Decoder (SD), whose computational complexity is independent of the total number of possible transmit vectors. SDs achieves similar performance to ML decoder with reasonable computational complexity. This is due to the fact that SD examine only the vector candidates which fall within a sphere of a given radius $\sqrt{C}$ centered at the received vector y, instead of examining the entire possible transmit vectors as shown in fig. 1.

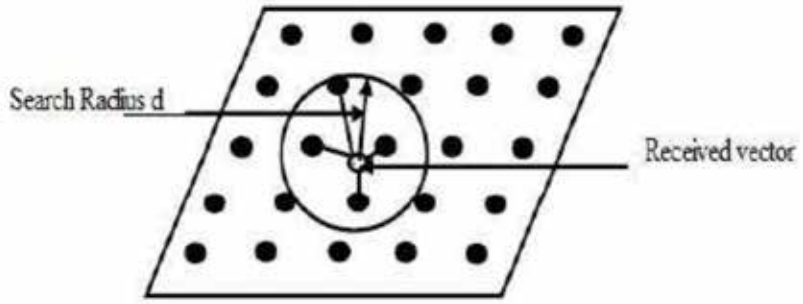

Fig.1: A 2- Dimensional Geometric Representation of Sphere Decoding [5]

II. THE MIMO MODEL

Consider the linear MIMO system as shown in fig.2 to communicate over the channel. We have to find the detection of a set of M transmitted symbols from a set of N observed signals.

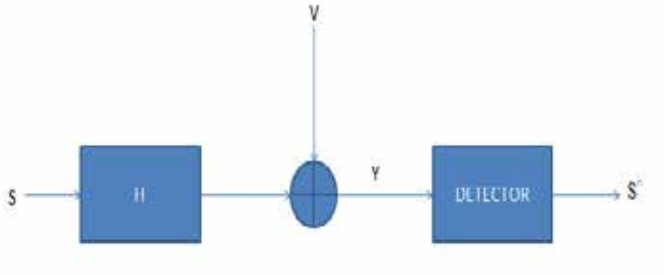

Fig.2: MIMO Communication system diagram [6]

MIMO channel is given below:

$$y = Hs + v \quad (1)$$

where $s \in S_m$ is the finite set of transmitted vector symbols , $y \in F_n$ is the received signal vector, $H \in F^{nxm}$ is the channel matrix and $v \in F^n$ is the additive white Gaussian noise. Here F is the set of real or complex numbers [6]. In the most general term, a detector or receiver refers to a mapping which takes the vector of received signal y and the channel matrix H as inputs and thus produces an estimated symbol vector, ŝ as output. That is, a detector is defined by some (possibly random) map.

$$\phi: F^n \quad F^{nxm} \rightarrow s^m \quad (2)$$

where $\hat{s} = \Phi (y, H)$ and F is real or complex. Computation of Φ relates to the implementation of the detector. The possibility that the minimum probability of error provided by the receiver in case of transmitted messages $s \in S^m$, is the ML receiver expressed as:

$$||y - H\hat{s}||^2 \quad (3)$$

III. SD STRATEGIES

SD is an efficient strategy that computes all the lattice points within a sphere with a certain radius. This strategy is based on integer lattice theory. The concept behind the sphere decoding is to limit the count of possible code words by considering only those which are within a sphere centered at the received signal vector. This enumeration strategy was first introduced in digital communications by Viterbo and Biglieri.

The SD algorithm for Spatial Modulation (SM) MIMO systems has two types of searching strategies, the Fincke - Pohst (FP) and the Schnorr-Euchner (SE).

3.1 FP Strategy

The FP strategy is considered to be the original sphere decoding algorithm [7]. This method considers all hypotheses in natural order and the search is starting with the first one as shown in fig. 3.

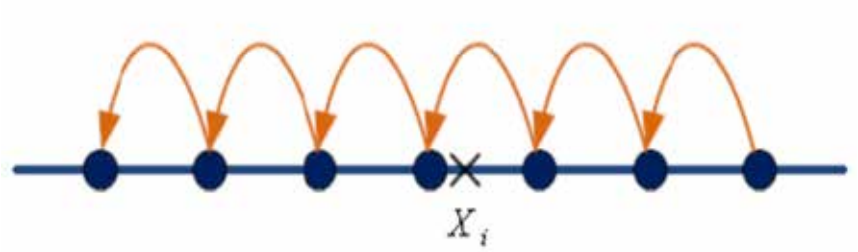

Fig.3: Fincke - Pohst Strategy [5]

An important characteristic of the FP strategy is that a search radius $\sqrt{C}$ must be specified. However, if C is too large, many lattice points will have to be computed and a large number of points may also be cancelled out. If it is too small, no lattice points will be found and then decoder must be restarted with a larger search radius. Both of these factors negatively impact the overall computation time and thus it is well-known that one of the main weaknesses of the FP decoder is the sensitivity of its performance to the choice of C. A typical choice is the distance to the Babai point (BP) [8].

A simplified SD algorithm is given below:

Step 1: Input y, C, H and S.

Step 2: Compute Gram matrix G := $H^T H$ and find QR decomposition $\{q_{ij}\}$:= Q-Chol(G).

Step 3: Compute $\rho := H^{-1}y$

Step 4: Initialize $d^2 := C$, $T_n := C$, $S_n := \rho_n$, i = n

Step 5: Evaluate the followings:

U_i := Q-Up($\sqrt{(Ti/qii)} + S_i$, S);

L_i := Q-Low($-\sqrt{(Ti/qii)} + S_i$, S);

N_i :=len(L_i, U_i, S);

y_i :=find(L_i, U_i, S);

z_i := sort(y_i, U_i, S);

Step 6: Output $s_i = z_i(1)$

Step 7: Next i [9].

3.2 SE Strategy

Schnorr and Euchner introduced an algorithm which does not require an initial radius estimate [2]. It added a small but significant improvement to the FP approach. The FP strategy search for the valid nodes without any ordering, whereas in SE strategy, the valid nodes of each level are spanned in a zigzag order starting with the closest middle point as depicted in fig.4.

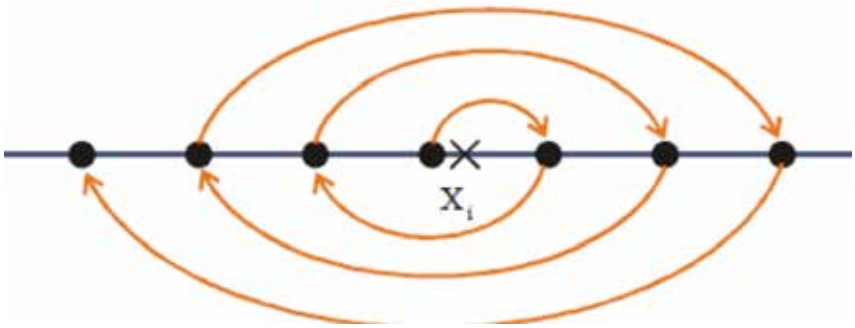

Fig.4: Schnorr-Euchner Strategy [5]

SE strategy considers symbol close to the BP solution and if a point is found, then the radius is updated (reduced) and so on. The SE enumeration is more efficient than FP and is less complex in terms of computations than FP. The tree is explored depth-first and child nodes at level i are prioritized in the increasing order of Partial Euclidean Distances (PEDs). Initially, the search radius $\sqrt{C}$ is set to infinity and is updated with the PED of each new candidate solution. The SE enumeration finds eligible solutions faster and is the foundation for most of SD extensions.

IV. VARIANTS OF SD ALGORITHM

The basic idea of SD algorithm is to search in a hyper sphere of radius $\sqrt{C}$ centered at the received vector y. Even though points in this hyper sphere are searched exhaustively, calculations are performed recursively, based on a search tree to enable reusing intermediate computations [10].

4.1 SE Variant of SD Algorithm

Recently, a variant of the SD algorithm appeared in both [11] and [12]. Since this version of SD algorithm was first used by Schnorr and Euchner, it is abbreviated as the SE-SDA [11]. For SE Decoder, the algorithm is based on two stages. The first stage consists in searching for the BP, which represents a first estimation, but is not necessarily, the closest point. Finding the BP gives a bound on the error. In the second stage, the BP is modified until the closest point is reached. We zigzag around each BP component in turn to build the closest point.

4.2 SD Algorithm with Increasing Radius Search (IRS)

This algorithm is initially mentioned in [13]. For a fixed search radius, there is always a probability that no candidate is found. Hence, increasing the radius is needed to achieve ML or near-ML performance while maintaining the SD algorithm's efficiency. The SD algorithm with IRS is as follows. Let $r_{p1} < r_{p2} < \ldots.. < r_{pn}$ be a set of sphere radii. Execute the SD algorithm with search radius r_{p1}. If a candidate is found, terminate the program; otherwise, run SD algorithm again with the next radius until r_{pn} .

4.3 SD Algorithm with Improved Increasing Radius Search (IIRS)

IRS can improve the computational efficiency of the conventional SD algorithm. However, there is an apparent waste of computations in the SD algorithm with IRS. Because for any sphere radius r_{pi}, there is always a probability that this sphere does not contain any valid lattice point. At this time, the SD algorithm increases the search radius from r_{pi} to r_{pi+1} and searches again. To reduce this loss and to lower search complexity, SD algorithm with IIRS is used.

The intuition behind the new IIRS is as follows. Whenever the SD algorithm search with radius fails, an incomplete search tree is constructed, from which promising paths can often be identified. An incomplete tree for a four dimensional (4-D) binary search is depicted in fig. 5, where the initial radius is r_{pi}. Each branch in the kth level of the tree is associated with a candidate of s. Starting from the root; each complete path corresponds to a candidate of s. From fig.5, it can be observed that paths 1 and 2 are more promising than path 3 [10].

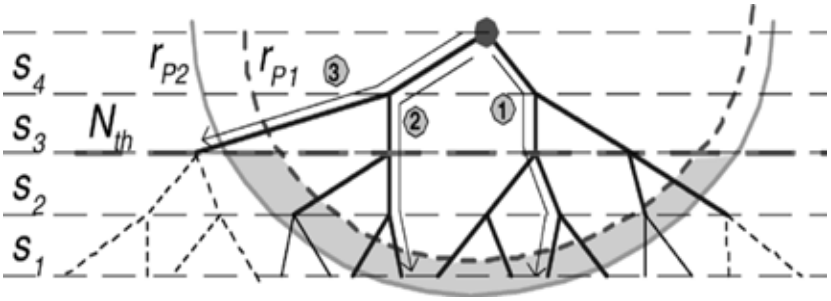

Fig.5: Search tree of the SDA [10]

4.3.1 Ordering Promising Paths

To check paths efficiently, promising paths are examined according to an ascending order of their predicted average Euclidean distances. When the SD algorithm search with radius r_{pi} fails, a path in an N-dimensional problem often consists of two segments. The first segment comprises n_1 branches, where branch metrics have been calculated. Let the sum of these branch metrics be $d^2_{n1} > r^2_{pi}$. The parameters n_1 and d^2_{n1} are generated by the SDA search with r_{pi}. The second segment comprises n_2 branches. Here, checking paths in an ascending order of their average distances maximizes the average probability to find the vector with minimum distance early.

4.3.2 Additional SD Algorithm Constraints

Ordering promising paths results in an undesirable exponentially growing memory. To reduce memory requirements, several additional constraints are assumed. First, two sphere radii $r_{pi} < r_{pi+1}$ in a single SD algorithm search are used. The radius r_{pi} plays the role of search radius as in the conventional SD algorithm, whereas r_{pi+1} upper bounds distance of promising paths when the r_{pi} search with r_{pi} fails. Second, a threshold N_{th} is used to confine the search to promising paths. This divides paths in two categories: promising or unlikely. If a path satisfies $n_2 < N_{th}$, it is a promising path and is ordered according to its average distance otherwise, it is unlikely and is ignored.

4.3.3 IIRS-A

Based on the parameters r_{pi}, r_{pi+1} and N_{th}, SD algorithm with IIRS-A called SDA-A is as follows. Before any candidate is found within r_{pi} during an SD algorithm search, the average distance for each path satisfying $n_2 < N_{th}$ and $r_{pi} < d_{n1} < r_{pi+1}$ is calculated, retaining only information about the most promising path. Whenever the SD algorithm with r_{pi} fails, SDA-A either provides information about the most promising path, or indicates that there is no such path. If the latter is true or the actual distance of the most promising path is greater than r_{pi+1}, then SDA-A fails; otherwise, it returns the candidate corresponding to the most promising path.

4.3.4 IIRS-B

To obtain near-ML performance, SD algorithm with IIRS-B called SDA-B with parameters r_{pi}, r_{pi+1} and N_{th} is as follows. Before any candidate is found within r_{pi} during an SD algorithm search, the average distance for each path satisfying $n_2 < N_{th}$ and $r_{pi} < d_{n1} < r_{pi+1}$ is calculated and complete information about the three most promising paths is kept. Whenever SD algorithm fails, SDA-B provides more information on promising paths than SDA-A. If no such path exists or no candidate within r_{pi+1} can be determined from these paths, SDA-B fails; otherwise, the first candidate found with distance < r_{pi+1} is tested. Suppose that n2 and d_{n1} are the parameters of the next promising path. If they are not available, then N_{th} and r_{pi} are used [10].

4.4 K-Best SD Algorithm

The SD algorithm can be divided into depth-first and breadth-first groups based on their search strategy. The depth-first algorithms process one candidate symbol vector at a time. The breadth-first algorithms process all the partial candidate symbol vectors on each level before moving to the next level. The K-best algorithm [14] is a breadth-first search based algorithm and keeps the K nodes which have the smallest accumulated Euclidean distances at each level. If the PED is greater than the squared sphere radius *d*, the corresponding node will not be expanded.

4.5 List Sphere Decoder (LSD) Algorithm

A LSD algorithm [15] is a variant of the SD algorithm. It provides a list of candidates L and their Euclidean distances as an output.

4.5.1 K-Best-LSD algorithm

The K-best LSD is a modification of the K-best algorithm and it outputs a list of candidate vectors and the corresponding Euclidean distances. The size N_{cand} of the output list L has an impact on the performance of the SD. With a small N_{cand}, the complexity is lower and the detection process faster, but the performance can be worse than with a full list.

4.5.2 Increasing Radius (IR)-LSD Algorithm

The IR-LSD algorithm [16] uses the metric-first search strategy. The algorithm is optimal in the sense of visited number of nodes in the tree structure. The search proceeds by calculating one branch extension at a time and stores the partial candidate to a stack memory. Then the search is always continued with the partial candidate with the lowest PED. The output of the algorithm is the candidates with lowest EDs.

V. GAP IN RESEARCH & OPEN ISSUES

The pros and cons of existing sphere decoding algorithms are shown in table 1.

Table 1: Various SD Methods

Variants of SD	Pros	Cons
SE variant of SD algorithm [17], [11], [18]	· The search phase of SE is less complex than SD. · It provides good performance	· Using QR decomposition, predecoding and initialization phases for SE are heavier than

	for a lower no. of antennas using slowly fading channels	the SD. · For lower SNR, the BP is very far from closest point, so the algorithm takes much more time to converge.
SD algorithm with IRS [1],[18],[19]	· IRS improves computational efficiency of the conventional SD algorithm. · It is effective for the medium-to-high SNR regime.	· In IRS, if for radius r_{pi}, sphere does not contain any valid lattice point then SD algorithm increases the search radius from r_{pi} to r_{pi+1}. Computations for radius r_{pi} are discarded, but they are recalculated in the search with radius r_{pi+1}. · The weakness of IRS algorithm is that it does not depend on any particular structure. In IRS, the search time for highly structured lattice is high.
SD algorithm with IIRS-A or SDA-A [18]	· It provides less decoding complexity as compared to IRS. · It provides most promising path which enables near ML performance with linear memory.	· To reduce computational complexity, IIRS-A degrades the symbol error rate (SER) performance by 0.5dB.
SD algorithm with IIRS-B or SDA-B [18]	It offers two improvements over SDA-A. · The three most promising paths are tracked by SDA-B, which enables near-ML performance with linear memory. · In SDA-B, the testing is an effective mechanism to guarantee the reliability of a candidate.	· The testing mechanism relies only on the AWGN model.
K- Best SD algorithm [14],[20]	· This algorithm is preferable in terms of hardware implementation since it has fixed complexity and memory usage.	· For this algorithm, the performance of MIMO in terms of bit error rate (BER) is degraded, especially when the number of candidate symbols

		kept at each level, is small.
K- Best LSD algorithm [21]	· The K-Best LSD algorithm guarantees a fixed throughput and complexity.	· The K-Best LSD requires a larger list size compared to the IR-LSD to obtain as accurate approximation and performance.

From study of existing algorithms and their pros and cons, it can be concluded that these algorithms show the following major weaknesses:

- The sphere decoder performance is very sensitive for the most current proposals in order to choose the search radius parameter. The successful termination of the algorithm which provides the result as an optimal solution is highly dependent on the search radius.
- Secondly, at high spectral efficiencies which are required to support higher communication rates, SNR is low and the complexity coefficient can become very large.

The issues for future research in field of sphere decoder are given below:

- To improve the performance of MIMO-OFDM using existing / modified detection.
- To improve the BER performance and to reduce computational complexity for existing sphere decoding algorithms.

VI. CONCLUSION

Different SD algorithms along with their modified forms have been studied. The existing search strategies are described in a unified framework and their pros and cons have been discussed.

REFERENCES

[1] P.W Wolniansky, G. J. Foschini, G. D. Golden and R. A. Valenzuela, V-BLAST: an architecture for realizing very high date rates over the rich-scattering wireless channel, in *International Symposium on Signals, Systems and Electronics*, pp. 295-300, 1998.

[2] H. Liao, A zero forcing and sphere decoding joint detector for multiple input multiple output LAS-CDMA system, *IEEE WRI International Conference on Communications and Mobile Computing*, pp. 246-249, 2009.

[3] E.G. Larsson, MIMO detection methods: How they work, *IEEE Signal Processing Magazine*, May 2009.

[4] K. Su, I. Berenguer, I. J. Wessell and X. Wang, Efficient maximum-likelihood decoding of spherical lattice codes, *IEEE Transactions On Communications, vol.57, no. 8*, pp. 2290-2300, Aug. 2009.

[5] R. P. Yadav, G. Mathur, S. Mrinalee and H. P. Garg, Improved radius selection in sphere decoder for MIMO system, *International Conference on Computing for Sustainable Global Development*, pp. 183-186, March 2014.

[6] MD.S.Alam, On sphere detection for OFDM based MIMO systems, *Blekinge Institute of Technology*, pp. 33-37, Sept. 2010.

[7] U.Fincke and M.Pohst, Improved methods for calculating vectors of short length in lattice including a complexity analysis, *AMS Mathematics of Computation, Vol. 44, No. 170,* pp. 463-471, April 1985.

[8] C. Schnorr and M. Euchner, Lattice basis reduction: Improved practical algorithms and solving subset sum problems, *Springer, Mathematical Programming, Vol. 66, Issue 1-3*, pp. 181–199, Aug. 1994.

[9] N. K. Noordin, B. M. Ali, S. S. Jamuar and M. Ismail, A simplified sphere decoding algorithm for MIMO transmission system, *University Putra, Malaysia*.

[10] W. Zhao and G. Giannakis, Sphere decoding algorithms with improved radius search, *IEEE Trans. Commun., vol. 53,* pp. 1104–1109, July 2005.

[11] E. Argell, E. Eriksson, A. Vardy and K. Zeger, Closest point search in lattices, *IEEE Trans. Inform. Theory, vol. 48,* pp. 2201–2214, Aug. 2002.

[12] G. Rekaya and J.-C. Belfiore, Complexity of ML lattice decoders for the decoding of linear full rate space-time codes, *IEEE Trans. Inform. Theory*, pp. 206, July 2003.

[13] E. Viterbo and J. Boutros, A universal lattice code decoder for fading channel, *IEEE Trans. on Inform Theory, vol. 45, no. 5*, pp. 1639-1642, July 1999.

[14] K. Wong, C. Tsui, R.-K. Cheng and W. Mow, A VLSI architecture of a K-best lattice decoding algorithm for MIMO channels, in *Proc. IEEE Int. Symp. Circuits and Systems, Helsinki, Finland, vol. 3,* pp. 273–276, June 2002.

[15] B. Hochwald and S. ten Brink, Achieving near-capacity on a multiple-antenna channel, *IEEE Transactions on Communications, vol. 51, no. 3*, pp. 389–399, March 2003.

[16] M. Myllyla, J. Cavallaro and M. Juntti, A list sphere detector based on Dijkstra's algorithm for MIMO-OFDM systems, in *Proc. IEEE Int.Symp. Pers., Indoor, Mobile Radio Commun. (PIMRC), Athens, Greece*, Sept. 12 - 19, 2007, pp. 1-5.

[17] A. M. Chan and I. Lee, A new reduced-complexity sphere decoder for multiple antenna system, *IEEE Conference on Communications, ICC2002*, pp.460-464.

[18] M.O. Damen, H. E. Gamal and G. Caire, On maximum-likelihood detection and the search for the closest lattice point, *IEEE Transactions on Information Theory, Vol. 49, No. 10*, pp. 2389-2402, Oct. 2003.

[19] B. Hassibi and H. Vikalo, On the sphere-decoding algorithm I. expected complexity, *IEEE Transactions on Signal Processing, Vol. 53, No. 8,* pp.2806-2818, Aug. 2005.

[20] B. Shim and I. Kang, On radius control of tree-pruned sphere decoding, in *Proceedings of the IEEE International conference on Communications*, pp. 2469-2472, 2009.

[21] M. Myllyla, M. Juntti and J. R. Cavallaro, Implementation aspects of list sphere decoder algorithms for MIMO-OFDM systems, *Signal Processing 90,* April 2010, pp. 2863–2876.

A SURVEY ON ANALYSIS OF LOW POWER AND LOW VOLTAGE OF COMPARATORS

N.Megala[1], M.Navitha[2]

[1,2] *Department Of Electronics And Communication Engineering,*
SNS College of Technology, (India).

ABSTRACT

Design of low voltage double-tail Comparator with pre-amplifier and latching stage is reported in this paper. Design has specially concentrated on delay of both single tail comparator and double-tail comparator, which are called clocked regenerative comparator. Based on a new dynamic comparator is proposed, where the circuit of conventional double tail dynamic comparator is modified for low power and fast operation even in small supply voltages. Simulation results in 0.25µm CMOS technology confirm the
analysis results. It is shown that proposed dynamic comparator both power consumption and delay time reduced. Both delay and power consumption can be reduced by adding two NMOS switches in the series manner to the existing comparator. The supply voltages of 1.5V while consuming 1 5µw in proposed comparator and 16 µw in existing comparator respectively.

Keywords: Double Tail Comparator, Low-Power Analog Design, Power Gating Technique, Tanner EDA Tool.

I. INTRODUCTION

Comparator is one of the fundamental building blocks in Analog-to-digital converters. designing high speed comparator is more challenging when the supply voltage is smaller. in other words to achieve high speed, larger transistors are required to compensate the reduction of supply voltage, which also means that more die area and power is needed. Developing a new circuit structures which avoid stacking too many transistors between the supply rails is preferable for low voltage operation, especially if they do not increase circuit complexity.

Additional circuitry is added to the conventional dynamic comparator to enhance the comparator speed in low voltage operation.

Many high speed ADC's such as flash ADC's requires high speed, low power comparators with small chip area. A new dynamic comparator is presented, which does not require boosted voltage or stacking of too many transistors. Merely by adding a few minimum-size transistors to the conventional double-tail dynamic comparator, latch delay time is profoundly reduced. This modification also results in considerable power savings when compared to the conventional dynamic comparator and double-tail comparator.

II. CLOCKED REGENERATIVE COMPARATORS

Clocked regenerative comparators have found wide applications in many high-speed ADCs since they can make fast decision due to the strong positive feedback in the regenerative latch. Recently many comprehensive

analyses have been presented, which investigate the performance of these comparators from different aspects, such as noise, offset and random decision errors and kickback noise

2.1 Conventional Dynamic Comparator

This comparator widely used in A/D converters with high input impedance, rail-to-rail output swing and no static power consumption. Fig 1 shows the Schematic diagram of the conventional Dynamic comparator.

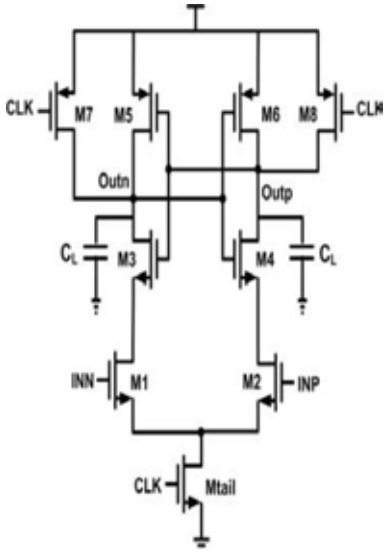

Fig. 1 Schematic diagram of a conventional Dynamic Comparator

The operation of the comparator is as follows. During the reset phase when CLK = 0 and Mtail is off ,reset transistors (M7– M8) pull both output nodes Outn and Outp to VDD to define a start condition and to have a valid logical level during reset. After when CLK = VDD, transistors M7 and M8 are off, and Mtail is on. Output voltages (Outp, Outn), which had been pre- charged to VDD, start to discharge with different discharging rates depending on the corresponding input voltage (INN/INP). Assuming the case where VINP > VINN, Outp discharges faster than Outn, hence when Outp (discharged by transistor *M*2 drain current), falls down to VDD–|Vthp| before Outn (discharged by transistor *M*1 drain current), the corresponding PMOS transistor (*M*5) will turn on initiating the latch regeneration caused by back-to-back inverters and M4, M6). Thus, Outn pulls to VDD and Outp discharges to ground. If VINP < VINN, the circuits works vice versa. The simulation of the comparator is shown in Fig 2.

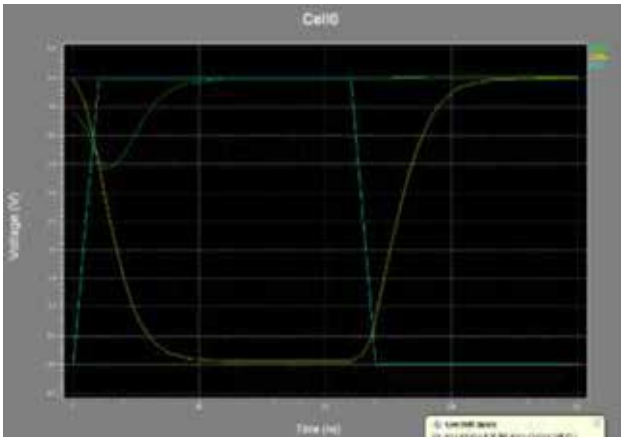

Fig.2. Transient simulation of the conventional dynamic comparator

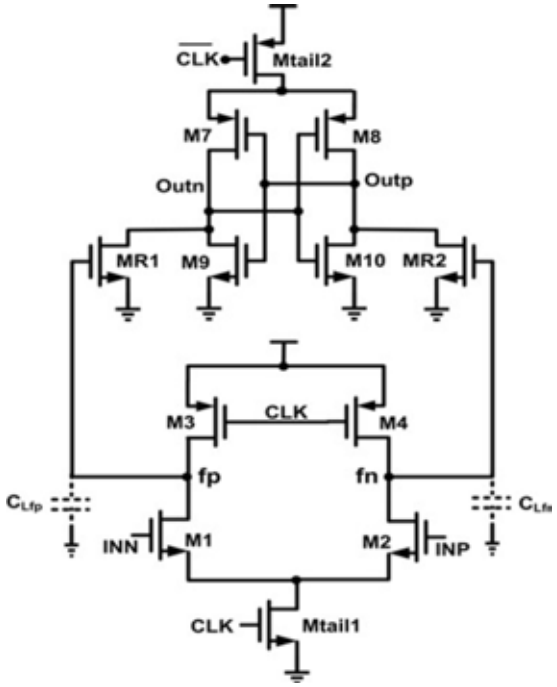

Fig.3 Schematic diagram of the conventional double-tail dynamic comparator.

2.2 Conventional Double Tail Dynamic Comparator

A conventional double-tail comparator is shown in Fig .3. This topology has less stacking and therefore can operate at lower supply voltages compared to the conventional dynamic comparator. The double tail enables both a large current in the latching stage and wider Mtail2, for fast latching independent of the input common-mode voltage (Vcm), and a small current in the input stage (small Mtail1), for low offset. During reset phase (CLK = 0, Mtail1, and Mtail2 are off), transistors M3-M4 pre-charge fn and fp nodes to VDD, which in turn causes transistors MR1 and MR2 to discharge the output nodes to ground.

During decision-making phase (CLK = VDD, Mtail1 and Mtail2 turn on), M3-M4 turn off and voltages at nodes fn and fp start to drop with the rate defined by I Mtail1/Cfn(p) and on top of this, an input dependent differential voltage ΔVfn(p) will build up. The intermediate stage formed by MR1 and MR2

passes ΔVfn(p) to the cross coupled inverters and also provides a good shielding between input and output, resulting in reduced value of kickback noise. Fig 4 shows the simulation of this comparator.

Similar to the conventional dynamic comparator, the delay of this comparator comprises two main parts, t0 and tlatch. The delay t0 represents the capacitive charging of the load capacitance CLout (at the latch stage output nodes, Outn and Outp) until the first n-channel transistor (M9/M10) turns on, after which the latch regeneration starts; thus t0 is obtained where IB1 is the drain current of the M9 and approximately equal to the half of the tail current.

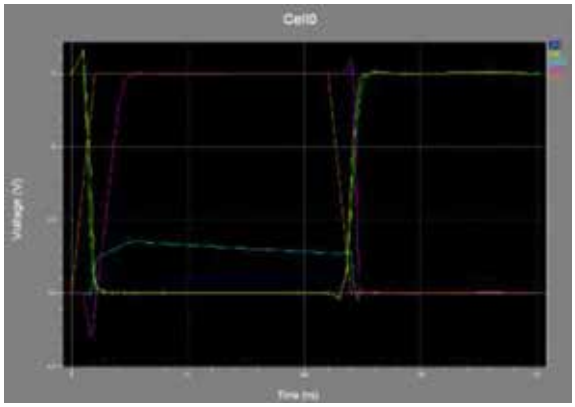

Fig.4. Transient simulation of the conventional double tail dynamic comparator

III. PROPOSED DOUBLE TAIL DYNAMIC COMPARATOR

Fig 5 Shows the Schematic diagram of the proposed method. The operation of the proposed comparator is as follows. During reset phase (Clk=0 Mtail1 and Mtail2 are off avoiding static power),M3 and M4 pulls both fn and fp nodes to VDD hence Mc1 and Mc2 are cut off .Intermediate stage transistor MR1 and MR2 reset both latch outputs to ground.

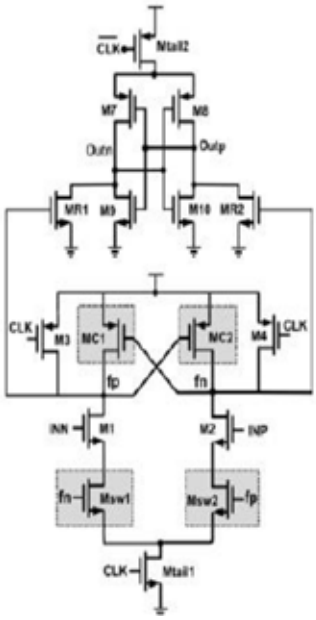

Fig.5.Schematic diagram of proposed double-tail dynamic comparator

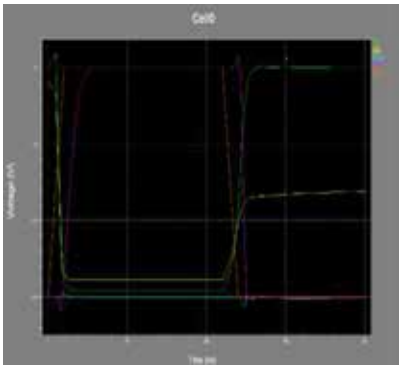

Fig.6 Transient simulation of the proposed double-tail dynamic comparator

During decision making phase (CLK=VDD Mtail1,and Mtail2 are on), transistors M3 and M4 turn off. Furthermore, at the beginning of this phase, the control transistors are still off (since fn and fp are about VDD). Thus, fn and fp start to drop with different rates according to the input voltages. Suppose VINP>VINN, thus fn drops faster than fp, (since M2 provides more current than M1). As long as fn continues falling, the corresponding PMOS control transistor (Mc1 in this case) starts to turn on, pulling fp node back to the VDD; so another control transistor (Mc2) remains off, allowing fn to be discharged completely. In other words, unlike conventional double-tail dynamic comparator, in which ΔVfn/fp is just a function of input transistor transconductance and input voltage difference, in the proposed structure as soon as the comparator detects that for instance node fn discharges faster, a PMOS transistor (Mc1) turns on, pulling the other node fp back to the VDD. Therefore by the time passing, the difference between fn and fp (ΔVfn/fp) increases in an exponential manner, leading to the reduction of latch regeneration time.

Despite the effectiveness of the proposed idea, one of the points which should be considered is that in this circuit, when one of the control transistors (e.g.,Mc1) turns on, a current from VDD is drawn to the ground via input and tail transistor (e.g., Mc1, M1, andMtail1) as shown in Fig 6, resulting in static power consumption. To overcome this issue, two NMOS switches are used below the input transistor.

At the beginning of the decision making phase, due to the fact that both fn and fp nodes have been precharged to VDD (during the reset phase), both switches are closed and fn and fp start to drop with different discharging rates. As soon as the comparator detects that one of the fn/fp nodes is discharging faster, control transistors will act in a way to increase their voltage difference. Suppose that fp is pulling up to the VDD and fn should be discharged completely, hence the switch in the charging path of fp will be opened (in order to prevent any current drawn from VDD) but the other switch connected to fn will be closed to allow the complete discharge of fn node. In other words, the operation of the control transistors

with the switches emulates the operation of the latch. Future work is the delay of the proposed double tail dynamic comparator to be reduced from the present delay value.

IV. PERFORMANCE COMPARISON

TABLE 1

Comparator Structure	**Single Tail Comparator**	**Conventional Double Tail Comparator**	**Proposed Double Tail Comparator**	**Modified Double Tail Comparator**
Technology CMOS	180 nm	180 nm	180 nm	180 nm
Supply voltage (v)	0.8v	0.8v	0.8v	0.8v
Power Consumption (watts)	7.04 x 10-6 watts	1.50 x 10-5 watts	1.29 x 10-5 watts	9.50 x 10-6 watts
Delay (sec)	6.61 x 10-8 sec	7.51 x 10-9 sec	7.48 x 10-9 sec	4.84 x 10-9 sec

V. SIMULATION RESULTS

In order to compare the proposed comparator with the single tail comparator and the conventional double tail comparators, all circuits have been simulated in 180 nm CMOS technology, VDD = 0.8v. Tanner EDA Tool is a leading provider of easy to use, PC based electronic based design automation (EDA) software solution for the design, layout and verification of analog – mixed signal integrated circuits. The result is simulated in T-SPICE platform and the circuit has been drawn using S-EDIT and got the output waveform in W-EDIT. Using the Tanner EDA Tool each comparator circuits has been simulated and got the output waveforms, which show the corrective working of the designed circuits. T-SPICE gives the power consumption and delay analysis results. For the simulation of all comparator structures, the supply voltage (VDD) given is 0.8v, the input voltage INP given is 0.7v and INN given is 0.5v. For each circuit structures the number of transistors used varies. The simulation results show that for the proposed double tail comparator, the power consumption is reduced drastically when comparing all other comparator structures.

VI. CONCLUSION

The paper, presented a comprehensive delay analysis for clocked dynamic comparators. Two common structures of conventional dynamic comparator and conventional double-tail dynamic comparators were analyzed. Also, based on theoretical analyses, a new dynamic comparator with low-voltage low-power capability was proposed in order to improve the performance of the comparator. Post-layout simulation results in 0.18-µm CMOS

technology confirmed that the delay and energy per conversion of the proposed comparator is reduced to a great extent in comparison with the conventional dynamic comparator and double-tail comparator.

REFERENCES

[1] B. Goll and H. Zimmermann, "A comparator with reduced delay time in 65-nm CMOS for supply voltages down to 0.65," *IEEE Trans. Circuits Syst. II, Exp. Briefs*, vol. 56, no. 11, pp. 810–814, Nov. 2009.

[2] S. U. Ay, "A sub-1 volt 10-bit supply boosted SAR ADC design in standard CMOS," *Int. J. Analog Integr. Circuits Signal Process.*, vol. 66, no. 2, pp. 213–221, Feb. 2011.

[3] A. Mesgarani, M. N. Alam, F. Z. Nelson, and S. U. Ay, "Supply boosting technique for designing very low-voltage mixed-signal circuits in standard CMOS," in *Proc. IEEE Int. Midwest Symp. Circuits Syst. Dig. Tech. Papers*, Aug. 2010, pp. 893–896.

[4] B. J. Blalock, "Body-driving as a Low-Voltage Analog Design Technique for CMOS technology," in *Proc. IEEE Southwest Symp. Mixed-Signal Design*, Feb. 2000, pp. 113–118.

[5] M. Maymandi-Nejad and M. Sachdev, "1-bit quantiser with rail to rail input range for sub-1V __ modulators," *IEEE Electron. Lett.*, vol. 39,no. 12, pp. 894–895, Jan. 2003.

[6] Y. Okaniwa, H. Tamura, M. Kibune, D. Yamazaki, T.-S. Cheung,J. Ogawa, N. Tzartzanis, W. W. Walker, and T. Kuroda, "A 40Gb/s CMOS clocked comparator with bandwidth modulation technique," *IEEE J. Solid-State Circuits*, vol. 40, no. 8, pp. 1680–1687, Aug. 2005.

[7] B. Goll and H. Zimmermann, "A 0.12 μm CMOS comparator requiring 0.5V at 600MHz and 1.5V at 6 GHz," in *Proc. IEEE Int. Solid-State Circuits Conf., Dig. Tech. Papers*, Feb. 2007, pp. 316–317.

FREQUENCY DOMAIN FLUTTER ANALYSIS OF AIRCRAFT WING IN SUBSONIC FLOW

Ms.K.Niranjana[1], Mr.A.Daniel Antony[2]

[1]*UG Student, Department of Aerospace Engineering, Karunya University, (India)*

[2]*Assistant professor, Department of Aerospace Engineering, Karunya University, (India)*

ABSTRACT

This paper presents simple binary flutter model developed with the simplified unsteady terms. Binary flutter is the most important of all aero elastic phenomena and it is difficult to predict. The Aero elastic equation of motion which is frequency dependent, along with its dynamic aero elastic behavior for the flapping and pitching of the wing is derived. Further the equation is scripted as a MATLAB code and the figure obtained while the command is executed. From which the frequencies and damping ratio at different airspeed is calculated and the velocity at the flutter point is found.

Keywords: Cessna 152,Crictical Velocity, Damping ratio,Flutter point, Frequency

I INTRODUCTION

Flutter is a dynamic aero elasticity phenomena and in most cases it is very difficult to predict it is an unstable self-excited vibration in which the structure extracts energy from the air stream and often results in catastrophic structural failure [1]. It is a dynamic instability of an elastic structure in a fluid flow, caused by positive feedback between the body deflection and the force exerted by the fluid flow. Classical binary flutter occurs when the aerodynamics forces associated with the motion in two modes of vibration because the modes to couple in unfavorable manner that causes flutter In a linear system 'flutter point' is the point at which the structure is undergoing simple harmonic motion-zero net damping and so any further decrease in net damping will result in self-oscillation and eventual failure.Net damping is the sum of the structure's natural positive damping and the negative damping of the aerodynamics force[2].

Flutter is classified into two types: hard flutter and soft flutter.

- Hard flutter is net damping decreases very suddenly and very close to flutter point.
- Soft flutter is net damping decrease gradually [1].

Fig.1.1Collar's triangle diagram

1.1 Literature Review

Based on aerodynamic identification technology in which unsteady CFD (computational fluid dynamics) is used, the unsteady aerodynamic reduced order models (ROM) are constructed. Coupled with structural equations, we get the analyzable models for transonic aeroelasticity in state-space. A Mach number flutter trend of a typical airfoil section with a control surface is analyzed and agrees well with that of CFD/CSD (computational structural dynamics) direct coupling method. Then we study the effect of the structural parameters (natural frequency and the flap static unbalance) of the control surface on the transonic flutter system [3].

The aerodynamic lift and moment deduced from the aerodynamic theories, one Gaussian white noise force was also added to the lift force. Then the spectral density of response was calculated with respect to the frequency response of the system as well as the spectral density of the excitation. The variance of the response was determined with respect to the airspeed. The flutter speed was obtained by investigating the variation of the response-variance against the airspeed [4].

II EQUATION OF MOTION

Consider 2D aerofoil with flexural axis positioned a distance ec after of the aerodynamics centre and ab after mid chord.

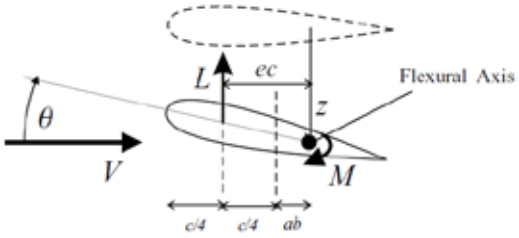

Fig 2.1 2-D aerofoil with flexural axis

Classical solution for lift and moment about flexural axis, per unit span for an aerofoil undergoing oscillatory harmonic motion (flutter)

$$L=\pi\rho b^2\left[\ddot{z}+V\dot{\theta}-ba\ddot{\theta}\right]+2\pi\rho bc(k)\left[\dot{z}+V\theta+b\left(\tfrac{1}{2}-a\right)\dot{\theta}\right] \quad (1)$$

$$M=\pi\rho b^2\left[ba\ddot{z}-Vb\left(\tfrac{1}{2}-a\right)\theta-b^2\left(\tfrac{1}{8}+a\right)\ddot{\theta}\right]+2\pi\rho Vb^2\left(\tfrac{1}{2}+a\right)c(k)\left[\dot{z}+V\theta+b\left(\tfrac{1}{2}-a\right)\dot{\theta}\right] \quad (2)$$

Aerodynamic damping and stiffness

$k=\frac{\omega b}{V}$; $z=z_0e^{i\omega t}$; $\dot{z}=i\omega z_0e^{i\omega t}$; $\theta=\theta_0e^{i\omega t}$; $\dot{\theta}=i\omega\theta_0e^{i\omega t}$

By substituting aerodynamic damping and stiffness in equation 1 & 2

We get,

The lift and moment per unit span for an airfoil for a particular reduced frequency

$$L=\rho V^2\left(L_Z Z+L_{\dot{z}}\frac{b\dot{z}}{V}+L_\theta b\theta+L_{\dot{\theta}}\frac{b^2\dot{\theta}}{V}\right) \quad (3)$$

$$M=\rho V^2\left(M_Z bz+M_{\dot{z}}\frac{b^2\dot{z}}{V}+M_\theta b^2\theta+M_{\dot{\theta}}\frac{b^2\dot{\theta}}{V}\right) \quad (4)$$

Where V- True airspeed, ρ - Density

Pitching term ($M_{\dot{\theta}}$) is negative but initially it is considered to be constant and also it differs numerically by a factor of four, which occurs because the unsteady aerodynamic derivatives are derived in terms of the reduced frequency k rather than the frequency parameter v.

III AERO ELASTIC EQUATION OF MOTION

3.1 Derivation

Consider a rectangular wing of span s and chord c is rigid. It has a 2 rotational spring at root to provide flap (k) and pitch (θ)degrees of freedom. The spring is attached in the flexural axis shown in fig 3.1.1. The wing is assumed to have uniform mass distribution and the mass axis lies on the mid chord.

The displacement z on the wing due to aileron and flap movement

$$z(x,y,t) = yk(t) + (x - x_f)\theta(t) \quad (5)$$

Where

k – Generalized coordinate for pitch angle

θ – Generalized coordinate for flap angle

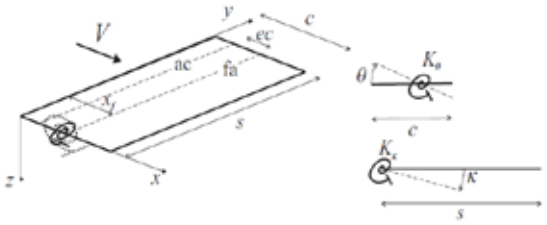

Fig 3.1.1 Aircraft wing with springs attached

The equation of motion can be found using LaGrange's equations. Total energy can be calculated by kinetic energy and potential energy.

The kinetic energy due to dynamic motion

$$T = \int_{wing} \frac{1}{2} dm\, \dot{z}^2 \quad (6)$$

Differentiating z w.r.t x&y

$$\dot{z} = y\dot{k} + (x - x_f)\dot{\theta}$$

$$T = \int_0^s \int_0^c \left[y\dot{k} + (x - x_f)\dot{\theta}\right]^2 dx\, dy \quad (7)$$

The potential energy due to spring at the root of the wing

$$U = \frac{1}{2} K_k k^2 + \frac{1}{2} K_\theta \theta^2 \quad (8)$$

Applying Lagrange's equation (i.e. Kinetic energy & Potential energy) for both generalised coordinates

We get,

$$\frac{dT}{dt}\left(\frac{\partial T}{\partial \dot{k}}\right) = m\left[\frac{s^3 c}{3}\ddot{k} + \frac{s^2}{2}\left(\frac{c^2}{2} - x_f c\right)\ddot{\theta}\right] \quad (9)$$

$$\frac{dT}{dt}\left(\frac{\partial T}{\partial \dot{\theta}}\right) = m\left[\frac{s^2}{2}\left(\frac{c^2}{2} - x_f c\right)\ddot{k} + s\left(\frac{c^3}{3} - c^2 x_f + x_f^2 c\right)\ddot{\theta}\right] \quad (10)$$

$$\frac{\partial U}{\partial k} = K_k k \quad (11)$$

$$\frac{\partial U}{\partial \theta} = K_\theta \theta \quad (12)$$

Where

K_k- Flapping coefficient

K_θ-Pitching coefficient.

Writing the equations in a matrix form which leading to equation of motion for the wing, without any aerodynamics forces

$$\begin{bmatrix} \frac{ms^2c}{3} & \frac{ms^2}{2}\left(\frac{c^2}{2} - x_f c\right) \\ \frac{ms^2}{2}\left(\frac{c^2}{2} - x_f c\right) & ms\left(\frac{c^3}{3} - c^2 x_f + x_f{}^2 c\right) \end{bmatrix} \begin{Bmatrix} k \\ \theta \end{Bmatrix} + \begin{bmatrix} K_k & 0 \\ 0 & K_\theta \end{bmatrix} \begin{Bmatrix} k \\ \theta \end{Bmatrix} = \begin{Bmatrix} 0 \\ 0 \end{Bmatrix}$$

Assuming inertia matrix

$$\begin{bmatrix} \frac{ms^2c}{3} & \frac{ms^2}{2}\left(\frac{c^2}{2} - x_f c\right) \\ \frac{ms^2}{2}\left(\frac{c^2}{2} - x_f c\right) & ms\left(\frac{c^3}{3} - c^2 x_f + x_f{}^2 c\right) \end{bmatrix} \quad \begin{bmatrix} I_k & I_{k\theta} \\ I_{k\theta} & I_\theta \end{bmatrix}$$

Where,

$$I_k = \int_0^s y^2 dm \quad (13)$$

$$I_\theta = \int_0^c \int_0^s (x - x_f) y dm \quad (14)$$

$$I_{k\theta} = \int_0^c (x - x_f)^2 dm \quad (15)$$

These terms are the moment of inertia in flap and pitch and the product moment of inertia

The pitch and flap natural frequencies are

$$\omega_k = \sqrt{\frac{K_k}{I_k}} \quad (16)$$

$$\omega_\theta = \sqrt{\frac{K_\theta}{I_\theta}} \quad (17)$$

Generalised forces $Q_k$and Q_θ (i.e. assumed unsteady aerodynamic forces) will act on the wing. It is written in terms of aerodynamics derivatives for a particular reduced frequency.

Applying strip theory,

Lift and pitching moment about the flexural axis for each elemental strip theory dy of

$$dL = \frac{1}{2}\rho V^2 c dy a_w \left(\frac{y}{k} + \theta\right) \quad (18)$$

$$dM=\frac{1}{2}\rho V^2 c^2\left[ea_w\left(\frac{\dot{yk}}{V}+\theta\right)+M_\theta\frac{\theta c}{4V}\right] \quad (19)$$

Where

$\dot{yk}$- Effective heave velocity

The incremental work done over the wing due to aerodynamic force and moment through incremental deflection δk & $\delta\theta$ of the wing is

$$\delta W=\int_{wing}[dL(-y\delta k)+dM\delta\theta$$

And therefore the generalised forces are

$$Q_k=\frac{\partial(\delta W)}{\partial(\delta k)}=-\int_0^s ydL$$

$$Q_k=-\frac{1}{2}\rho V^2 cs^2 a_w\left(\frac{ks}{2V}+\frac{\theta}{2}\right) \quad (20)$$

$$Q_\theta=\frac{\partial(\delta W)}{\partial(\delta\theta)}=\int_0^s dM$$

$$Q_\theta=\frac{1}{2}\rho V^2 sc^2\left[ea_w\left(\frac{ks}{2V}+\theta\right)+M_\theta\frac{\theta c}{4V}\right] \quad (21)$$

Above equations can be written in the matrix to form,

The full aero elastic equation of motion become

$$\begin{bmatrix}I_k & I_{k\theta}\\ I_{k\theta} & I_\theta\end{bmatrix}\begin{Bmatrix}\ddot{k}\\ \ddot{\theta}\end{Bmatrix}+\rho V\begin{bmatrix}\frac{cs^2a_w}{6} & 0\\ -\frac{ea_w s^2c^2}{4} & -\frac{sc^2}{8}M_{\dot{\theta}}\end{bmatrix}\begin{Bmatrix}\dot{k}\\ \dot{\theta}\end{Bmatrix}+\left\{\rho V^2\begin{bmatrix}0 & \frac{cs^2a_w}{4}\\ 0 & -\frac{ea_w sc^2}{2}\end{bmatrix}+\begin{bmatrix}K_k & 0\\ 0 & K_\theta\end{bmatrix}\right\}\begin{Bmatrix}k\\ \theta\end{Bmatrix}=\begin{Bmatrix}0\\ 0\end{Bmatrix}$$

The mass and the stiffness matrices are symmetric while the aerodynamic matrices are non-symmetric. Thus the 2 DoF are coupled and it is coupled that can give rise to flutter.

General Form of the Aero Elastic Equation

$$A\ddot{q}+(\rho VB+D)\dot{q}(\rho V^2C+E)q=0$$

Where,

A – Structural inertia

B – Aerodynamic damping

C – Aerodynamic stiffness

D – Structural damping

E – Structural stiffness matrices

3.2 MATLAB Baseline parameter

The dynamic aero elastic behavior for the flapping/pitching wing can be determined at different airspeed and altitude for each flight condition and then calculating the corresponding frequencies and damping ratio.

The baseline system parameters considered, (Cessna 152) [7]

- Mass axis is at the semi-chord x_m = 0.5c=0.725m
- Flexural axis is at x_f = 0.48c=0.696m from the leading edge.

- Semi-span s=5.1m
- Chord c=1.45m
- Mass per unit area=100kg/m^2
- Flap stiffness (K_k)= $I_k(5*2\pi)^2$

  Sub the values in equation 13, we get

  $I_k = 6411.465m$

  Hence, K_k= 6327862.318m

  Sub these 2 values in equation 16,$\omega_k = 10$ hertz
- Pitch stiffness (K_θ)= $I_k(10*2\pi)^2$

  Sub the values in equation 14, we get $I_\theta = 130.188$m

  Hence, K_θ= 513963.52m

  Sub these 2 values in equation 17,$\omega_\theta = 5$ hertz
- Lift slope curve a=2π
- Non dimensional pitch damping derivative M_θ= -1.2

Using the aero elastic equation of motion, the MATLAB program have been scripted and the baseline system parameter of Cessna 152 is given as the input, the frequency and damping ratio has been found for different airspeed.

IV RESULTS AND DISCUSSION

The figure given below obtained from MATLAB code, when the command is executed.

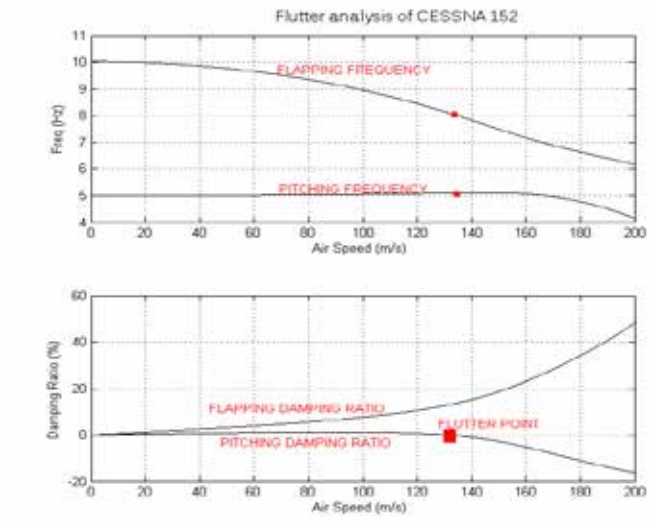

Fig 3.2.1 MATLAB Figure

The figure 3.2.1 shows how frequency and damping ratio values varies for this classical binary flutter behavior. As the airspeed increases, the frequencies begins to converge. Initially both of the damping ratio increases, but the flapping damping ratio continuous to increase, the pitching damping ratio starts to decrease and become zero at the flutter speed of 132m/s. Beyond this airspeed the pitching damping ratio becomes negative and flutter

occurs. The two frequencies do not coalesce, but rather move close enough in frequency for the two modes to couple unfavorably.

Limitation:

Using this method only approximate flutter velocity can be obtain not the exact critical flutter velocity.

REFERENCES

[1] http://en.wikipedia.org/wiki/Aeroelasticity Flutter

[2] Jan R. Wright, Jonathan E. Cooper,"Introduction to aircraft aeroelasticity and loads", John Wiley& sons limited, 2007.

[3]WeiweiZhang,ZhengyinYe,"Effect of control surface on airfoil flutter in transonic flow",Acta Astronautica 66,999–1007,2010.

[4] S. Irani, S. Sazesh,"A new flutter speed analysis method using stochastic approach", Elsevier, Journal of Fluids and Structures 40,105-114,2013.

[5] Feng-Ming Li, "Active aero elastic flutter suppression of a supersonic plate with piezoelectric material", Elsevier, International Journal of Engineering Science 51,190–203,2012.

[6] R.J. Zwaana, B.B. Pranantab,"Fluid structure interaction in numerical aeroelastic simulation" International Journal of Non-Linear Mechanics 37,987–1002,2002.

[7] http://en.wikipedia.org/wiki/Cessna_152

EFFECT OF CHEMICAL REACTION ON UNSTEADY HYDRO-MAGNETIC CONVECTIVE FLOW PAST A VERTICAL POROUS PLATE IN POROUS MEDIUM WITH HEAT SOURCE AND SOLUTION WITH C-PROGRAMING

Ruchi Chaturvedi[1], Mohd. Salim Ahamad[2]

[1]*Department of Mathematics, FET-Agra College, Agra, (India)*

[2]*Department of Mathematics, Hindustan College of Science & Technology, Mathura, (India)*

ABSTRACT

The purpose of this paper is to analyze the effect of chemical reaction on unsteady hydro magnetic free convective flow of a viscous incompressible electrically conducting fluid past an infinite vertical porous plate in presence of constant suction and heat source. The governing equations of the flow field are solved using multi parameter perturbation technique and approximate solutions using C-programming are obtained for velocity field, temperature field, concentration distribution, skin friction and the rate of heat transfer.

Keywords: Porous, Unsteady, Convection, Hydro-Magnetic, Heat Transfer

I. INTRODUCTION

The theory of hydro-magnetic flow with heat and mass transfer in an electrically conducting fluid past a porous plate embedded in a porous medium has varied applications in many engineering problems such as MHD generators, plasma studies, nuclear reactors, oil exploration, geothermal energy extractions and in the boundary layer control in the field of aerodynamics. Heat transfer in laminar flow is important in problems dealing with chemical reactions and in dissociating fluids.

In view of its wide applications, Hasimoto (1957) initiated the boundary layer growth on a flat plate with suction or injection. Soundalgekar (1974) showed the effect of free convection on steady MHD flow of an electrically conducting fluid past a vertical plate.Yamamoto and Iwamura (1976) explained the flow of a viscous fluid with convective accelerationthrough a porous medium. Mansutti et al. (1993) have discussed the steady flow of a non-Newtonianfluid past a porous plate with suction or injection. Chandran and associates (1998) have discussed the unsteady free convection flow of an electrically conducting fluid with heat flux and accelerated boundary layer motion in presence of a converse magnetic field. The unsteady free convective MHD flow with heat transfer past a semi-infinite vertical porous moving plate with variable suction has been studied by Kim (2000). Singh and Thakur (2002) have given an exact solution of a plane unsteady MHD flow of a non-Newtonian fluid. Sharma and Pareek (2002) explained the behavior of steady free convective MHD flow past a vertical porous moving surface. Singh and his co-workers (2003) have analyzed the effect of heat and mass transfer in MHD flow of a viscous fluid past a vertical plate under oscillatorysuction velocity. Makinde et al.

(2003) discussed the unsteady free convective flow with suction on an accelerating porous plate.Sarangi and Jose (2005) studied the unsteady free convective MHD flow and mass transfer past a vertical porous plate with variable tempature. Das and his associates (2006) estimated the mass transfer effects on unsteady flow past an accelerated vertical porous plate with suction employing finite difference analysis. Das et al.(2007) investigated numerically the unsteady free convective MHD flow past an accelerated vertical plate with suction and heat flux. Das and Mitra (2009) discussed the unsteady mixed convective MHD flow and mass transfer past an accelerated infinite vertical plate with suction. Recently, More recently, Das et al. (2010) investigated the hydro-magnetic convective flow past a vertical porous plate through a porous medium with suction and hear source.

The study of stellar structure on solar surface is connected with mass transfer phenomena. Its origin is attributed to difference in temperature caused by the non-homogeneous production of heat which in many cases can rest on only in the formation of convective currents but also in violent explosions. Mass transfer certainly occurs within the mantle and cores of plates of the size of or larger than the earth. In the present study we therefore, propose to analyze the effect of mass transfer on unsteady free convective flow of a viscous incompressible electrically conducting fluid past on infinite vertical porous platewith constant suction and heat source in presence of a transverse magnetic field. Das et al. also studied the effect of mass transfer on hydo-magnetic flow in presence of suction and heat source. In this paper we have extended the work done by Das to analyze the effect of chemical reaction.

II. FORMULATION OF THE PROBLEM

Consider the unsteady free convective mass transfer flow of a viscous incompressible electrically conducting fluid past an infinite vertical porous plate in presence of constant suction and heat source and transverse magnetic field. Let the x-axis be taken in vertically upward direction along the plate and y-axis normal to it. Neglecting the induced magnetic field and the Joulean heat dissipation and applying Boussinesq's approximation the governing equations of the flow field are given by:

Continuity equation:

$$\frac{\partial v'}{\partial y'} = 0 \Rightarrow v' = -v'_0 \text{ (Constant)} \tag{1}$$

Momentum equation:

$$\frac{\partial u'}{\partial t'} + v'\frac{\partial u'}{\partial y'} = g\beta(T' - T'_\infty) + g\beta^*(C' - C'_\infty) + \nu\frac{\partial^2 u'}{\partial y'^2} - \frac{\sigma B_0^2}{\rho}u' - \frac{\nu}{K'}u' \tag{2}$$

Energy equation:

$$\frac{\partial T'}{\partial t'} + v'\frac{\partial T'}{\partial y'} = k\frac{\partial^2 T'}{\partial y'^2} + \frac{\nu}{C_p}\left(\frac{\partial u'}{\partial y'}\right)^2 + S'(T' - T'_\infty) \tag{3}$$

Concentration equation:

$$\frac{\partial C'}{\partial t'} + v'\frac{\partial C'}{\partial y'} = D\frac{\partial^2 C'}{\partial y'^2} - K_1 C' \tag{4}$$

The boundary conditions of the problem are:

$$u' = 0, v' = -v_0', T' = T_w' + \epsilon(T_w' - T_\infty')e^{i\omega' t'},$$
$$C' = C_w' + \epsilon(C_w' - C_\infty')e^{i\omega' t'} \text{ at } y' = 0, \quad (5)$$
$$u' \to 0, T' \to T_\infty', C' \to C_\infty' \text{ at } y' \to \infty,$$

Introducing the following non-dimensional variables and parameters,

$$y = \frac{y' v_0'}{\nu}, t = \frac{t' v_0'^2}{4\nu}, \omega = \frac{4\nu\omega'}{v_0'^2}, u = \frac{u'}{v_0'}, v = \frac{h_0}{r},$$
$$M = \left(\frac{\sigma B_0^2}{r}\right)\frac{\nu}{v_0'^2}, K_p = \frac{v_0'^2}{\nu^2}, T = \frac{T' - T_\infty'}{T_w' - T_\infty'},$$
$$C = \frac{C' - C_\infty'}{C_w' - C_\infty'}, P_r = \frac{\nu}{k}, G_r = \frac{\nu g \beta (T_w' - T_\infty')}{v_0'^3}, \quad (6)$$
$$G_c = \frac{\nu g \beta^* (C_w' - C_\infty')}{v_0'^3}, S_c = \frac{\nu}{D}, S = \frac{4S'\nu}{v_0'^2},$$
$$E_c = \frac{v_0'^2}{C_p (T_w' - T_\infty')}$$

Where $g, r, \sigma, \nu, \beta, \beta^*, \omega, h_0, k, T, T_w, T_\infty, C, C_w, C_\infty,$ $C_p, D, P_r, S_c, G_r, G_c, S, K_p, E_c$ and M

Are respectively the acceleration due to gravity, density, Electrical conductivity, coefficient of kinematic viscosity, volumetric coefficient of expansion for heat transfer ,volumetric coefficient of expansion for mass transfer ,angular frequency, coefficient of viscosity, thermal diffusivity, temperature, temperature at the plate, temperature at infinity, concentration, concentration at the plate, concentration at infinity, specific heat at constant pressure, molecular mass diffusivity, Prandtl number, Schimdt number, Grashof number for heat transfer, Grashof number for mass transfer, heat source parameter, permeability parameter, Eckert number and Hartmann number.

Substituting equation (6) in equations (2), (3) and (4) under boundary conditions (5), we get:

$$\frac{1}{4}\frac{\partial u}{\partial t} - \frac{\partial u}{\partial y} = G_r T + G_c C + \frac{\partial^2 u}{\partial y^2} - \left(M + \frac{1}{K_p}\right)u \quad (7)$$

$$\frac{1}{4}\frac{\partial T}{\partial t} - \frac{\partial T}{\partial y} = \frac{1}{P_r}\frac{\partial^2 T}{\partial y^2} + \frac{1}{4}ST + E_c\left(\frac{\partial u}{\partial y}\right)^2 \quad (8)$$

$$\frac{1}{4}\frac{\partial C}{\partial t} - \frac{\partial C}{\partial y} = \frac{1}{S_c}\frac{\partial^2 C}{\partial y^2} - K_1 C \quad (9)$$

The Corresponding boundary conditions are:

$$u = 0, T = 1 + \epsilon e^{i\omega t}, C = 1 + \epsilon e^{i\omega t} \text{ at y=0},$$
$$u \to 0, T \to 0, C \to 0 \text{ as } y \to \infty \quad (10)$$

III. METHOD OF SOLUTION

To solve equation (7),(8)&(9), we assume ϵ to be very small and the velocity , temperature and concentration distribution of the flow field in the neighbourhood of the plate as

$$u(y,t) = u_0(y) + \epsilon e^{i\omega t} u_1(y) \quad (11)$$

$$T(y,t) = T_0(y) + \epsilon e^{i\omega t} T_1(y) \quad (12)$$

$$C(y,t) = C_0(y) + \epsilon e^{i\omega t} C_1(y) \quad (13)$$

Substituting equations (11)-(13) in equations (7)-(9) respectively, equating the harmonic and non-harmonic terms and neglecting the coefficients of ϵ^2 , we get

Zeroth order:

$$u_0'' + u_0' - \left(M + \frac{1}{K_p}\right) u_0 = -G_r T_0 - G_c C_0 \quad (14)$$

$$T_0'' + P_r T_0' + \frac{P_r S}{4} T_0 = -P_r E_c \left(\frac{\partial u_0}{\partial y}\right)^2 \quad (15)$$

$$C_0'' + S_c C_0' = 0 \quad (16)$$

First Order:

$$u_1'' + u_1' - \left(\frac{i\omega}{4} + M + \frac{1}{K_p}\right) u_1 = -G_r T_1 - G_c C_1 \quad (17)$$

$$T_1'' + P_r T_1' - \frac{P_r}{4}(i\omega - S) T_1 = -2 P_r E_c \left(\frac{\partial u_0}{\partial y}\right)\left(\frac{\partial u_1}{\partial y}\right) \quad (18)$$

$$C_1'' + S_c C_1' - \left(\frac{i\omega S_c}{4} + K_1 S_c\right) C_1 = 0 \quad (19)$$

The corresponding boundary conditions are

$$y = o:\ u_0 = 0,\ T_0 = 1,\ C_0 = 1,\ u_1 = 0,\ T_1 = 1,\ C_1 = 1$$

$$y \to \infty:\ u_0 = 0,\ T_0 = 0,\ C_0 = 0,\ u_1 = 0,\ T_1 = 0,\ C_1 = 0 \quad (20)$$

Solving equations (16) and (19) under boundary condition (20), we get

$$C_0 = e^{-Ay} \quad (21)$$

$$C_1 = e^{-m_1 y} \quad (22)$$

Using multi parameter perturbation technique and assuming $E_c << 1$, we assume

$$u_0 = u_{00} + E_c u_{01} \quad (23)$$

$$T_0 = T_{00} + E_c T_{01} \quad (24)$$

$$u_1 = u_{10} + E_c u_{11} \quad (25)$$

$$T_1 = T_{10} + E_c T_{11} \quad (26)$$

Now using equations (23)-(26) in equations (14),(15),(17) & (18) and equating the coefficients of like powers of E_c neglecting those of E_c^2 we get the following set of differential equations:

Zeroth Order:

$$u_{00}'' + u_{00}' - \left(M + \frac{1}{K_p}\right) u_{00} = - G_r T_{00} - G_c C_0 \quad (27)$$

$$u_{10}'' + u_{10}' - \left(M + \frac{1}{K_p} + \frac{iw}{4}\right) u_{10} = - G_r T_{10} - G_c C_1 \quad (28)$$

$$T_{00}'' + P_r T_{00}' + \frac{P_r S}{4} T_{00} = 0 \quad (29)$$

$$T_{10}'' + P_r T_{10}' - \frac{P_r}{4}(iw - S) T_{10} = 0 \quad (30)$$

The corresponding boundary conditions are

$$y = 0 : \; u_{00} = 0, \; T_{00} = 1, \; u_{10} = 0, \; T_{10} = 1$$

$$y \to \infty : \; u_{00} = 0, \; T_{00} = 0, \; u_{10} = 0, \; T_{10} = 0 \quad (31)$$

First Order:

$$u_{01}'' + u_{01}' - \left(M + \frac{1}{K_p}\right) u_{01} = - G_r T_{01} \quad (32)$$

$$u_{11}'' + u_{11}' - \left(M + \frac{1}{K_p} + \frac{iw}{4}\right) u_{11} = - G_r T_{11} \quad (33)$$

$$T_{01}'' + P_r T_{01}' + \frac{P_r S}{4} T_{01} = - P_r \left(u_{00}'\right)^2 \quad (34)$$

$$T_{11}'' + P_r T_{11}' - \frac{P_r}{4}(iw - S) T_{11} = - 2 P_r \left(\frac{\partial u_{00}}{\partial y}\right)\left(\frac{\partial u_{10}}{\partial y}\right) \quad (35)$$

The corresponding boundary conditions are,

$$y = 0 : \; u_{01} = 0, \; T_{01} = 0, \; u_{11} = 0, \; T_{11} = 0$$

$$y \to \infty : \; u_{01} = 0, \; T_{01} = 0, \; u_{11} = 0, \; T_{11} = 0 \quad (36)$$

Solving equations (27)-(30) subject to boundary condition (31), we get

$$u_{00} = A_0 e^{-m_3 y} + A_1 e^{-S_c y} - A_2 e^{-m_7 y} \quad (37)$$

$$T_{00} = e^{-m_3 y} \quad (38)$$

$$u_{10} = A_3 e^{-m_5 y} + A_4 e^{-m_1 y} - A_5 e^{-m_9 y} \quad (39)$$

$$T_{10} = e^{-m_5 y} \quad (40)$$

Solving equations (32)-(35) subject to boundary condition (36), we get

$$T_{01} = A_6 e^{-2S_c y} + A_7 e^{-2m_3 y} + A_8 e^{-2m_5 y} + A_9 e^{-(m_3+S_c)y} + A_{10} e^{-(m_7+S_c)y} + A_{11} e^{-(m_3+m_7)y} - A_{12} e^{-m_3 y} \quad (41)$$

$$T_{11} = A_{13} e^{-(m_3+m_5)y} + A_{14} e^{-(m_1+m_3)y} + A_{15} e^{-(m_3+m_9)y} + A_{16} e^{-(m_5+S_c)y} + A_{17} e^{-(m_1+S_c)y} + A_{18} e^{-(m_9+S_c)y} + A_{19} e^{-(m_5+m_7)y} + A_{20} e^{-(m_1+m_7)y} + A_{21} e^{-(m_7+m_9)y} - A_{22} e^{-m_5 y} \quad (42)$$

$$u_{01} = A_{23} e^{-2S_c y} + A_{24} e^{-2m_3 y} + A_{25} e^{-2m_7 y} + A_{26} e^{-(m_3+S_c)y} + A_{27} e^{-(m_7+S_c)y} + A_{28} e^{-(m_3+m_7)y} + A_{29} e^{-m_3 y} - A_{30} e^{-m_7 y} \quad (43)$$

$$u_{11} = A_{31} e^{-(m_3+m_5)y} + A_{32} e^{-(m_1+m_3)y} + A_{33} e^{-(m_3+m_9)y} + A_{34} e^{-(m_5+S_c)y} + A_{35} e^{-(m_1+S_c)y} + A_{36} e^{-(m_9+S_c)y} + A_{37} e^{-(m_5+m_7)y} + A_{38} e^{-(m_1+m_7)y} + A_{39} e^{-(m_7+m_9)y} + A_{40} e^{-m_5 y} - A_{41} e^{-m_9 y} \quad (44)$$

Substituting the values of C_0 and C_1 from equations (21) and (22) in equation (13) the solution for concentration distribution of the flow field is given by

$$C = e^{-Ay} + \epsilon e^{i\omega t} e^{-m_1 y} \quad (45)$$

3.1 Skin Friction

The skin friction at the wall is given by

$$\tau_w = \left(\frac{\partial u}{\partial y}\right)_{y=0}$$

$$= -m_3 A_0 - S_c A_1 + m_7 A_2 - E_c[2S_c A_{23} + 2m_3 A_{24} + 2m_7 A_{25} + (m_3 + S_c) A_{26} + (m_7 + S_c) A_{27} + (m_3 + m_7) A_{28} + m_3 A_{29} - m_7 A_{30}] - \epsilon e^{i\omega t} \{m_5 A_3 + m_1 A_4 - m_9 A_5 + E_c[(m_3 + m_5) A_{31} + (m_1 + m_3) A_{32} + (m_3 + m_9) A_{33} + (m_5 + S_c) A_{34} + (m_1 + S_c) A_{35} + (m_9 + S_c) A_{36} + (m_5 + m_7) A_{37} + (m_1 + m_7) A_{38} + (m_7 + m_9) A_{39} + m_5 A_{40} - m_9 A_{41}]\} \quad (46)$$

3.2 Heat Flux

The heat flux at the wall in terms of Nusselt number is given by

$$N_u = \left(\frac{\partial T}{\partial y}\right)_{y=0}$$

$$\begin{aligned}
&= -m_3 - E_c[2S_cA_6 + 2m_3A_7 + 2m_5A_8 \\
&- (m_3 + S_c)A_9 + (m_7 + S_c)A_{10} \\
&+ (m_3 + m_7)A_{11} - m_3A_{12}] + \varepsilon e^{i\omega t} \\
&\{-m_5 - E_c[(m_3 + m_5)A_{13} + (m_1 + m_3)A_{14} \\
&+ (m_3 + m_9)A_{15} + (m_5 + S_c)A_{16} + (m_1 + S_c)A_{17} \\
&+ (m_9 + S_c)A_{18} + (m_5 + m_7)A_{19} \\
&+ (m_1 + m_7)A_{20} + (m_7 + m_9)A_{21} - m_5A_{22}]\}
\end{aligned} \qquad (47)$$

Where

$$A = \left(\frac{S_c + \sqrt{S_c^2 + 4K_1S_c}}{2}\right)$$

$$m_1 = \frac{1}{2}\left[S_c + \sqrt{S_c^2 + \left(\frac{i\omega S_c}{4} + K_1S_c\right)}\right]$$

$$m_2 = \frac{1}{2}\left[-S_c + \sqrt{S_c^2 + \left(\frac{i\omega S_c}{4} + K_1S_c\right)}\right]$$

$$m_3 = \frac{1}{2}\left[P_r + \sqrt{P_r^2 - SP_r}\right]$$

$$m_4 = \frac{1}{2}\left[-P_r + \sqrt{P_r^2 - SP_r}\right]$$

$$m_5 = \frac{1}{2}\left[P_r + \sqrt{P_r^2 - P_r(S - i\omega)}\right]$$

$$m_6 = \frac{1}{2}\left[-P_r + \sqrt{P_r^2 - P_r(S - i\omega)}\right]$$

$$m_7 = \frac{1}{2}\left[1 + \sqrt{1 + 4\left(M + \frac{1}{K_p}\right)}\right]$$

$$m_8 = \frac{1}{2}\left[-1 + \sqrt{1 + 4\left(M + \frac{1}{K_p}\right)}\right]$$

$$m_9 = \frac{1}{2}\left[1 + \sqrt{1 + 4\left(M + \frac{1}{K_p} + \frac{i\omega}{4}\right)}\right]$$

$$m_{10} = \frac{1}{2}\left[-1+\sqrt{1+4\left(M+\frac{1}{K_p}+\frac{iw}{4}\right)}\right]$$

$$A_0 = \frac{G_r}{(m_7 - m_3)(m_8 + m_3)}$$

$$A_1 = \frac{G_c}{(m_7 - S_c)(m_8 + S_c)}$$

$$A_2 = A_0 + A_1$$

$$A_3 = \frac{G_r}{(m_9 - m_5)(m_{10} + m_5)}$$

$$A_4 = \frac{G_c}{(m_9 - m_1)(m_{10} + m_1)}$$

$$A_5 = A_3 + A_4$$

$$A_6 = \frac{P_r S_c^{\,2} A_1^{\,2}}{(m_3 - 2S_c)(m_4 + 2S_c)}$$

$$A_7 = \frac{-P_r m_3 A_0^{\,2}}{(m_4 + 2m_3)}$$

$$A_8 = \frac{P_r m_7^{\,2} A_2^{\,2}}{(m_3 - 2m_7)(m_4 + 2m_7)}$$

$$A_9 = -\frac{2A_0 A_1 m_3 P_r}{(m_3 + m_4 + S_c)}$$

$$A_{10} = \frac{2P_r S_c A_1 A_2 m_7}{(m_3 - m_7 - S_c)(m_4 + m_7 + S_c)}$$

$$A_{11} = \frac{2A_0 A_1 m_3 P_r}{(m_3 + m_4 + m_7)}$$

$$A_{12} = A_6 + A_7 + A_8 + A_9 + A_{10} + A_{11}$$

$$A_{13} = -\frac{2P_r A_0 A_5}{(m_3 + m_5 + m_6)}$$

$$A_{14} = \frac{2P_r A_0 A_4 m_1 m_3}{(m_5 - m_3 - m_1)(m_6 + m_3 + m_1)}$$

$$A_{15} = \frac{2P_r A_0 A_5 m_3 m_9}{(m_9 - m_5 + m_3)(m_9 + m_6 + m_3)}$$

$$A_{16} = -\frac{2P_r A_1 A_3 m_5}{(m_6 + m_5 + S_c)}$$

$$A_{17} = \frac{2P_r S_c A_1 A_4 m_1}{(m_5 - m_1 - S_c)(m_6 + m_1 + S_c)}$$

$$A_{18} = \frac{2P_r S_c A_1 A_5 m_9}{(m_9 - m_5 + S_c)(m_9 + m_6 + S_c)}$$

$$A_{19} = \frac{2P_r A_2 A_3 m_5}{(m_7 + m_6 + m_5)}$$

$$A_{20} = \frac{2P_r A_2 A_4 m_1 m_7}{(m_7 - m_5 + m_1)(m_7 + m_6 + m_1)}$$

$$A_{21} = \frac{2P_r A_2 A_5 m_7 m_9}{(m_9 + m_7 + m_5)(m_9 + m_7 + m_6)}$$

$$A_{22} = A_{13} + A_{14} + A_{15} + A_{16} + A_{17} + A_{18} + A_{19} + A_{20} + A_{21}$$

$$A_{23} = \frac{G_r A_6}{(m_7 - 2S_c)(m_8 + 2S_c)}$$

$$A_{24} = \frac{G_r A_7}{(m_7 - 2m_3)(m_8 + 2m_3)}$$

$$A_{25} = \frac{-G_r A_8}{m_7 (m_8 + 2m_3)}$$

$$A_{26} = \frac{G_r A_9}{(m_7 - m_3 - S_c)(m_8 + m_3 + S_c)}$$

$$A_{27} = \frac{-G_r A_{10}}{S_c (m_8 + m_3 + S_c)}$$

$$A_{28} = \frac{-G_r A_{11}}{m_3 (m_8 + m_7 + m_3)}$$

$$A_{29} = \frac{G_r A_{12}}{(m_3 - m_7)(m_8 + m_3)}$$

$$A_{30} = A_{23} + A_{24} + A_{25} + A_{26} + A_{27} + A_{28} + A_{29}$$

$$A_{31} = \frac{G_r A_{13}}{(m_9 - m_5 - m_3)(m_{10} + m_5 + m_3)}$$

$$A_{32} = \frac{G_r A_{14}}{(m_9 - m_3 - m_1)(m_{10} + m_3 + m_1)}$$

$$A_{33} = \frac{-G_r A_{15}}{m_3 (m_{10} + m_9 + m_3)}$$

$$A_{34} = \frac{G_r A_{16}}{(m_9 - m_5 - S_c)(m_{10} + m_5 + S_c)}$$

$$A_{35} = \frac{G_r A_{17}}{(m_9 - m_1 - S_c)(m_{10} + m_1 + S_c)}$$

$$A_{36} = \frac{-G_r A_{18}}{S_c (m_{10} + m_9 + S_c)}$$

$$A_{37} = \frac{G_r A_{19}}{(m_9 - m_7 - m_5)(m_{10} + m_7 + m_5)}$$

$$A_{38} = \frac{G_r A_{20}}{(m_9 - m_7 - m_1)(m_{10} + m_7 + m_1)}$$

$$A_{39} = \frac{-G_r A_{21}}{m_7 (m_{10} + m_9 + m_7)}$$

$$A_{40} = \frac{G_r A_{22}}{(m_9 - m_5)(m_{10} + m_5)}$$

$$A_{41} = A_{31} + A_{32} + A_{33} + A_{34} + A_{35} + A_{36} + A_{37} + A_{38} + A_{39} + A_{40}$$

IV. RESULTS AND DISCUSSIONS

The effect of chemical reaction on unsteady free convective flow of a viscous incompressible electrically conducting fluid past an infinite vertical porous plate with constant suction and heat source with mass transfer in presence of a transverse magnetic field has been studied. The governing equations of the flow field are solved employing multi parameter perturbation technique with C-programming and approximate solutions are obtained for velocity field, temperature field and concentration distribution. The effects of chemical reaction parameter on the flow field are analyzed and discussed with the help of velocity profiles(Fig. 1), temperature profiles(Fig. 2). Concentration distribution (Fig. 3). To be more realistic , during numerical calculations we have chosen the values of $P_r = 0.71$ representing air at $20^0 C$, S_c representing H_2O vapour, $G_r > 0$ corresponding to cooling of the plate and $S > 0$ representing heat source.

4.1 Velocity Field

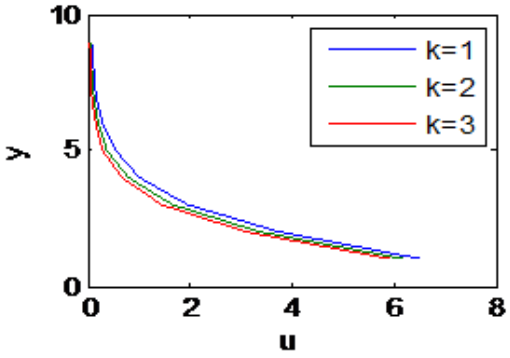

Fig. 1

The velocity of the flow field is found to change more or less with the variation of the flow parameters. The major factors affecting the velocity of the flow field are Hartmann number M, permeability parameter K_p, Grashof numbers for heat and mass transfer G_r, G_c, Schmidt number S_c, heat source parameter S and Prandtl number P_r.

Fig. 1 depict the effect of chemical reaction parameter on velocity (mean and transient) of the flow field. It is observed that a growing chemical reaction parameter decelerates velocity of the flow field at all points due to the magnetic pull of the Lorentz force acting on the flow field.

4.2 Temperature Field

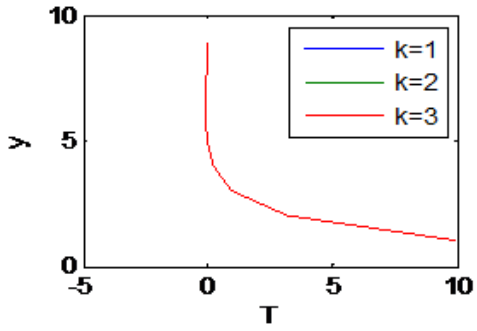

Fig. 2

The temperature of the flow field does not show a significant or major effect of chemical reaction parameter change. These variations are shown in Fig. 2.

4.3 Concentration Distribution

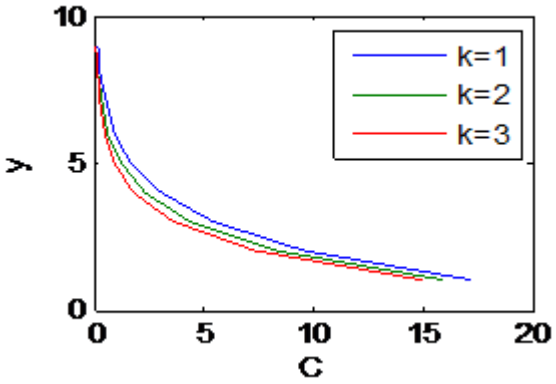

Fig. 3

The variation in the concentration boundary layer of the flow field is shown in Fig. 3 due to the change in the chemical reaction parameter. In the curves of the said figure it is observed that a growing chemical reaction parameter decreases the concentration boundary layer thickness of the flow field at all points.

V. ACKNOWLEGEMENT

For the C- programming of mathrmatical equations used in our paper Shaurabh Srivastava (B.Tech- CS, FET, Agra College Agra) and Shubham Sharma (B.Tech- CS, FET, Agra College Agra) have given their full cooperation and support so we acknowledge their work for our paper.

REFERENCES

1. Chandran,P., N.C. Sacheti and A.K. Singh(1998). Unsteady hydromagnetic free convection flow with heat flux and accelerated boundary motion. J. Phys. Soc.Japan, 124-129.
2. Das S. S., S. K. Sahoo and G.C. Dash(2006). Numerical Solution of mass transfer effects on unsteady flow past an accelerated vertical porous plate with suction. Bull. Malays. Math. Sci. Soc. 29(1), 33-42.
3. Das S.S., A. Sathpathy, J.K. Das and S.K. Sahoo(2007). Numerical solution of unsteady free convective MHD flow past an accelerated vertical plate with suction and heat flux. J. Ultra Sci. Phys. Sci. 19(1), 105-112.
4. Das S.S., A. Sathpathy, J.K. Das and J.P. Panda(2009). Mass transfer effect on MHD flow and heat transfer past a vertical porous plate through a porous medium under oscillatory suction and heat source. Int. J. Heat mass transfer 52,5962-5969.
5. Das S.S., U.K. Tripathy and J.K. Das(2010). Hydromagnetic convective flow past a vertical porous plate through a porous medium with suction and heat source. Int. J. Of Energy and environment 1(3),467-478.
6. Hasimoto, H. (1957). Boundary layer growth on a flat plate with suction or injection, J. Phys. Sci. Japan 12,68-72.
7. Kim, Y.J.(2000). Unsteady MHD convective heat transfer past a semi-infinite vertical porous moving plate with variable suction. Int. J. Engg. Sci. 38,833-845.
8. Makinde, O.D., J.M. Mango and D.M. Theuri(2003). Unsteady free convection flow with suction on an accelerating porous plate . AMSE J. Mod. Meas. Cont., B72(3), 39-46.
9. Mansutti, D., G. Pontrelli and K.R. Rajagopal(1993). Steady flows of non-Newtonian fluids past a porous plate with suction or injection. Int. J. Num. Methods fluids 17, 927-941.
10. Sarangi,K.C. and C.B. jose(2005). Unsteady free convective MHD flow and mass transfer past a vertical porous plate with variable temperature, Bull. Cal. Math. Soc. 97(2), 137-146.
11. Sharma, P.R. and D. Pareek (2002). Steady free convection MHD flow past a Vertical porous moving surface, Ind. J. Theo. Phys. 50,5-13.
12. Singh, A.K.,A.K. Singh and N.P.Singh(2003). Heat and mass transfer in MHD flow of a viscous fluid . past a vertical plate under oscillatory suction velocity. Ind. J. Pure Appl. Math. 34(3), 429-442.
13. Singh , B. And C. Thakur(2002). An exact solution of plane unsteady MHD non-Newtonian fluid flows . Ind. J. Pure appl. Math. 33(7), 993-1001.
14. Soundalgekar, V.M.(1974). Free convective effects on steady MHD flow past a vertical porous plate. J. Fluid Mech. 66, 541-551.
15. Yamamoto, K. And N. Iwamura(1976). Flow with convective acceleration through a porous medium. Engg. Math. 10,41-54.
16. Chaturvedi,Ruchi.et al
17. Das S.S. et al.(2011).Mass Transfer Effects on Unsteady HydromagneticConvective Flow past aVertical Porous Plate in a Porous Medium with Heat Source.Journal of Applied Fluid

A COMPREHENSIVE REVIEW OF SIGNIFICANT RESEARCHES ON PAPR REDUCTION TECHNIQUES IN OFDM SYSTEMS

V. Murugan[1], D. Sivakumar[2]

[1]Research Scholar , [2]Professor & Head, Dept. of CSE, Eswari Engineering College, Ramappuram, Chennai (India)

ABSTRACT

One of the challenging issues for Orthogonal Frequency Division Multiplexing (OFDM) system is its high Peak-to-Average Power Ratio (PAPR). In this paper, we review and analysis different OFDM PAPR reduction techniques, based on computational complexity, bandwidth expansion, spectral spillage and performance. We also discuss some methods of PAPR reduction for multiuser OFDM broadband communication systems.

Index Terms: Orthogonal Frequency Division Multiplexing (OFDM), Peak-To-Average Power Ratio (PAPR)

I. INTRODUCTION

As an attractive technology for wireless communications, Orthogonal Frequency Division Multiplexing (OFDM), which is one of multi-carrier modulation (MCM) techniques, offers a considerable high spectral efficiency, multipath delay spread tolerance, immunity to the frequency selective fading channels and power efficiency,. As a result, OFDM has been chosen for high data rate communications and has been widely deployed in many wireless communication standards such as Digital Video Broadcasting (DVB) and based mobile worldwide interoperability for microwave access (mobile WiMAX) based on OFDM access technology

As one of characteristics of the PAPR, the distribution of PAPR, which bears stochastic characteristics in OFDM systems, often can be expressed in terms of Complementary Cumulative Distribution Function (CCDF). Recently, some researchers have reported on determination of the PAPR distribution based on different theoretics and hypotheses –. Moreover, various approaches also have been proposed to reduce the PAPR including clipping –, coding schemes –, phase optimization,, nonlinear companding transforms –, Tone Reservation (TR) and Tone Injection (TI),, constellation shaping –, Partial Transmission Sequence (PTS) and Selective Mapping (SLM) – and other techniques such as pre-scrambles proposed in. These schemes can mainly be categorized into signal scrambling techniques, such as block codes and PTS etc., and signal distortion techniques such as clipping.

In this paper, firstly we investigate the distribution of PAPR based on the characteristics of the OFDM signals. Then, we analyze five typical techniques of PAPR reduction and propose the criteria of PAPR reduction in OFDM systems in details. Finally, we briefly discuss the issue of PAPR in some broadband communication systems correlative with OFDM technology, such as multiuser OFDM systems.

II PAPR REDUCTION TECHNIQUES IN LITERATURE

The most challenging contents for Orthogonal Frequency Division Numerousxing (OFDM) structure is the high Peak-to-Average Power Ratio (PAPR).

Any classic methods of PAPR reduction are analyzed here.

2.1 Clipping and Filtering

The easiest and most popularly used method of PAPR reduction is to primarily clip the parts of the signals that are exterior the permitted segment. Usually, clipping is executed at the transmitter. Nevertheless, the receiver has to evaluate the clipping that has happened and to balance the received OFDM symbol properly. Commonly, at most one clipping happens per OFDM symbol, and thus the receiver has to evaluate two variables: position and magnitude of the clip. Nevertheless, it is hard to get these data. Hence, clipping method initiate both in band deformation and out of band emission into OFDM signals, which devalues the structure operation including BER and spectral efficiency. Filtering can lessen out of band emission after clipping while it cannot lessen in-band deformation. Nevertheless, clipping may create peak regrowth so that the signal after clipping and filtering will overshoot the clipping level at any points.

2.2 Effects of Clipping and Filtering

Several alternative solutions have been presented to lessen the crest factor (CF) of the signal input to the amplifier. One of these approaches, and the simplest, is to deliberately clip the OFDM signal before amplification. In particular, since the huge peaks occur with very low prospect, clipping could be an effectual method for CF reduction. Nevertheless, clipping is a nonlinear process and may create operative in-band deformation, which devalues the bit-errorrate (BER) operation, and out-of-band noise, which lessens the spectral efficiency. Filtering after clipping can lessen the spectral splatter but may also create any peak regrowth.

2.3 Estimation and Compensation of Clipping

Soft clipping lessens the magnitude of huge signals to a predefined threshold while leaving their phase unchanged. Clipping noise introduced by the magnitude deformation devalues the structure operation. Any approaches have been investigated to mitigate the noise, including decision aided reconstruction, iterative clipping noise estimation, and over-sampling based clipping noise reconstruction. Estimation and compensation for clipping noise in the downlink of OFDMA structures faces special challenges as each user only has limited knowledge of the whole signal. Since there are flexible modulation plans for different users, it is not always possible for a particular user to know the modulation plans of all other users. Most of the clipping noise estimation plans presented for OFDM structures are based on the decision directed approach which requires demodulated data symbols. Lack of modulation knowledge at any of the subcarriers prevents these plans from being applied in OFDMA structures.

2.4 Coding Plans

Jones was introduced simple block coding plans. Its fundamental design is that plotting 3 bits data into 4 bits watchword by attaching a Simple Odd Parity Code (SOBC) at the last bit over the mediums. The foremost disadvantage of SOBC method is that it can lessen PAPR for a 4-bit watchword. Later, Wulich applied the

Cyclic Coding (CC) to lessen the PAPR. In 1998, Fragiacomo presented an methodical Simple Block Code (SBC) to lessen the PAPR of OFDM signals. Nevertheless, it is ended that SBC is not effectual when the structure magnitude is huge. Later, Complement Block Coding (CBC) and Modified Complement Block Coding (MCBC) plans were presented to lessen the PAPR in need of the limitation of structure magnitude. CBC and MCBC are more appealing due to their pliability on selecting the coding rate, structure magnitude and low implementation complication. CBC and MCBC make use of the harmonious bits that are added to the genuine data bits to lessen the prospect of the peak signals incident.

2.5 PTS and SLM

In a classic OFDM structure with PTS approach to lessen the PAPR, the input data block in is divided into disjoint Subblocks. The known subblock dividing methods can be categorized into three classes: adjoining separation, interleaved separation and pseudorandom separation. Then, the subblocks are modified into time-doforemost partial transmit orders

These partial orders are alone revolved by phase factors. The intension is to ideally merge the subblocks to acquire the timedoforemost OFDM signals with the lowest PAPR. Hence, there are two main contents should be solved in PTS: high computational complication for searching the optimal phase factors and the overhead of the optimal phase factors as side data required to be transferred to receiver for the accurate decoding of the transferred bit order. While PTS and SLM are main possibility plans for PAPR reduction, it was previously known that SLM can make numerous time doforemost OFDM signals that are asymptotically independent, whereas the alternative OFDM signals generated by PTS are interdependent.

2.6 Nonlinear Companding Transforms

Operation including PAPR reduction and BER, low implementation complication and no bandwidth expansion. The primary nonlinear companding modification is the law companding, which is eastablished on the speech processing algorithm -law, and it has shown better operation than that of clipping method. law primarly focuses on enlarging signals with small amplitude and holding peak signals unchanged, and thus it increase the average power of the reassigned signals and possibly results in overshooting the saturation segment of HPA to make the structure operation worse.

Nonlinear companding transform is a kind of nonlinear process that may lead to operative deformation and operation loss by companding sound. Companding noise can be explained as the noises that are produced by the peak regrowth after DAC to produce in-band deformation and out-band noise, by the excessive channel noises magnified after inverse nonlinear companding transform etc.

2.7 TR and TI

TR and TI are two methodical methods to decrease the PAPR of OFDM signals. In TR, the intension is to get the time front most signal to be added to the genuine time foremost signal to lessen the PAPR.

The TI method is more elusive than the TR method since the injected signal populate the frequency band as the data bearing signals. Also, the alternative constellation points in TI method have an enhanced energy and the implementation complication enhances for the calculation of the optimal translation vector.

2.8 Nonlinear Companding Transform

The nonlinear characteristic of the HPA is very reactive to variation in signal amplitudes. Unluckily, the variation of OFDM signal amplitudes is very beamy with high peak-to-average power ratio (PAPR). Huge PAPR also claims analog-to-digital converters (ADC's) with huge driving range. Also, OFDM transmit signals

displays Gaussian distribution for huge number of sub-carriers, which implies that peak signals quite seldom occur and parallel quantization by the ADC's is not appreciable. So it is main to diminish the PAPR in OFDM structure.

A companding transform act that can reduce the PAPR effectually with a low implementation complication. The scheme includes methods by which the input signal is altered before amplification and then is restored at the receiver. The scheme is relevant with any modulation format. Unlike other known companding processes, the presented scheme works on statistical distribution of OFDM transmit signals, which is well developed by Gaussian distribution, and changes the distribution into uniform distribution, so it can be acheived with a technical device (such as a smooth limiter).

2.9 Exponential Companding Method

Nonlinear signal deformation occurs and leads to high adjoining channel interference and poor structure operation. A recent nonlinear companding method called "exponential companding", to decrease or reduce the PAPR of OFDM signals. It can successfully transform the genuine Gaussian-distributed OFDM signals into uniform-distributed (companded) signals in need of changing the average power level. Unlike the -law companding scheme, which primarily focuses on increasing small signals, our exponential companding plans set both small and huge signals in need of bias so that it is able to proffer better operation in terms of PAPR reduction, Bit-Error-Rate (BER) and phase error for OFDM structures.

Non-Symmetric De companding for Improved Operation of Companded OFDM Structures

Recently, companding transforms have been demonstrated by several authors to reduce PAPR. It has been demanded that the companding transforms exceeded the operation of the clipping by a fair margin. However, in these works, the impact of filtering out OBR has not been taken in detail.

The impact of filtering out OBR on the operation of companded OFDM structures. This method is established on the use of curve fitting method to figure out a desirable polynomial to be used for de companding at the receiver. To the best knowledge of the authors, this non-symmetric companding and de companding process has not been considered in the literature yet.

2.10 Complement Block Coding

In 1994 a simple block coding scheme was presented by Jones. The fundamental model of this scheme is that plotting 3 bits of data into 4 bits of watchword by linking a simple odd parity code (SOPC) at the last bit over the mediums lessens the PAPR, and can reduce PAPR by 3.54 dB. The primary disadvantage of this process is that it can only reduce PAPR for a 4-bit watchword. This is recreated if SOPC is used for longer codes, the high-powered watchwords will not be ruled out. Later, Fragiacomo presented a modified and methodical version of the simple block coding (SBC) scheme to reduce the PAPR of OFDM signals, but this method is not legal when the structure magnitude is huge. Later, a modified SBC (MSBC) scheme was presented and blended with the sub block processing method to make SBC effectual for OFDM structures with huge structure magnitudes. But in practice, compared to SBC, the operation of the MSBC scheme is no development when the coding rate R > 5/6. Moreover, the operation of OFDM structures can only be improved by MSBC under the lower coding rate when the structure magnitude is large.

2.11 Merged Selective Plotting and Binary Cyclic Codes

This approach of presenting an algorithm with focus on binary cyclic codes. The algorithm includes decomposing a binary cyclic code into a direct sum of two cyclic subcodes, a accurateion subcode for encoding

data bits and a scrambling subcode for encoding PAPR bits. The resulting code of OFDM orders is built by selecting a proper subcode from the direct sum of these two cyclic component codes.

2.12 Novel Low-Complication SLM Plans

Traditional SLM plans have a improved bandwidth efficiency, but needs a bank of inverse fast Fourier transforms (IFFTs) to make candidate signals, resulting in a dramatic increase in computational complication. To overcome this drawback, Wang and Ouyang presented a low-complication scheme by which the IFFTs were replaced by conversion vectors required by taking the IFFT of the phase rotation vectors. Unfortunately, for most of the conversion vectors demonstrated in the elements of the corresponding phase rotation vectors do not have the same magnitude, leading to operative degradation in bit error rate (BER) operation.

2.13 PTS and Error- Accurateing Code Subblocking

In the partial transmit order (PTS) approach, disjoint subblocks of OFDM subcarriers are phase shifted individually after the IFFT is calculated. If the subblocks are ideally phase shifted, they show a minimum PAPR and consequently reduce the PAPR of the merged signal. The number of sub blocks and their dividing scheme check out the PAPR reduction. The search for optimum subblock phase factors is computationally complex, but this can be reduced with adaptive PTS or sphere decoding. Normally, the receiver requires side data corresponding to the optimal phases in PTS and the reassign orders in SLM.

One of the major fault of PTS arises from the computation of numerous IFFTs, which result in a high complication proportional to the number of sub blocks. In an attempt to reduce this complication, intermediate signals within the IFFT using decimation in time (DIT) have been used to achieve the PTS sub blocks. The experimental results shows that the PAPR reduction decreases as the number of stages after PTS dividing decreases. Hence, to accomblish PAPR reduction close to that of genuine PTS (O-PTS), there should be a substantial number of stages in the IFFT after the splitting into PTS sub blocks. Hence, the computational complication is not operatively reduced. As a result, the key question is how to minify the complication while foremost taining a PAPR reduction close to that of O-PTS.

2.14 Partial Transmit techniques With Low Computational Complication

The big matter of finding the optimal phase combination for PTS order is composite and hard when the number of subcarriers and the order of modulation are enhanced. To reduce the computational complication, many extensions of PTS plans have been implemented recently, such as adaptive PTS approach. However, for all these searching methods, either the PAPR reduction is suboptimal or the complication is still more. As an example, iterative flipping algorithm has been demonstrated to lessen the PAPR with less complex and more easily implementation. Moreover, the combination of its phase factors is suboptimal. A novel solution is presented to reduce the complication while keeping the optimal combination of the phase factors to decrease the PAPR hugely. Specifically, we apply the simulated annealing (SA) to find the optimal combination of phase factors with highly less complication. Numerical results implies that the presented scheme can accomplish better PAPR reduction with lower computational complication when compared to that of the former approaches.

2.15 Joint Channel Estimation and PTS

A novel method, which merges the channel estimation and T-PTS method to minify the PAPR of OFDM signals, called as the CE-PTS method. Especially, a virtual channel frequency response is considered as the combination of the traditional channel frequency response and the phase rotation factors of the T-PTS method. Thus, the genuine OFDM signals could be instantly recovered via channel estimation in need of any knowledge

of the SI at the receiver. Hence, the structure does not need to hold extra bits to deposit and protect the phase rotation factors. A novel pilot arrangement also demonstrated, in which the pilot tones are alone inserted into each sub block to reach an accurate channel estimation.

2.16 Hexagonal Constellation method

A novel PAPR reduction method that is based on hexagonal constellation. By using a hexagonal constellation rather than quadrature amplitude modulation (QAM) constellation, it is possible to have more signal points in a given area and these extra degrees of freedom can be make use of for this PAPR reduction. The application of the hexagonal constellation to the tone injection method was demonstrated by the authors. In this paper, we use partial transmit order (PTS) method and selected plotting (SLM) method as applications of the presented hexagonal constellation data rate loss because of the side data in PTS method and SLM method by applying the presented method to them.

2.17 Low-Complication PTS-Based Radix FFT Method

A low complication IFFT based PAPR reduction method is presented. The analysis is based on the corresponding fast Fourier transform (FFT). PTS sub blocking is done in the middle stages of the -point radix FFT DIF or DIT algorithm. It is clear that DIT has a majority of its complex multiplication operations towards the end of the computation stages, and DIF has a majority towards the beginning. Thus, DIF has lower multiplicative complication in producing PTSs compared to DIT, and the same PAPR reduction. Moreover, it is shown that high radix algorithms succeed better PAPR reduction per stage in comparison with low radix algorithms, while providing lower multiplicative complication. Lastly, we present a low complication PTS scheme (decomposition PTS) which has a small number of transform computations compared and O-PTS, and mostly the same PAPR reduction as O-PTS. We divide the FFT stages into subsets of stages, and each subset uses a different number of PTS sub blocks.

2.18 Fountain Codes

High PAPR leads to the conorders that the OFDM receiver detection efficiency becomes very sensitive to the device nonlinearity in the signal processing loop, which may severely impair the communication structure operation. Properly, many PAPR reduction plans have been presented in the literature, among which, coding-based approaches are the most appealing.

A novel coding scheme is presented to control the PAPR of OFDM signals. Unlike all existing coding plans for PAPR reduction, the presented scheme deploys fountain codes to control PAPR at a desired level. Theoretical analysis, numerical examples, and simulation results show that the presented scheme could aquire superior operation in terms of PAPR and throughput, with random structure magnitudes and rateless codes.

Signal make a peak power, when they are attach with the same phase which is times the average power. Therefore, the good PAPR reduction can be acquire when some counts are taken to lessen the event prospect of the same phase of the signals, which is the main plan of the coding schemes.

An easy block coding scheme was established and its primary plan is that mapping 3 bits data into 4 bits codeword by adding an Simple Odd Parity Code (SOBC) at the least bit across the medium. The main drawback of SOBC method is that it can lessen PAPR for a 4-bit codeword. Later, the Cyclic Coding (CC) is applied to lessen the PAPR. An efficient Simple Block Code (SBC) is proposed to lessen the PAPR of OFDM signals. Later, Complement Block Coding (CBC) and Modified Complement Block Coding (MCBC) schemes were proposed to lessen the PAPR without the reduction of frame size. CBC and MCBC are more agreeable due to

their flexibility on choosing the coding rate, frame size and low implementation complexity. The comparisons are showed in table I and II.

Method	BER	SNR
Clipping	$10^{-0.6}$	33
Error companding	$10^{-0.54}$	19
Tone Reservation	$10^{-0.5}$	17.6
Optimal PTS	$10^{-0.43}$	17
Exponential companding	$10^{-0.41}$	17.2

Table I

N	n	R	PAPR reduction (dB)				
			CBC	SBC	MCBC	SOPC	CC
4	1	¾	3.56	3.56	-	3.56	3.56
8	1	7/8	2.59	2.52	-	2.52 (R=7/8)	3.66 R=(3/4)
	2	¾	2.67	3.72	2.81		
16	1	15/16	2.74	1.16	-	1.18 (R=15/16)	3.74 R=(3/4)
	2	7/8	2.74	2.52	-		
	3	13/16	2.74	-	-		
	4	3/4	2.74	2.98	3.46		

Table II

III. CONCLUSION

We proposed a novel BICM-OFDM method, to reduce the PAPR without side information in OFDM systems. Theoretical analysis and simulation results showed that the proposed method could achieve the PAPR reduction than the PTS and SLM methods. The BER performance of the proposed methods is also better than the existing methods with perfect side information in uncoded and coded OFDM systems over AWGN and fading channels, respectively.

In future our system can be extended to a relay assisted distributed BICM -OFDM system, and a complexity-reduced implementation method. This system can reduce the PAPR further more so that the efficiency of the system can be increased.

IV. ACKNOWLEDGEMENTS

This research was partially supported by the SEARCHiN project (FP6-042467, Marie Curie Actions). We would like to also thank Ala Hawash, Andreas Manoli, Anton Deik, Bilal Farraj, and Constantinos Savvides for their support and help in the implementation of Mash QL.

REFERENCES

[1] Y.Wu and W. Y. Zou, “Orthogonal frequency division multiplexing: A multi-carrier modulation scheme,” *IEEE Trans. Consumer Electronics*, vol. 41, no. 3, pp. 392–399, Aug. 1995.

[2] W. Y. Zou and Y. Wu, "COFDM: An overview," *IEEE Trans. Broadcasting*, vol. 41, no. 1, pp. 1–8, Mar. 1995.

[3] T. Jiang, W. Xiang, H. H. Chen, and Q. Ni, "Multicast broadcasting services support in OFDMA-based WiMAX systems," *IEEE Communications Magazine*, vol. 45, no. 8, pp. 78–86, Aug. 2007.

[4] S. Shepherd, J. Orriss, and S. Barton, "Asymptotic limits in peak envelope power reduction by redundant coding in orthogonal frequency-division multiplex modulation," *IEEE Trans. Communications*, vol. 46, no. 1, pp. 5–10, Jan. 1998.

[5] R. van Nee and A. deWild, "Reducing the peak to average power ratio of OFDM," in *Proceedings of the 48th IEEE Semiannual Vehicular Technology Conference*, May 1998, vol. 3, pp. 2072–2076.

[6] H. Ochiai and H. Imai, "On the distribution of the peak-to-average power ratio in OFDM signals," *IEEE Trans. Communications*, vol. 49, no. 2, pp. 282–289, Feb. 2001.

[7] N. Dinur and D. Wulich, "Peak-to-average power ratio in high-order OFDM," *IEEE Trans. Communications*, vol. 49, no. 6, pp. 1063–1072, Jun. 2001.

[8] S. Litsyn and G.Wunder, "Generalized bounds on the crest-Factor distribution of OFDM signals with applications to code design," *IEEE Trans. Information Theory*, vol. 52, no. 3, pp. 992–1006, Mar. 2006.

[9] S. Q. Wei, D. L. Goeckel, and P. E. Kelly, "A modem extreme value theory approach to calculating the distribution of the peak-to-average power ratio in OFDM Systems," in *IEEE International Conference on Communications*, Apr. 2002, vol. 3, pp. 1686–1690.

[10] T. Jiang, M. Guizani, H. Chen, W. Xiang, and Y. Wu, "Derivation of PAPR distribution for OFDM wireless systems based on extreme value theory," *IEEE Trans. Wireless Communications*, 2008.

REUSE OF INDUSTRIAL BUILT HERITAGE FOR RESIDENTIAL: CASE STUDY EX TABACO WAREHOUSE IN SHKOZET, DURRES, ALBANIA

Phd Candidate Arch. Boriana Vrusho (Golgota)

Department of Engineering Sciences, "Aleksander Moisiu" University, Durres, Albania

ABSTRACT

This paper was done as part of PhD studies from the author at Epoka University, Albania.
It is about Adaptive Reuse of ex-Industrial Buildings transformed for residential houses. As a case study was taken the ex-Tabaco warehouse transformed into two stores apartment building, located in Shkozet, Durres, Albania.
The analysis first starts by taking in consideration international close resemblance cases which will help in the comparison and conclusion phase. Research continues with a deep analysis of available project data of ex-Tabaco warehouse, such as construction documents, proceeds with the further direct site in observation and interviews. After the classification of problems, the questionnaire for the present inhabitants is developed and their evaluation of the design solution is taken.
The outcome of this paper is a set of guidelines which allows to avoid the common design problems and to provide better spatial and energy sufficient solutions.

Keywords: Adaptive Reuse, Spatial Analysis, Questionnaire.

I. INTRODUCTION

The process of industrialization in Albania started at the second half of XIX century, during the second Industrial Revolution. First industrial production activities were mostly domestic and handcraft activities like textile, brick and oil production. Manufacturing processes took place in citizen's houses. Later on, at the end of XIX century and the beginning of XX century, the industrialization process incurred a big change because of production of first motors. Because of the presence of foreign industrial companies in Albania, new processes and technologies were put to work. In this period the process of industrialization was accompanied by construction of new warehouses, for example food and textile industry; or many other fabrics for refinement processes. After the Second World War, many of the destroyed warehouses were reconstructed and reused for industrial purposes. They were also nationalized by the state, which now was represented by the communist regime. Through fifty years many industrial warehouses were built with the help of communist countries of that time[1]. In 1949 state factories were built with the help of ex-Yugoslavia, 1948-1959 with the help of ex BRSS and 1961-1978 with the help of RP China. Most of the time, these new industrial buildings imposed their presence for the city layout. Many new residential buildings were built near production areas to accommodate new workers, which were brought from all over the country.

1 Parangoni, I. (2010) Assessment of Industrial Heritage in Central Albania, p 11.

After the fall of communist regime, many industries were abandoned and forgotten for many years. Instead of being energizing points of production and economic profit, these site now represent urban and social problematic areas. They have lost identity and do not represent any more important values to be identified. As stated by Beccu, Calace, Martines, Menghini and Ruggiero (2014), …*with the abandonment of the old production cycles these structures, often very impressive and extensive, have quickly evolved from "engine" to the economic and social identity of the city, in actual tumor agents of urban, social and hygienic decay*[2].

Migration and emigration of Albanians was accompanied with huge problematic in housing field. Because of lack of apartments at the beginning of this transition period, many nun functional warehouses were adapted for residential use. Most of them were used for accommodation of ex workers if the respective industry. However, these was an awkward solution used because of the minimal spaces provided for the residents. Most of apartments were adapted in 1+1 areas, which do not fulfill life quality requirements of resident's.

After successive discussions with different stakeholders (inhabitants in these buildings, engineers, commercialists) about the possibilities of reconstruction and reuse of old industrial buildings, most of them think that these objects should remain for industrial purposes as for production and service industry or various warehouses. A considerable part think that they should be reused for commercial centers, social centers. A few on them think that they should be used as mixed use buildings like production lines, retail stores and administrative center. The smallest part of the people interviewed have expressed their opinion that old industrial buildings should be adapted and reconstructed for public building and living residences.

II. STUDY APPROACH AND METHODOLOGY

In this paper is studied the process of transformation of an old industrial building for residential houses by using adaptive reuse methodology. It is based on the transformation of an ex Tabaco warehouse adapted for residential use in 1995, which is located in Shkozet, Durres.

The most difficult part of this paper writing was finding theoretical analysis of reuse of industrial heritage in Albania. Most of reports have analyzed the history of construction of industrial buildings and recorded some of the remains of them. A few studies that take in consideration the reuse of ex industrial buildings but none of them have considered analysis of reuse of ex industrial buildings for residential purposes. This paper will be a good start in the academic research in the field of adaptive reuse of ex industrial buildings in Albania.

The aim of this paper is to evaluate the quality of reconstruction of ex industrial buildings into housing, by taking in consideration these parameters:

1. Spatial quality (location on urban plan, neighborhood development, apartment areas, number of inhabitants/area)
2. Construction quality (materials used)
3. Environment quality (temperature, light conditions, insulation, overheat, ventilation)

Research starts from the analysis of available project data, such as construction document, proceeds with the further direct site observation and interviewees. After formulation of the main spatial, construction and environmental quality problems, the questionnaire is developed in order to verify the theoretical proposals and

2 Beccu, M., Calace, F., Martines, G., Menghini, A., Ruggiero F. (2014) Industrial Heritage in Albania: Architecture and Landscape. A New Resource for Fier, p 2.

to receive the evaluation of the results of the common problems and possible transformation done at the reconstruction of ex-Tabaco warehouse.

The outcome of the paper is a set of design guidelines which allows to avoid the common problems and to provide better spatial and energy sufficient solutions from the analysis of adaptive reuse of ex industrial Tabaco building. Within the last part of the research are presented the evaluations of the design solutions by inhabitants, by identifying the common problems of the reconstruction of this building and the set of design criteria, which may help to avoid the poor design and construction solutions in future.

Qualitative data collection methodology used in this paper by desk research (documents, scientific periodic, articles, books, magazines that talk about adaptive reuse) to gather information on some over world case studies and to formulate the main strategies of the reconstruction of industrial building into housing. Based on the international experience the analysis of the construction project, documentation of the ex-Tabaco warehouse with the further observation and photography is done. Furthermore, inhabitant's questionnaires and interviews of engineers who have been part of the process of projecting this case study transformation will be part of this paper.

III. INTERNATIONAL CASES

Adaptive reuse of ex industrial buildings is a methodology used worldwide nowadays especially in countries which have inherited these buildings since the first industrial revolution. As Candell says, *adaptive reuse came into mainstream architectural parlance during the 1960s and 1970s due to the growing concern for the environment*[3]. Hence, it is a broadly discussed theme among architects, planners and politicians. During the 1980s and 90s many warehouses were converted into residential apartments, creating a dominate type of adaptive re-use that remodeled robust building fabric into individual dwellings[4]. Many of these old industrial sites have been registered as historic heritages. However, there are some ex industrial buildings, like the one taken as case study in this paper, which does not contain architectural or urban values but are part of memory of citizens and workers of those warehouses.

The terminology of adaptive reuse is being a trend of these decades because of the emergent need of reusing old industrial heritage. It is the process of changing the functionality of a building by taking in consideration reparation and preservation. As quoted by Kee, T (2014), adaptive reuse is "*the method of reusing old buildings for new purposes, instead of demolishing and rebuilding new buildings on the site*"[5]. According to Plevoets, B.; Van Cleempoel, K.This, it is "*the case for buildings that cannot be used anymore for the function they were initially designed for and which have to be adapted to a completely diferent function*"[6]. Adaptive reuse is also a tool to preserve the identity of a city and to conserve its cultural and historical heritage.

Following are illustrated some examples of international cases in which adaptive reuse have been used as a successful tool for adaptation of ex industrial buildings.

3 Cantell, S. F. (2005) The Adaptive Reuse of Historic Industrial Buildings: Regulation Barriers, Best Practices and Case Studies, p 3.

4 ODASA Design Guidance Note (2014) Adaptive re-use, p.2.

5 Kee, T. (2014) Adaptive Reuse of Industrial Buildings for Affordable Housing in Hong Kong, p. 3.

6 Plevoets, B.; Van Cleempoel, K. (March 2012) Adaptive Reuse as a strategy towards conservation of Cultural Heritage: a survey of 19th and 20th century theories, p 3.

Fig.1: Orient House (photo from Mengüşoğlu, N. & Boyacioğlu, E. (2013) Reuse of industrial built heritage for residential purposes in Manchester. METU JFA. 2013/1 (30:1) 126)

Fig.2: Middle WareHouse (photo from Mengüşoğlu, N. & Boyacioğlu, E. (2013) Reuse of industrial built heritage for residential purposes in Manchester. METU JFA. 2013/1 (30:1) 126)

Fig.3: Britania Mills (photo from Mengüşoğlu, N. & Boyacioğlu, E. (2013) Reuse of industrial built heritage for residential purposes in Manchester. METU JFA. 2013/1 (30:1) 128)

Fig.4: Albert Mill (photo from Mengüşoğlu, N. & Boyacioğlu, E. (2013) Reuse of industrial built heritage for residential purposes in Manchester. METU JFA. 2013/1 (30:1) 129)

Fig.5: Murray's Mill (photo from Mengüşoğlu, N. & Boyacioğlu, E. (2013) Reuse of industrial built heritage for residential purposes in Manchester. METU JFA. 2013/1 (30:1) 129-130)

Fig.6: Royal Mills (photo from Mengüşoğlu, N. & Boyacioğlu, E. (2013) Reuse of industrial built heritage for residential purposes in Manchester. METU JFA. 2013/1 (30:1) 131)

Fig.7: De Enk, a Dutch case (photo from Remoy H., Van Der Voordt, Th. (2014) Adaptive reuse of office buildings: opportunities and risks of conversion into housing. Building Research & Information 42:3, 381-390)

Fig.8: Twentec building, a Dutch case (photo from Remoy H., Van Der Voordt, Th. (2014) Adaptive reuse of office buildings: opportunities and risks of conversion into housing. Building Research & Information 42:3, 381-390)

Another international case that could be compared with this paper case study is the adaptation of former industrial buildings since 2005, in Durham USA, part of Tabaco manufacturing plant (fig 8). The interesting part is that most of tenants who move here are active in what is called "the creative economy"[7] as most of all are with higher education.

Fig.8: The new courtyard inside American Tabacco (photo from Legnér, M. (2007) Redevelopment through rehabilitation. The role of historic preservation in revitalizing deindustrialized cities: Lessons from the United States and Sweden, p 63.)

From the above literature Albanian specialists could adapt some methods on ways to reuse old industrial buildings and to find financial solutions for support. In Albanian case, most of the reused building examples from industrial to housing are from years 1995-1999. Nowadays industrial heritage is forgotten, although it's bad condition. As many of construction plot in the city are consumed, it is a starting point to consider as a good

7 Legnér, M. (2007) Redevelopment through rehabilitation. The role of historic preservation in revitalizing deindustrialized cities: Lessons from the United States and Sweden, p 63.

alternative to reuse old industrial buildings for housing. The difference between the above literature and Albanian cases, is that most of old industrial buildings are built away from city center. A few of them, only the one of light industry, are located near the city center. So it is very important to make an extensive analysis on how these buildings could be reused.

IV. CASE STUDY DESCRIPTION

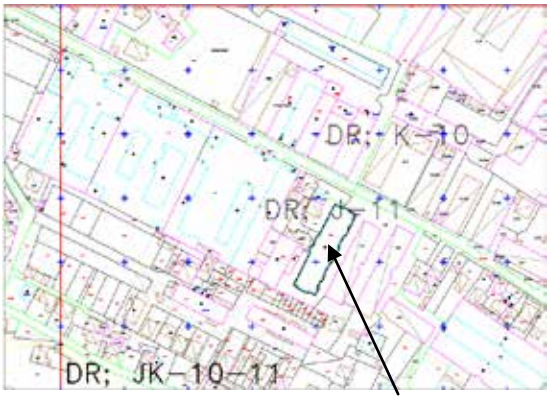

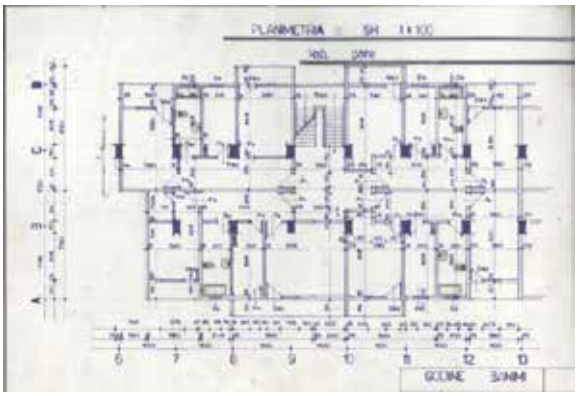

Fig. 9, 10: Site map and Plan of ex Tabaco warehouse reused for housing (Location in Shkozet, Durres)

Fig. 11: North-west façade of ex Tabaco warehouse

Fig. 12: South-east façade of ex Tabaco warehouse

This paper case study is a 3 stores high ex industrial building, built in the 1950, located in neighborhood nr.14 in Shkozet, Durres, Albania (Fig 9-12). It is approximately 2 km away from Durres City Center and 1.5km from the seashore. It has served for 45 years as industrial tobacco warehouse. Adaptive reuse of the building was made in 1995. The ex-Tabaco Enterprise Durres requested the adaption of building for housing requirements. New tenants were workers when it functioned as Tabaco warehouse.

Before 1990 this area was used for industrial purposes only. Today it is mixed use for industrial and residential. It is not a developed commercial area, it predominantly consists of industrial buildings, which are changing in daily basis from simple warehouses to small private production plants. Small shoe production lines, confection production, car service, cleaning solution production lines, etc. can be found in this area. Residential buildings are mainly low and with a maximum of 5 stores. Inhabited area coefficient is 30% and the remaining are warehouses and industrial buildings. Industrial buildings are also low consisting of 3 to 4 for stores or 21 meter high industrial plants.

The plan of the original object was organized with stairs in between and two warehouses on the edges. The structure of the object remained unchanged. Interventions primarily consist of floor reinforcement, divisor walls and sanitary areas construction, reconstruction and repairing of the ceiling. Isolation, stairs and granite works were entirely redone. Building was constructed by brick wall and precast floor called “SAP”. Floor reinforcement was made by adding 6cm of reinforced concrete. The apartments inside walls were made using 10

cm hollow bricks, whereas the in-between apartment walls are 20 cm. All wall plastering, internal and external, was redone using standard plaster and lime. The building was not plastered from the outside.

The object is 15.3m x 66.4m and covers an area of 1001 m^2. Building plan was organized in small living 1+1 apartments. To maximally utilize the area the apartments were placed along both sides of a long corridor. As a result the apartments were either east or west oriented. Apartment have an area of around 60 m^2. Building organization was perfectly optimized so that the common areas took only 6% of the construction. It has 12 apartments and around 95 inhabitants. Here is a summary table of nr of entrances, nr of apartments and inhabitants.

Building its oriented north-south in its length with a 25° incline to east. It has a considerable height at h=3.75m with abundant light openings. The windows used for reconstruction were single glass aluminum frame and not of a good quality, this because in the time the reconstruction occurred Albania did not have the possibility of using contemporary technologies.

From the interviews of the inhabitants are pointed the following problems. The apartments created are all 1+1, so they offer very small areas with no possible alternative changes. The environmental quality of the building is not satisfactory. Windows used were not were single glazed. The high height of the apartments, because of the existing building structure, makes it difficult to heat in winter. Energy preservation is very poor because of the low quality materials used (low insulation). Hereinafter will be explained concrete results from the questionnaires made to this building tenants.

V. QUESTIONNAIRE

The model of questionnaire attached to the appendix, in Albanian language, was done to the inhabitants of the ex-Tobacco Warehouse building. In total 22 persons were questioned which lived at ground floor and at first floor. In order to obtain inclusive information, careful selection of interviewees was done. Each apartment were given a number, so each questionnaire was done based on that number (Fig 13, 14). The questionnaire is composed by these parts: the head which introduces for which source these questionnaires will be used and the information about the nr of apartment and floor, the second part is composed by intro questions (age, education, employment status, family members), the third part is composed by info about spatial properties of their houses (bedrooms, dining + living, bathroom, storage), the fourth part is about environmental characteristics (heating, cooling, water warming) and the last about mainly problematic that they could evident and changes that they had done in order to improve living quality. After completing the questionnaires, the results were placed in a summary table. From this, graphics were designed to compare different important elements that could be pointed out from the questionnaires.

Fig. 13: Plan Of Ground Floor Of Case Study Building

Fig. 14: Plan Of First Floor Of Case Study Building

5.1 Spatial Properties

According to the inhabitants, they had done these spatial changes in their houses (fig 15): they have closed loggias which were used some as bedrooms and some as loggias but bordered with protective bars, they have changed interior walls to connect dining with living room, and they have added tents at the façade and new installations for conditioner or wood stove. Most common changes were closage of loggia (63%), use of tents and protective bars (86%).

Spatial changes about close of loggias to use as bedroom or wall changes to connect dining with living room, were made because of insufficient area according to nr of persons living in the apartment. Below is shown the graphic of spatial changes made by inhabitants. At the horizontal axis is showed total number of apartments which have done each of changes and also which one (Ap. nr). At the vertical axis is showed which changes are concretely done.

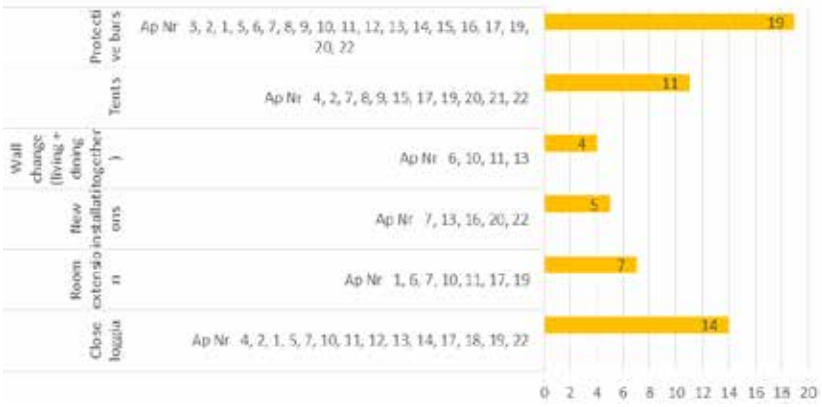

Fig. 15: Spatial changes

Spatial changes were made according to nr of persons/ap. For example, 5 % of interviewed said that they are 5 family members and they sleep 2-3 persons in bedroom and others in living room (Fig 16). 9 % of interviewed said that they are 3 family members and they sleep 2 persons in bedroom and other in living room. 59 % of interviewed said that they are 3-4 family members and they sleep 2 persons in bedroom and others in living room. 27 % of interviewed said that they are 4 family members and they sleep 2 persons in bedroom (they have two bedrooms).

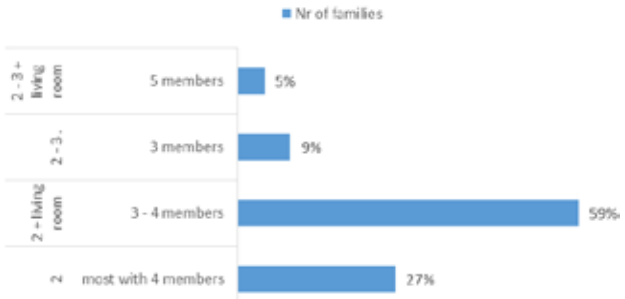

Fig. 16: Persons sleeping in bedroom vs. nr of family members

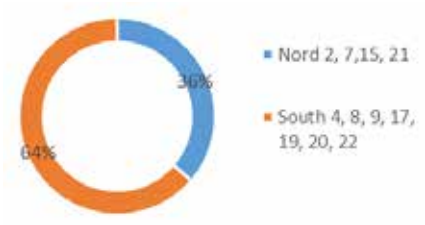

Fig. 17: Tent installation

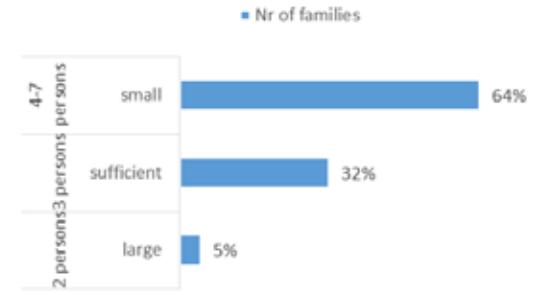

Fig. 18: How do inhabitants consider their house area

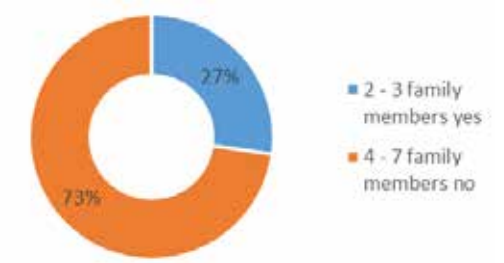

Fig. 19: Enough Storage and toilet area

As showed in fig 18, 67 % of the interviewed consider their apartment with insufficient area (families with 4-7 members), 32 % consider it sufficient (mostly with 3 family members) and only 5% think their house is large (2 family members). Furthermore, as showed in fig 19, 73 % of the interviewed think they don't have enough storage or bathroom area and only 27% think the opposite (2-3 family members).

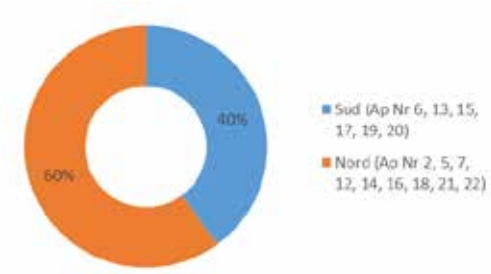

Fig. 20: Moisture

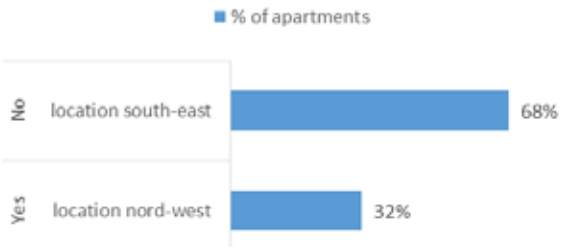

Fig. 21: Turn on light during day

Most of families which compalint for moisture (60 %) have their house oriented to nord and only 40 % to south. In graph nr 20, are also showed which apartment are located to nord and which to sud. Most of apartments which have use tent in façade (64 %), were oriented to south (fig 20) and they also complaint for direct sunlight, so they have used tents (fig 17). Most of them, 68 %, do not turn on lights during day at their living rooms, orientation south-east (fig 21). The others, located nord-west, do turn on light during day and they also complaint for insufficient light (Fig 27).

5.2 Environmental Properties

One of the most problematic environmental issue in this apartments are heating and cooling elements. Many of these families have low incomes, so most of them (10 families) used ventilators as a heating tool. The others, 5 families used wood stove, 4 families used conditioner and 3 families used gas stove in winter time (fig 22). At the vertical axis of the graph is also showed which families used each of equipment. As cooling tool during

summer, 18 families (81%) used ventilators and only 4 families used conditioner. At fig nr 23 is also showed which family numbers used each cooling equipment. Again, this is related to economical state.

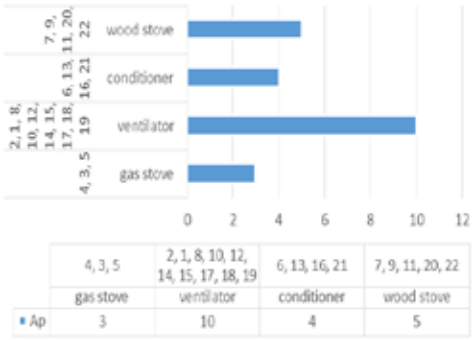

Fig. 22: Heating Tool

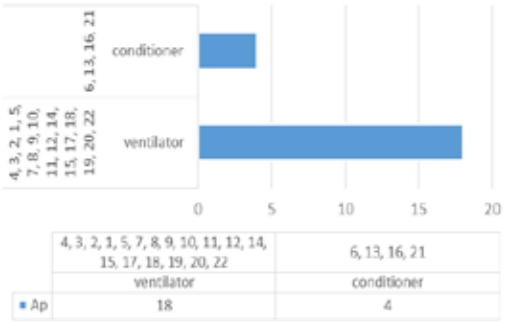

Fig. 23: Cooling Tool

As showed in fig 24, 12 interviewers (also are showed which apartment nr) said that they adjusted heating during winter in very cold days and 10 interviewers adjusted during all winter. Meanwhile, 12 interviewers said that they adjusted cooling during very hot days and only 8 interviewers during all summer (fig 25).

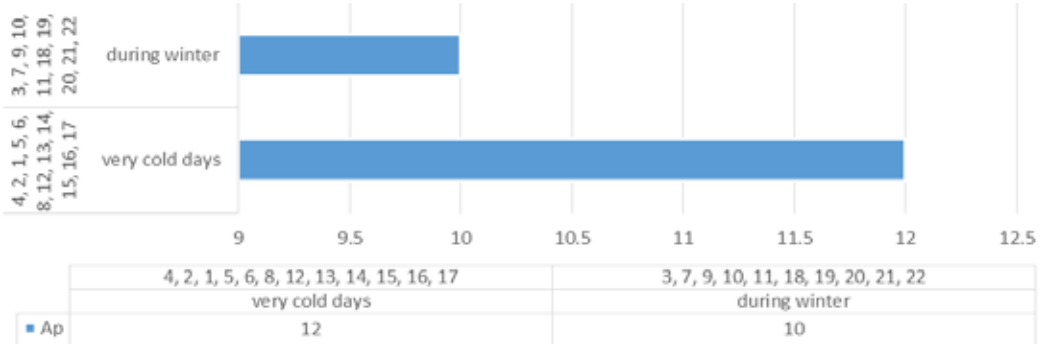

Fig. 24: Adjust heating

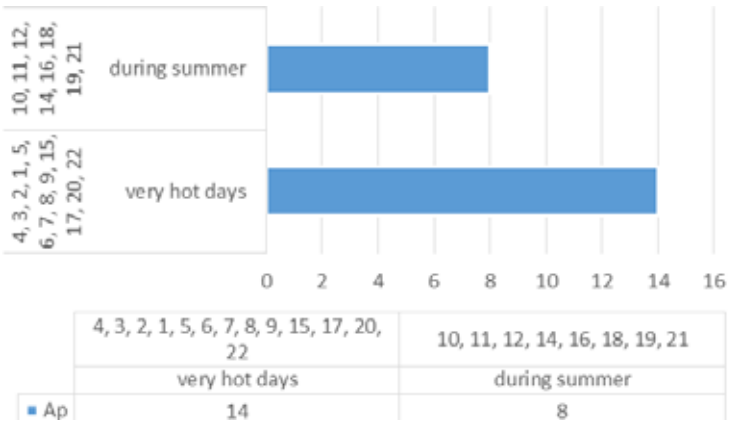

Fig. 25: Adjust cooling

5.3 Changes Made By Inhabitants

Results from questionnaires show that 100 % of families have added water deposits in building terrace, 86% have plastered their walls inside and outside, 50 % of them have added outside tents (most of them located in south-east), 45 % of them have changed their windows and only 9 % have added insulation to walls (Fig 26). Most of the families which did not changed original windows, complained more for indoor environment than the

others who did change them. Furthermore, building materials use a huge role in this case, because walls of ground floor were done all by complete bricks. At the first floor are used full bricks in building façade and bricks with holes during apartments division. This is why also, the apartments at the middle of the building complaint more of noise from neighbors than the others located at the perimeter (Fig 27). According to questionnaire results, 27 % of interviewed complaint for insufficient light (mostly apartment located at north), 64 % of the interviewed complaint for moisture (most of them located in first floor because of terrace leak), 45 % of them complaint for direct sunlight (most of them located in south-east) and 55 of them complaint for noise from neighbors.

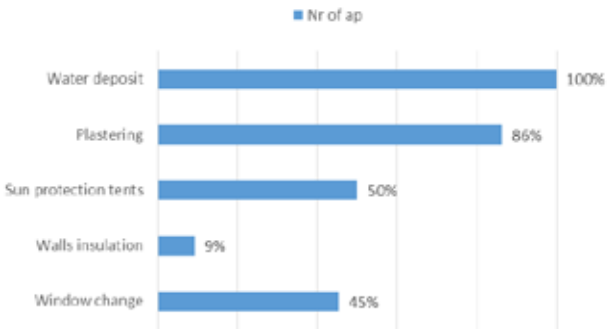

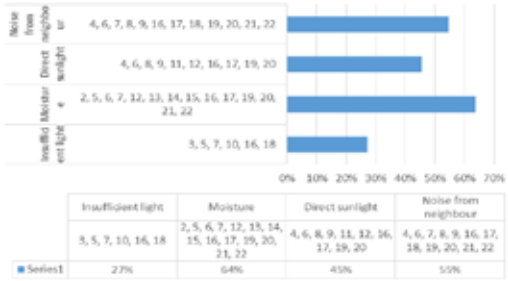

Fig. 26: Actions To Improve Indoor Environmental Quality Fig. 27: Indoor Environmental Problems

VI. CONCLUSIONS

Adaptive reuse is considered a very good strategy to be used in case of lack of construction sites. Most of Albanian ex industrial buildings are not located in the city center. This means that industrial sites can be used not only to regenerate abandoned areas, but also to create new sustainable neighborhoods. These objects can be reused for housing, commercial and leisure purposes. However, as many Albanian investors have expressed their intention to invest in industrial services, some of these ex industrial sites could be reused for light industry, production and service industry, or as various warehouses.

This process also needs the support of government. First of all, it is needed that the term “industrial archeology” should be added in law of monuments preservation. That it could be legally possible to change function from industrial to other uses. Municipalities can collaborate with local investors and other stakeholders to make real this transformation process in the most efficient and sustainable way possible.

Being driven by the results of the questionnaires done to the inhabitants of the ex-industrial Tabaco building, which was adapted as residential building, some important key points could be taken in consideration. Firstly it is important that adaptive reuse of ex industrial buildings should be done properly in terms of materials used, as they play crucial role in indoor environment. Most of reused buildings of this type were adapted in 1+1 apartments, which mostly offer not sufficient areas for inhabitants. Apartment changes, room extensions, loggia closed are consequences of spatial insufficiency. Hence, it is important to take in consideration apartment areas since the first stages of adaptive design projects.

At the end, my opinion is that adaptive reuse is a very good and efficient way to implement for ex industrial buildings. Albania have many industrial buildings, part of heritage of last century, which have not been used properly and are degrading day after day. Responsible adaptive procedures can be used for this buildings and ex industrial sites to regenerate dead brown fields in country.

BIBLIOGRAPHICAL NOTE

Ms. Boriana Vrusho (Golgota) is working as e lecturer at "Aleksander Moisiu" University Durres, Albania and is taking a PhD degree in Architecture at "Epoka" University, Tirana, Albania.

BIBLIOGRAPHY

[1] KEE, K. (June 2014) Adaptive Reuse of Industrial Buildings for Affordable Housing in Hong Kong, *Journal of Design and Built Environment*. [Online] Vol. 14(1). Availabe from: http://umrefjournal.um.edu.my/filebank/published_article/6443/Adaptive%20Reuse%20of%20Industrial%20Buildings%20for%20Affordable%20Housing%20in%20Hong%20Kong.pdf [Accessed 25/01/2015].

[2] Remøy, H. T. & Vander Voordt, D.J.M. (2014) Adaptive reuse of office buildings: opportunities and risks of conversion into housing. *Building Research & Information.* [Online] 42:3, 381-390. Availabe from: http://www.tandfonline.com/doi/abs/10.1080/09613218.2014.865922#.VMffCmjF8pU [Accessed 25/01/2015].

[3] Mengüşoğlu, N. & Boyacioğlu, E. (2013) Reuse of industrial built heritage for residential purposes in Manchester. *METU JFA.* [Online] 2013/1 (30:1) 117-138. Availabe from: http://jfa.arch.metu.edu.tr/archive/0258-5316/2013/cilt30/sayi_1/117-138.pdf [Accessed 26/01/2015].

[4] Cantell, S. F. (May 2005) The Adaptive Reuse of Historic Industrial Buildings: Regulation Barriers, Best Practices and Case Studies. Submitted in partial fulfillment of the requirement for the degree Master of Urban and Regional Planning *Virginia Polytechnic Institute and State University*. Availabe from: http://sig.urbanismosevilla.org/Sevilla.art/SevLab/r001US1_files/r001_US_1.pdf [Accessed 26/01/2015].

[5] Northcountry Cooperative Foundation and Jeff Allman, P.E., Principal, Allman & Associates (2006) Too Good to Throw Away: The Adaptive Reuse of Underused Buildings. *www.harriscompanyrec.com* [Online] Availabe from: http://www.harriscompanyrec.com/files/AdaptiveReuseFINAL_1_.pdf [Accessed 26/01/2015].

[6] Beccu, M., Calace, F., Martines, G., Menghini, A., Ruggiero F. (May 2014) Industrial Heritage in Albania: Architecture and Landscape. A New Resource for Fier. Submitted in 2nd ICAUD, Epoka University, Tirana, Albania [Online] Paper No. 211

[7] Parangoni, I. (2010) Assessment of Industrial Heritage in Central Albania, Report from the Albanian Heritage Foundation

[8] ODASA Design Guidance Note (July 2014) Adaptive re-use.

[9] Plevoets, B., and K. Van Cleempoel. (March 2012) Adaptive Reuse as a strategy towards conservation of Cultural Heritage: a survey of 19th and 20th century theories.

[10] Plevoets, B., and K. Van Cleempoel. (March 2012) Adaptive reuse within the retail design discipline: exploring the concept of authenticity. In First International Congress on Architectural Design, Teaching and Research, Bari, Italy, May 3-7, 2011.

[11] Legnér, M. (April 2007) Redevelopment through rehabilitation. The role of historic preservation in revitalizing deindustrialized cities: Lessons from the United States and Sweeden.

Appendix

Below is the model of the questionnaire used for this study.

EPOKA UNIVERSITY

FACULTY OF ARCHITECTURE AND ENGINEERING

DEPARTMENT OF PHD IN ARCHITECTURE

Questionnaire Nr____ Apartment Nr ____ Floor ____

1. **Gender**: **a.** Male **b.** Female
2. **Age: a.** Under 18 **b.** 18-24 **c.** 25-44 **d.** 45-65 **e.** Over 65
3. **Education: a.** No education **b.** 4 years **c.** 8-9 years **d.** High school **e.** University **f.** After University
4. **Employment status:**
   a. Employed **b.** Self-employed **c.** Student **d.** Pensioner **e.** Unemployed
5. **How many members are in your family? a**. Females__ **b.** Males __
6. **How do you consider your house area:**
   a. Small **c.** Sufficient area **b.** Large
7. **How do you use dining and living areas: a.** Separate__ **b.** Together __
8. **How many persons are usually sleeping in bedrooms?**
   a. One **b.** 1-2 __ **c.** 2 **d.** there is a sleeping place also in living room __
9. **How many bedrooms do you have in your apartment?**
10. **Is there enough storage in your apartment? a**. Yes__ **b.** No __
11. **Is there enough bathroom/toilet at your apartment**? **a**. Yes__ **b.** No __
12. **Which spatial changes did you made to your apartment**?
    a. Balcony __ **b.** Loggia__ **c.** Room extension__ **d.** New installations__ **e.** Wall demolishing or changing__ **f.** Tends__ **g.** Protective bars outside windows__ **h.** Other__
13. **What do you use for heating? _____**
14. **What do you use for cooling? _____**
15. **What do you use for water warming?**
16. **How often do you adjust heating during winter?**
17. **How often do you adjust cooling during summer?**
18. **Do you turn on lights during the day time in habitable rooms? a**. Yes__ **b.** No __
19. **Which actions were taken in order to improve indoor environmental quality?**

a. Changing the windows __ **b.** Insulation of walls__ **c.** Sun protection elements__ **d.** Plastering__ **e.** Other__

20. **What do you think are some indoor environmental problems at your house?**

a. Overheating __ **b.** Overcooling__ **c.** Insufficient light__ **d.** Moisture__ **e.** Direct sunlight__ **f.** Lack of natural ventilation__ **g.** Noise from street__ **h.** Noise from noighbours__ **i.** Other__

Thank you for your collaboration!

ENTREPRENEURSHIP AND BUSINESS INCUBATION PROGRAMME: THE SURE COUPLE

Nkem Okpa Obaji[1], Chikodi Onyemerela[2], Mercy Uche Olugu[3],

[1]Fakulti of Management, Universiti Teknologi Malaysia, Johor Baru, Malaysia

[2]British Council, Abuja, Nigeria

[3]Department of Statistics, Federal School of Statistics, Ibadan, Nigeria

ABSTRACT

This paper reviews the symbiotic relationship between entrepreneurship and business incubation programme. It is being suggested that for the development of entrepreneurship in any country, such business assistance programme like business incubators are the much needed business model to achieve it. The incubation development theory implies the offering of shared facilities such as working spaces, offices, hands-on organization support, and contact to financing, networking and publicity to important business and technical assistance that improve the achievement of ventures throughout incubation phase. The outcome of this symbiotic relationship between entrepreneurship and business incubation is economic development which is brought about by SMEs development, job creation as well as competitiveness of existing firms.

Keywords*: *Business incubation, Economic Development, Entrepreneurship, SMEs

I. INTRODUCTION

Generally speaking, an incubator is a mechanism in which babies who are born prematurely are kept warm and safe under controlled environment. In the same vein business incubation is a programme targeted at keeping young entrepreneurial firms warm and safe through an array of support services, until they are strong and sufficiently matured to move out of the incubator and flourish on their own. The key drive for a business incubation programme according to [1] is to encourage entrepreneurship.

The birthplace of business incubator was Batavia, New York in the United States in 1959 [2, 3]. Other countries universally have similarly accepted and adopted the policy tool specifically for economic development.

The rationale for this study is grounded on the premise that entrepreneurship development has not been really studied alongside with business incubation. Several studies on entrepreneurship have been concentrated on general entrepreneurship as well as business incubator studied separately. On the contrary, this study differs from past studies for the reason that in spite of the fact that research on business incubation especially in success factors or performance [4-7] the dearth of literature on the relationship between business incubation practice and entrepreneurship still exists.

This research aims to have a better understanding pertaining to entrepreneurship – business incubation process relationship in a broader context of developing countries. The paper is structured as follows: Section 2 provides the review of the literature related to entrepreneurship as well as business incubation, section 3 takes on the conclusion

II. LITERATURE REVIEW

As the SMEs are seen as engines and bedrock of the industrial and economic development and growth in many dynamic economies, government of various evolving nations have been performing a vital function in outlining strategies and agenda which sustain the enhancement of entrepreneurs from grassroots to medium enterprises, business incubation programmes are recognized by various national governments as the particular mechanism used to achieve such SMEs outcomes as incubators have been observed to fostering the enhancement of the entrepreneur way of life as well as performing as a mechanism intended for the growth of incorporated firm support arrangement which comprise along with others, institutions of higher education, entrepreneurial business, professionals and government bodies.

2.1 Entrepreneurship

SMEs have been recognized as critical in the economic and social development of most countries. They serve as a crucial element of technology dynamics of modern economies because of their flexibility and vicinity to clients [8]. They argued that despite their roles as agent of economic development, this group of entrepreneurs is most vulnerable, their vulnerability stems from their limitation to access basic factors of production, access to finance remains a dominant constraint, however, other very important constraints abound which militate against effective operations of small scale entrepreneurs, these include: lack of access to appropriate technology; this they also cited as having difficulty to get machines, spare parts, and raw materials [8]. Ayodeji and Balcioglu [9], also added that SMEs offer the preparatory environment for the growth and expansion of home-grown entrepreneurs.

Furthermore, SMEs help in the distribution of financially viable performance through promoting the expansion and transformation of these activities exterior to the main community neighbourhood. Much has been written in support of the importance attached to entrepreneurship and SME development [10-13]. On the contrary, [14] opposed the continued funding of start-ups of innovative businesses with marginal growth, rather attention should be given to businesses with high growth prospect. His divergent view relates to how entrepreneurial policies direct people to initiate negligible enterprises that are unlikely to be successful or have slight economic effect as well as creating minor employment. Furthermore, Musa and Danjuma [8] argue that increase in employment creation of SMEs is not continually associated with enhancement in productivity. Notwithstanding both arguments about the impact of SME on employment and job creation, the key function performed by these business enterprises cannot be ignored as SMEs have advantages above their larger scale rivals [8]

2.2 Business Incubation

Generally speaking, an incubator is a mechanism in which babies who are born prematurely are kept warm and safe under controlled environment. In the same vein business incubation is a programme targeted at keeping young entrepreneurial firms warm and safe through an array of support services, until they are strong and sufficiently matured to move out of the incubator and flourish on their own. Business incubator was first set up in the United States in 1959 in Batavia, New York [2, 3].

Technology business incubation is a trendy economic development instrument implemented in several parts of the globe to alleviate the altering situation and a range of industrial competitiveness caused by the effects of globalization. It encourages improvement and private enterprise way of life following the appearance of

innovative technologies and arrangements that improve country's stride towards industrialization. Business incubation is widely being used as an instrument for encouraging entrepreneurs and helping start-ups. Business incubators care for young companies especially when they are still prone to early start-up problems. They generally aid newly formed, innovative business, related to technical setting [15]. Several models of incubator as well as various arrangement alongside with levels of facilities they do according to the prerogative of those who funded and established it.

2.3 Entrepreneurship And Business Incubator: The Sure Couple

As SMEs are seen as engine and bedrock of the industrial and economic development and growth in many dynamic economies, government of various evolving nations have been performing a vital function in outlining strategies and agenda which sustain the enhancement of entrepreneurs from grassroots to medium enterprises [16].

Business incubation programmes are recognized by various national governments as the particular mechanism used to achieve such SMEs outcomes as incubators have been observed to fostering the enhancement of the entrepreneur way of life as well as performing as a mechanism intended for the growth of incorporated firm support arrangement which comprise along with others, institutions of higher education, entrepreneurial business, professionals and government bodies. Entrepreneurship and business incubator therefore act together as Siamese twins. The essence of establishing incubator centres is to assist entrepreneurs who are specially called the tenants or incubatees and are housed by the incubator, therefore the Small and Medium Enterprises (SMEs) and the incubators have a linear relationship.

It has been suggested in entrepreneurship literature that the essence of business incubator is to act as a stopgap that entrepreneur's lack. Such expediencies include both tangible and intangible resources. The lack of these resources have been the bane of entrepreneurs for entrepreneurial attainment. In line with this, Iwuagwu [17] noted that in the incubation centres, potential start-up firms would be fortified with business supports and programmes targeted at fostering them from scratch to adulthood.

Basically, business incubators contribute immensely to employment and wealth creation [15] in its environment. Anderson and Hanadi [18], state that international models of business incubation have proven to be a significantly useful element in economic advancement and job creation, innovation, technology transfer as well as diversification from the community economic system. Therefore business incubation system may probably be a good innovative scheme in bringing economic development at both local and global levels.

In a comparative study of incubator landscape in Europe and the Middle East conducted by Hanadi and Busler [19], the findings suggest that the major aim of incubator is economic development. This assertion is also consistent with several other authors [20-24]. Incubators have been assessed in relation to their influence on economic development particularly on employment formation, attainment of entrepreneurial company, job increment as well as sales [25].

2.4 Economic Development

Economic development has been defined by Al-Mubaraki and Busler [26] as the method of creating wealth by the gathering of human, financial, capital, physical and natural resources to produce marketable goods and services. Chandra [27], stated that many nations employ business incubators as a mechanism for economic

development. She emphasized that at large-scale level, incubators seek to encourage employment formation as well as economic development by connecting expertise, knowledge, resources, and technology in a valuable model to promote the development of innovative venture. She added that at the company level the incubator presents a value added assistance scheme for influencing capitalist organization.

Business incubators make a very important contribution to the economic development of the different tiers of government [28]. On the other hand, they contended that business incubator cannot transform an economy but instead have to be incorporated into a broader change of economic strategy, investing on infrastructure as well as funding. Incubator support from government is one of the attributes of majority of developing countries context of incubation programme; therefore the for-profit concept is foreclosed [29] and widely employed for economic development. As business incubators offer an array of future economic development advantages [28], their actual impacts on economic development have largely been examined by such simple quantifiable measures as number of job creation, level of company graduation and taxes received [30].

Nearly most of the countries of the world utilized Business incubators as an instrument for economic development. It generally offers a safe protection for the improvement of early stage business [31]. The safe haven provision by incubator is attained by an admixture of both physical and intangible services which include the provision of physical space as well as shared services together with administrative assistance, consulting, training/coaching/networking and access to funding [31]. The basic goals of business incubators are employment generation, revitalization, economic development, assistance to specific target clusters or businesses and companies' establishment [32]. Majority of the contemporary scholarly works on business incubation tackles economic development strategy and the use of business incubation services to encourage long term level of success while earlier studies considered business incubation as an economic development instrument [33]. The scholarly works of Campbell, 1989; Campbell et al. 1988 - for economic development can be corroborated by comparing these two-phased studies. And for economic development strategy, see the works of Al-Mubaraki [34]; Al-Mubaraki, Al-Karaghouli [28]. Prior studies were just focused on the usage of business incubation to improve economic development but contemporary scholars are likewise concerned not only as a tool for economic development but also as a policy for economic attainment of a country.

When an incubation initiative is implemented from the foreign countries to the developing countries, there is need for localized adaptation of the programme in order to suit the country's cultural milieu as well as other technological and infrastructural settings. When the incubation programme is well adapted to suit the needs of the local community, the extent to which the incubation programme will succeed will be high. And successful incubation programme will lead to economic development by increasing the number of SMEs, job creation, wealth creation as well as improving the competitiveness of existing businesses. Earlier researcher Markley and McNamara [25], had noted that incubators can cause an affirmative influence on the local economy through innovative business projects attainment level growth.

When there are many SMEs in the locality, there is the tendency for many people to be employed by these firms that have been standing on their own as a result of incubator assistance. When there is employment generation as well as increase in the number of entrepreneurs or SMEs, economic development or growth always takes place. Al-Mubaraki, Al-Karaghouli [28] declared that economic development is one of the objectives that drive each incubator. The other objectives according to them are technology transfer, innovation and cost-effective sustainable enterprise. In the same vein, earlier researchers [35-39] before [28] had postulated that incubation programme contribute to generation of new and also sustainable employment, business development

acceleration, acceleration of enterprises' expansion, reduction in the rate of failure of new enterprise, empowerment opportunities for specific groups of entrepreneurs and developing a role model for an entrepreneurial culture.

III. CONCLUSION

This paper has shown that, the quest for rapid entrepreneurship development in order to expedite economic development has remained pivotal to government administrations globally, particularly the developing countries. This is demonstrated by the diversity of support structures put in place by several countries governments. This is coming on the heels that entrepreneurship development play a very vital role to a nation's economic development. Entrepreneurs can play a catalytic role in social and economic development of country. They faced many obstacles particularly in funding and infrastructure. Business incubation is playing a vital role in the success of entrepreneurship development, particularly the early start-ups.

IV. ACKNOWLEDGEMENTS

Authors thank Ringa Kaingu Ringa for his constructive comments and suggestions. All errors are ours**.**

REFERENCES

[1] M. P. Rice and J. B. Matthews, *Growing New Ventures, Creating New Jobs: Principles and Practices of Successful Business Incubation*. 1995, Westport, CT: Quorum Books.

[2] S. M. Hackett and D. M. Dilts, *A systematic review of business incubation research.* The Journal of Technology Transfer, 2004. **29**(1): p. 55-82.

[3] D. A. Lewis, *Does Technology Incubation Work?: A Critical Review*. 2001: Economic Development Administration, US Department of Commerce.

[4] S. S. Lee and J. S. Osteryoung, *A Comparison of Critical Success Factors for Effective Operations of University Business Incubators in the United States and Korea*. Journal of Small Business Management, 2004. **42**(4): p. 418-26.

[5] R. W. Smilor, *Managing the incubator system: critical success factors to accelerate new company development.* Engineering Management, IEEE Transactions on, 1987(3): p. 146-155.

[6] H. Sun, W. Ni, and J. Leung, *Critical Success Factors for Technological Incubation: Case Study of Hong Kong Science and Technology Parks.* International Journal of Management, 2007. **24**(2).

[7] K. S. Kumar and D. S. R. Ravindran, *A Study on Elements of Key Success Factors Determining the Performance of Incubators.* European Journal of Social Sciences, 2012. **28**(1): p. 13-23.

[8] Y. W. Musa and D. Danjuma, *Small and medium scale enterprises: A veritable tool for sustainable job creation in Nigeria*. Journal of Business and Public policy, 2007. **1**(4): p. 1-25.

[9] A. R. Ayodeji and H. Balcioglu, *Financing Industrial Development In Nigeria: A Case Study Of The Small And Medium Enterprises In Kwara State.* Global Journal of Management And Business Research, 2010. **10**(3).

[10] Y. A. Gangi and E. Timan, *An empirical investigation of entrepreneurial environment in Sudan.* World Journal of Entrepreneurship, Management and Sustainable Development, 2013. **9**(2/3): p. 168-177.

[11] K. K. C. Deepthi and K. L. Latha, *Growth of Small Scale Entrepreneurship: A Case Study of Nellore District.* International Journal of Economics and Management, 2012. **6**(1): p. 98-114.

[12] C. Mason and R. Brown. *Entrepreneurial ecosystems and growth oriented entrepreneurship*. in *background paper for the International Workshop on Entrepreneurial Ecosystems and Growth Oriented Entrepreneurship*. 2013.

[13] V. Sriram and T. Mersha, *Stimulating entrepreneurship in Africa.* World Journal of Entrepreneurship, Management and Sustainable Development, 2010. **6**(4): p. 257-272.

[14] S. Shane, *Why encouraging more people to become entrepreneurs is bad public policy.* Small business economics, 2009. **33**(2): p. 141-149.

[15] M. Stefanović, G. Devedžić, and M. Eric, *Incubators in Developing Countries: Development Perspectives.* 2008.

[16] E. O. Oni and A. Daniya, *Development of small and medium scale enterprises: The role of government and other financial institutions.* Arabian Journal of Business and Management Review (OMAN Chapter) 2012. **1**.

[17] O. Iwuagwu, *The Cluster Concept: Will Nigeria's New Industrial Development Strategy Jumpstart the Country's Industrial Takeoff.* Afro Asian Journal of Social Sciences, 2011. **2**(2.4).

[18] B. B. Anderson and A. M. Hanadi, *The Gateway Innovation Center: exploring key elements of developing a business incubator*. World Journal of Entrepreneurship, Management and Sustainable Development, 2012. **8**(4): p. 208-216.

[19] A.-M. Hanadi and M. Busler, *A Comparative Study of Incubators' Landscapes in Europe and the Middle East.* European Journal of Business and Management, 2012. **4**(10): p. 1-10.

[20] A. Thierstein and B. Willhelm, *Incubator, technology, and innovation centres in Switzerland: features and policy implications.* Entrepreneurship & Regional Development, 2001. **13**(4): p. 315-331.

[21] S. Roper, *Israel's technology incubators: Repeatable success or costly failure?* Regional studies, 1999. **33**(2): p. 175-180.

[22] S. A. Mian, *Assessing and managing the university technology business incubator: An integrative framework.* Journal of Business Venturing, 1997. **12**(4): p. 251-285.

[23] H. Qian, K. E. Haynes, and J. D. Riggle, *Incubation push or business pull? Investigating the geography of US business incubators.* Economic Development Quarterly, 2011. **25**(1): p. 79-90.

[24] D. N. Allen and V. Levine, *Nurturing advanced technology enterprises: Emerging issues in state and local economic development policy*. 1986: Praeger New York.

[25] D. M. Markley and K. T. McNamara, *A business incubator: operating environment and measurement of economic and fiscal impacts.* Center for Rural Development, 1994.

[26] H. M. Al-Mubaraki and M. Busler, *Business Incubation as an Economic Development Strategy: A Literature Review.* International Journal of Management, 2013. **30**(1): p. 362-372.

[27] A. Chandra, *Approaches to business incubation: a comparative study of the United States, China and Brazil.* Networks Financial Institute Working Paper, 2007(2007-WP): p. 29.

[28] H. Al-Mubaraki, W. Al-Karaghouli, and M. Busler. *The Creation of Business Incubators in Supporting Economic Developments*. in *European, Mediterranean & Middle Eastern Conference on Information Systems 2010 (EMCIS2010)*. 2010.

[29] I. Akcomak, *Incubators as Tools for Entrepreneurship Promotion in Developing Countries*. 2009, World Institute for Development Economics Research.

[30] M. S. Lourenco, *Understanding Communication Network Development and Business Incubation: An Analysis of Three Incubators in Louisville, Kentucky.* University of Illinois at Urbana-Champaign's Academy for Entrepreneurial Leadership Historical Research Reference in Entrepreneurship, 2004.

[31] H. Al-Mubaraki and M. Busler, *Sustainable development through the inclusion of incubator: A SWOT analysis.* World Sustainable Development Outlook, 2010: p. 51-63.

[32] H. M. Al-Mubaraki and M. Busler, *Business Incubators Findings from a Worldwide Survey, and Guidance for the GCC States.* Global Business Review, 2010. **11**(1): p. 1-20.

[33] H. M. Al-Mubaraki and M. Busler, *Business incubators models of the USA and UK: A SWOT analysis.* World Journal of Entrepreneurship, Management and Sustainable Development, 2010. **6**(4): p. 335-354.

[34] H. Al-Mubaraki, *Procurement of international business incubation–Quantitative and Qualitative approaches.* Melrose Books, 2008.

[35] R. Lalkaka, *Assessing the performance and sustainability of technology business incubators.* International Centre for Science & High Technology, Trieste, Italy, 2000: p. 4-6.

[36] R. Lalkaka, *Technology business incubators to help build an innovation-based economy.* Journal of Change Management, 2002. **3**(2): p. 167-176.

[37] R. Lalkaka, *Lessons from international experience for the promotion of business incubation systems in emerging economies*. 1997: UNIDO, Small and Medium Industries Branch.

[38] R. Lalkaka, *Supporting the start and growth of new enterprises.* New York: United Nations Development Programme, 1997.

[39] L. DiCarlo, *Incubators on line support*. 2010.

BIOGRAPHICAL NOTES

N. O. Obaji just rounding off with his Ph.D. in Management Faculty (Specialization in Entrepreneurship) from Universiti Teknologi Malaysia (UTM), Skudai, Johor Baru, Malaysia

Mr. Chikodi Onyemerela is working as a Senior Manager in charge of business development, British Council, Abuja, Nigeria.

Mrs. M. U. Olugu is working as a Senior lecturer in Statistics Department, Federal School of Statistics, Ibadan, Nigeria.

A NOVEL TECHNIQUE BASED ON SELECTIVE MAPPING AND ITERATIVE FLIPPING PARTIAL TRANSMIT SEQUENCE ALGORITHM FOR PAPR REDUCTION IN OFDM SYSTEM

Shilpa Jaswal[1], Gaurav Jaswal [2]

[1]*Electronics and Communication Engineering, Department Career Point University, Hamirpur, H.P, (India)*

[2] *PhD Scholar, Electrical engineering Department, National Institute of Technology, Hamirpur, H.P, (India)*

ABSTRACT

The most serious issue of orthogonal frequency division multiplexing is high peak to average power ratio (PAPR). In this paper we proposed a new PAPR reduction technique that is developed by using new phase sequence selective mapping technique and Iterative flipping PAPR reduction technique for different numbers of sub blocks. This new technique (proposed technique) shows better PAPR reduction in comparison to new phase sequence SLM and iterative flipping partial sequence.

Key Words: Complementary Cumulative Distribution Function (CCDF), Orthogonal Frequency Division Multiplexing (OFDM), Partial Transmit Sequence (PTS), Peak To Average Power Ratio (PAPR), Selective Mapping Technique (SLM).

I INTRODUCTION

Now a day's OFDM become very attractive and promising technology for high rate wireless communication system. The first OFDM scheme is introduced by Chang in 1966 [1] for dispersive fading channels. OFDM was selected as high performance local area network's (HIPERLAN) transmission technique and it become the part of IEEE 802.11a wireless local area (WLAN) standard.

OFDM is a multicarrier modulation technique which provides high spectral efficiency, multipath delay spread and confrontation to frequency selective fading channels [2,3]. Despite of these advantages OFDM system has many drawbacks like high peak to average power ratio, co-channel interference in cellular OFDM and it is very sensitive to both time and frequency synchronization errors. One of the challenging issues in OFDM is high peak to average power ratio. Peak to average power ratio is proportional to the number of subcarriers. As subcarriers are add up coherently, large number of subcarriers cause high peak to average power. High PAPR also makes the implementation of analog to digital converter (A/D) and digital to analog converter (D/A) very complex. High PAPR also reduce the efficiency of RF amplifier. The high PAPR increase the in-band distortion and out-of-band distortion when the OFDM signal is fed into a nonlinear high power amplifier. In order to

reduce the distortion caused by a high power amplifier, several techniques have been introduced in literature that limits the peak of the envelope of the signal [3]. These techniques are referred as peak-to-average power ratio (PAPR) reduction techniques [4]. Mainly PAPR reduction techniques divided into two classes, Signal Scrambling and Signal Distortion Techniques. Signal scrambling techniques are all variations on how to scramble the codes to decrease the PAPR. Some signal scrambling techniques are selective mapping, partial transmit sequences, iterative flipping partial sequence transmit, interleaving, tone injection and tone reservation. The signal distortion techniques like peak windowing, clipping, companding etc. introduce both in-band and out-of-band interference and complexity to the system. These techniques reduce high peaks by distorting the signal prior to amplification directly.

The main objective of this paper is to design a new algorithm that will reduce PAPR of the OFDM system. In this paper, we propose a new PAPR reduction technique that is combination two existing techniques. First technique is SLM technique having new phase sequence generated by Riemann Matrix and second technique is iterative flipping. However, this technique is compared with conventional SLM technique, partial sequence transmit (PTS) technique, iterative flipping and original (without PAPR reduction).

The organization of this paper is as follow. Section 2 presents conventional SLM technique. Section 3 presents Riemann matrix based new phase sequence SLM technique. In. Section 4 presents iterative flipping technique. Section 5 &6 presents proposed technique and their simulation results. Section 7 draws conclusion and future scope.

II SELECTIVE MAPPING TECHNIQUE

The SLM technique was first introduced by Bauml.et.al.In the SLM, the input data sequences are multiplied by each of the phase sequences to generate alternative input symbol sequences [5]. IFFT operation is made on each of these alternative input data sequences. The signal having lowest PAPR is selected from a set of sufficiently different signals which all represents the same information. To allow the receiver to recover the original data, the multiplying sequence can be sent as side information [6].This technique is very flexible as it does not inflict any restriction on modulation applied or on number of sub-carrier [12].

III RIEMANN MATRIX BASED NEW PHASE SEQUENCE SLM TECHNIQUE

Selected Mapping technique is one of the promising PAPR reduction techniques for Orthogonal Frequency Division Multiplexing [10]. But this reduction technique results in a huge amount of computation complexity which is costly and time consuming. In SLM technique selecting of proper phase sequence is very important. Phase sequence set was chosen randomly from set[±1,±j] by Bauml, who first introduced SLM technique. In 2009, N. V.Irukulapati, V. K.Chakka and A. Jain projected a new technique for PAPR reduction using Riemann Matrix. This method is called SLM based new phase sequence technique [7,8].In this approach, rows of normalized Riemann matrix are used as phase rotation vectors. The Riemann matrix [9] is obtained by removing the first row and first column of the matrix A, where

$$A(i, j) = \begin{cases} i - 1 if, i - divides - j \\ -1, otherwise \end{cases}$$

(1)

Using Equation (1), Riemann Matrix (R) of order 4 can be written as:

$$R = \begin{bmatrix} 1 & -1 & 1 & -1 \\ -1 & 2 & -1 & -1 \\ -1 & -1 & 3 & -1 \\ -1 & -1 & -1 & 4 \end{bmatrix} \quad (2)$$

This technique is to make optimum use of the amplifier and to reduce the computation complexity of the selection of the data block. A threshold value of PAPR is decided based on the RF Power amplifier (PA) with a certain constant clipping threshold (not adaptive biased).If the Riemann matrix (R) is of size M * M, the entries in the normalized Riemann matrix (B) will be (1/M) R. In this technique the rows of the normalized Riemann matrix B is used as a phase sequence for SLM technique.

IV ITERATIVE FLIPPING PTS

Cimini and Sollenberger's Iterative flipping technique is developed as a sub-optimal technique for the PTS algorithm [11]. In PTS technique, to find the optimum set of phase factor, we need to evaluate all the combinations of phase factors. Due to this search complexity is increased. Thus a new simplified technique called iterative flipping algorithm has been introduced in which the computation complexity reduces to be linear with the number of sub-blocks M. In the iterative flipping algorithm, one keeps only one phase set in each sub-block. Even though the phase set chosen in the first sub block shows minimum PAPR in the first sub block that is not necessarily minimum if we allow it to change until we continue the procedure up to the end sub block [12,13].

For simplicity, the phase factor here is chosen as [1,-1]. These can be expanded to more phase factors. The algorithm is as follows. After dividing the data block into M disjoint sub blocks, one assumes that $b^{(m)}$= 1; (m = 1, 2…M) for all of sub-blocks and calculates PAPR of the OFDM signal. Then one changes the sign of the first sub-block phase factor from 1 to -1 ($b^{(1)}$= -1), and calculates the PAPR of the signal again. If the PAPR of the previously calculated signal is larger than that of the current signal, keep $b^{(m)}$= -1. Otherwise, revert to the previous phase factor, b^{m}= 1. Suppose one chooses b^{m}= -1. Then the first phase factor is decided, and thus kept fixed for the remaining part of the algorithm. Next, we follow the same procedure for the second sub-block. Since one assumed all of the phase factors were 1, in the second sub-block, one also changes $b^{(2)}$ = 1 to $b^{(2)}$ = -1, and calculates the PAPR of the OFDM signal. If the PAPR of the previously calculated signal is larger than that of the current signal, keep $b^{(2)}$ = -1. Otherwise, revert to the previous phase factor, $b^{(2)}$ = 1. This means the procedure with the second sub-block is the same as that with the first sub-block. One continues performing this procedure iteratively until one reaches the end of sub-blocks (M^{th}subblock and phase factor$b^{(m)}$) [12].

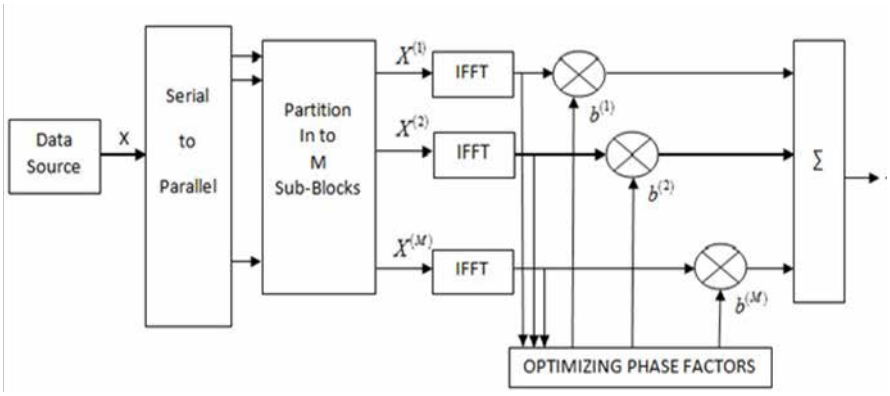

Figure: 2. Block diagram of partial transmit sequence technique

V PROPOSED TECHNIQUE

The novel technique (Proposed Technique2) is also based on new phase sequence SLM and Iterative flipping technique. In Proposed technique2 the rows of the normalized Riemann matrix are used as phase sequence set for PAPR reduction Here, in Proposed2, first SLM technique using rows of normalized Riemann matrix as a phase sequence set is applied to select the best combination of phase and input data which gives the minimum PAPR. After selecting the best combination of phase sequence and input data, apply this combination to the iterative flipping PTS technique using columns of normalized Riemann matrix as a phase sequence set for further reduction of PAPR.

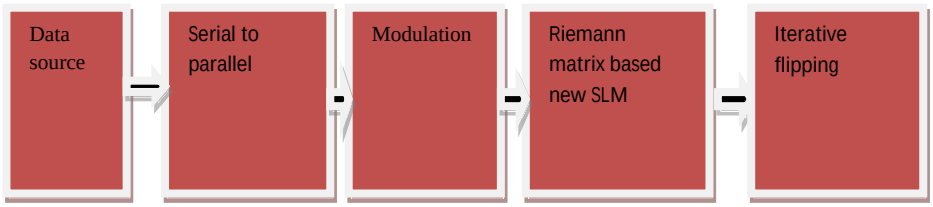

Figure 3: Block Diagram of Proposed Technique 2

The algorithm for this technique is described in following steps:

1: Sequences of data bits are mapped to constellation points M-QAM or BPSK to produce sequence symbols X_o, X_1,X_2…….

2: These symbol sequences are divided into blocks of length N. N is the number of subcarriers.

3: Each block X = $[X_0, X_1, X_2 \ldots\ldots\ldots X_{N-1}]$ is multiplied (point wise multiplication) by U different phase sequence vectors $[B^{(u)} = B_0^{(u)}, B_1^{(u)}, B_2^{(u)}, \ldots\ldots\ldots\ldots\ldots\ldots\ldots B_{N-1}^{(u)}]^T$ where each row of the normalised Riemann matrix B is taken as $B^{(u)}$, u =1,2, . . ., U.

4: A set of U different OFDM data blocks $X^{(u)}$= $[X_0^{(u)}, X_1^{(u)} \ldots\ldots\ldots\ldots\ldots\ldots\ldots\ldots X_{N-1}^{(u)}]^T$are formed, where $X_n^{(u)} = X_n * B_n^{(u)}$, n = 0, 1, . . ., N -1, u = 1, 2, . . . ,U.

5: Transform $X^{(u)}$ into time domain to get $x^{(u)}$ = IDFT $\{X^{(u)}\}$.

6: Select the one from $x^{(u)}$, u ¼ 1, 2, . . .,U, which has the minimum PAPR .

7: Select corresponding combination of phase sequence and input data before the IDFT operation i.e. $X^{(u)}$.

8: Apply $X^{(u)}$ as an input data to Iterative flipping technique with normalized Riemann matrix used as a phase sequence set.

9: Obtain signal with reduced PAPR after applying the iterative flipping technique with Riemann matrix.

VI SIMULATION & RESULTS

In this paper we have presented hybrid of two techniques to reduce the problem of higher PAPR in OFDM systems. Here New SLM technique is also compared with existing SLM technique and PTS is also compared with iterative flipping PTS. The PAPR reduction performance of the Proposed Technique2 is analysed by comparing with the New SLM, PTS, iterative flipping techniques & PAPR of original signal. In this method, the rows of the normalized Riemann matrix are used as phase sequence set.The programs implementing the PAPR reduction and comparison were written in MATLAB (Version 7.6.0.424). The different parameters considered for simulation purpose are shown below in Table 1.

Table 1: Simulation Parameters for the proposed techniques

Simulation Parameters	Value
Number of Sub carriers (N)	256
Number of Sub blocks	2,4,8,16
Oversampling Factor	4
Modulation Type	BPSK
Phase Factor	[1,-1]

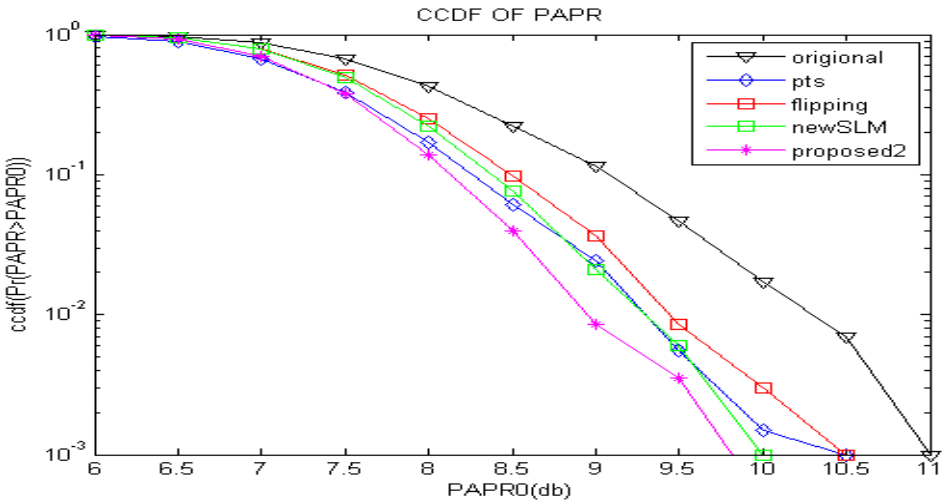

Figure 4: CCDF for comparison of PAPR reduction techniques for M=2 sub-blocks.

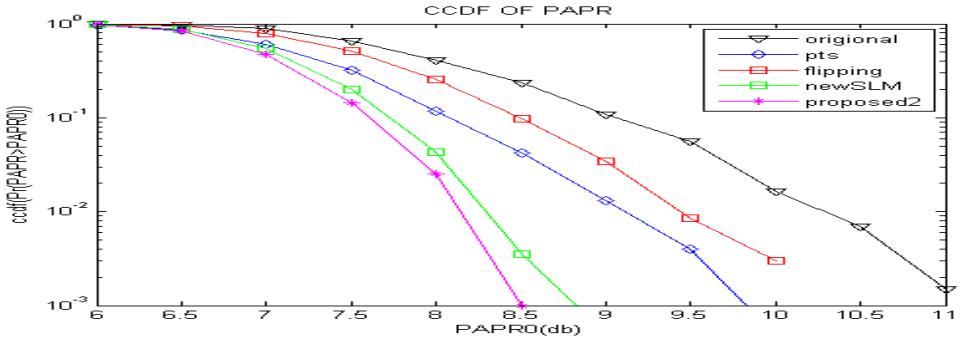

Figure 5: CCDF for comparison of PAPR reduction techniques for M=4 sub-blocks.

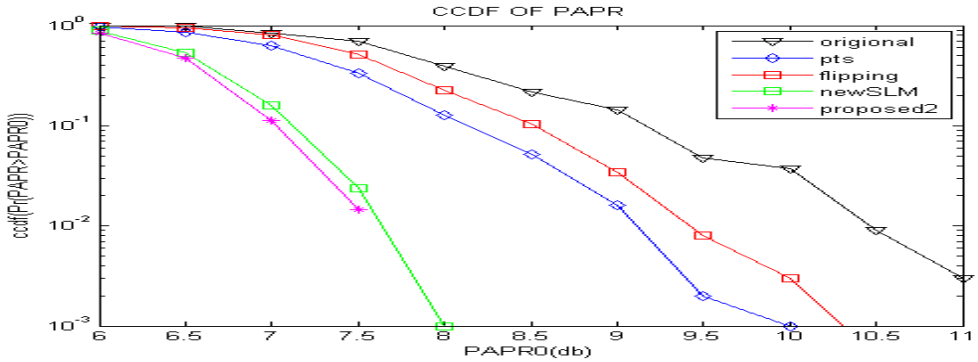

Figure 6: CCDF for comparison of PAPR reduction techniques for M=8 sub-blocks.

Figure 4 to Figure 7 show the graphs for the complement cumulative distribution function (CCDF) of PAPR in original, PTS, New SLM, Iterative flipping and Proposed 2 techniques for the different cases of M = 2; 4; 8; 16 sub-blocks respectively.

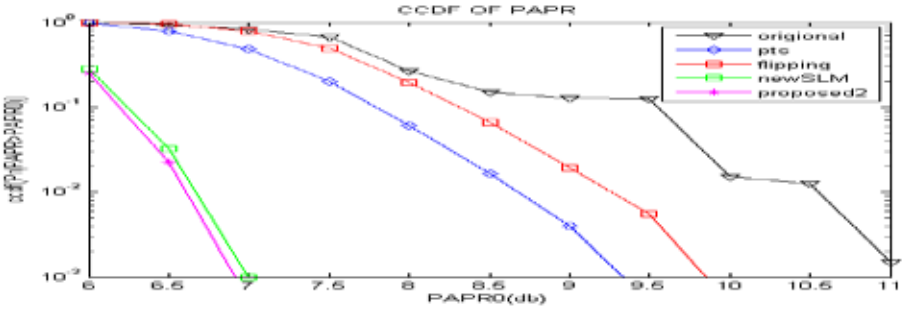

Figure 7: CCDF for comparison of PAPR reduction techniques for M=16sub-blocks.

VII CONCLUSION AND FUTURE SCOPE

From the simulation results, it can be seen that all these PAPR reduction techniques can reduce the PAPR of OFDM Signals. It is evident that the proposed technique2 based on Riemann matrix exhibit better PAPR reduction performance than the PTS, New SLM & iterative flipping techniques. However, because the Riemann matrix has been used to generate phase sequence set in Proposed technique2, therefore, the Proposed technique2 is more computationally complex. From Figure 4 to Figure 7, it is clear that as the number of sub-blocks increase, the PAPR reduction performance of the Proposed2 and New SLM techniques improves significantly. The performance of PTS & Iterative flipping techniques, however, is not affected much with the increase in

number of sub-blocks. From the simulation results, it is clear that Proposed Technique2 can achieve more PAPR reduction when compared to PTS, Iterative flipping and New SLM techniques. Moreover, the performance of Proposed Technique2 becomes better & better as the number of sub-blocks increase.

REFERENCES

[1]. Tao Jiang and Yiyan Wu, "An Overview: Peak to Average Power Reduction Techniques for OFDM Signals", *IEEE Transaction on Broadcasting, Vol.54,* June 2008.

[2]. V. Vijayarangan, R. Sukanesh, "An Overview Of Techniques For Reducing Peak To Average Power Ratio And Its Selection Criteria For Orthogonal Frequency Division Multiplexing Radio Systems", *Journal of Theoretical And Applied Information Technology*, 2009.

[3]. Van Nee and Wild. A:" Reducing the peak to average power ratio of OFDM ", *IEEE conference proceedings* , VTC, 1998.

[4]. Seung Hee Han andJae Hong Lee, "Overview of Peak to Average Power Ratio Reduction Techniques for Multicarrier Transmission", *IEEE Wireless Communication,* April 2005.

[5]. Anibal Luis Intini, "Orthogonal Frequency Division Multiplexing For Wireless Communication Systems", University Of California, December 2000.

[6]. R.W. Bauml ,R.F.H Fischer and J.B.Huber: "Reducing the peak-to-average power ratio of multicarrier modulation by selected mapping"; *IEEE Electronics Letters, 32(22), 1996.*

[7]. Saber Meymanatabadi, Javad Musevi Niya andBehzad Mozaffari, "Selected Mapping Technique for PAPR Reduction without Side Information Based On M-Sequence", *Springer Science &Business Media New York,* December 2012.

[8]. N.V. Irukulapati, V.K . Chakka and A.Jain: "SLM based PAPR reduction of OFDM signal using new phase sequence"; *IEEE Electronics Letters,* 45(24), 2009.

[9]. Ghassemi, A. , Gulliver, T.A. , "Partial Selective Mapping OFDM With Low Complexity IFFTs", *Communications Letter,IEEE ,Volume:12 , Issue: 1 ,ISSN :1089-7798,* January,2008.

[10]. ChihPeng Li, Sun-Hung Wang, Chin Liary Wang, "Novel Low-Complexity SLM Schemes For PAPR Reduction In OFDM Systems", *Signal Processing, IEEE Transactions Vol.58, Issue: 5 ,May 2010.*

[11]. Muller, S.H. And Huber, J.B., "*OFDM* with Reduced Peak to Average Power Ratio by Optimum Combination of Partial Transmit Sequences," *IEEE Electronics Letters, Vol.33,* Feb 1997.

[12]. N. R. Sollenberger, "Peak-to-Average Power Ratio Reduction of An OFDM Signal Using Partial Transmit Sequences," *IEEE Communication. Letter, Vol. 4, No. 3, Pp. 86-88,* Mar. 2000.

[13]. Cimini: "Peak-to-average power ratio reduction of an OFDM signal using partial transmit sequence", *IEEE Communication Letters, 4(3),*86-88..

[14]. Jones, Wilkinson,T.A and Barton: " Block coding scheme for reduction of peak to mean envelop power ratio of multicarrier schemes", *Electronics Letters,30(25),*Dec1994.

SYNTHESIS AND CHARACTERIZATION OF POLYANILINE DOPED WITH $Fe(NO_3)_3.9H_2O$

Smriti Sharma[1], Sneh Lata Goyal[2], Deepika Jain[3] and Nawal Kishore[4]

[1,2,3,4]*Department of Applied Physics, Guru Jambheshwar University of Science and Technology, Hisar, Haryana,(India)*

ABSTRACT

This paper describes the synthesis and characterization of polyaniline (PANI) doped with iron nitrate. The synthesis method is based on chemical oxidative polymerization of aniline added with various weight % of iron nitrate in the presence of ammonium persulphate as an oxidant. The composites were characterized by X-ray diffraction (XRD), Fourier Transform Infrared (FTIR) spectroscopy and Scanning Electron Microscopy (SEM). The variation in dc conductivity of these composites was also studied as a function of temperature and concentration and the results were compared with pure PANI. The XRD, FTIR and SEM results confirms the presence of iron nitrate in the composite. PANI/ iron nitrate composites show lower dc electrical conductivity as compared to PANI and it decreases regularly with increasing content of iron nitrate. The dc electrical conductivity increases with the increase of temperature.

Keywords: Fourier Transform Infrared (FTIR) spectroscopy, Polyaniline (PANI), Scanning Electron Microscopy (SEM), X-ray Diffraction (XRD)

I. INTRODUCTION

Conducting polymers such as polyaniline (PANI) and polypyrrole are becoming increasingly important for their technological importance due to their electrical, optical properties and their high air, chemical and electrical stability at ambient conditions and in field effect transistors [1–3]. Among the conducting polymers, polyaniline (PANI) has received a great deal of attention in last two decades due to its unique electrochemical and physicochemical behavior, environmental stability, and relatively easy synthesis [4, 5]. Furthermore, polymers possess unique optical, electronic and mechanical properties and thus have potential applications in various fields such as biosensors, electrochromic display devices, rechargeable batteries [6], anticorrosive coating [7, 8], and removal of toxic ions and in the fabrication of electronic devices like diodes [9, 10] and capacitors. Till now, although a number of studies on composites of PANI with different dopants are investigated but no studies are reported on synthesis of PANI/ $Fe(NO_3)_3.9H_2O$ composites.

In the present paper, the synthesis of PANI/ $Fe(NO_3)_3.9H_2O$ composites with different doping concentrations is reported. The characterization of all these samples has been conducted using X-ray diffraction (XRD), FTIR spectroscopy and SEM. The variation in dc conductivity of these composites has been studied as a function of temperature and concentration.

II. EXPERIMENTAL DETAILS

2.1 Synthesis of Pani

To prepare PANI, 0.2 M aniline hydrochloride (Aldrich) was oxidized with 0.25 M ammonium persulphate (Aldrich) in aqueous medium. Both solutions were left to cool in the refrigerator for 2-3 hours and then mixed in a beaker drop-wise, maintained at a temperature between 0-4 ^{0}C in an ice bath, stirred for 2 hours and left for 24 hours at rest to polymerize in refrigerator. Thereafter PANI precipitate was collected on a filter paper and was washed with 1 M HCl and acetone till the filtrate becomes colourless. Polyaniline (emeraldine) hydrochloride powder was dried in air and then in vacuum at 45^{0}C. Polyaniline prepared under these conditions was taken as standard sample.

2.2 Preparation of Pani/$Fe(No_3)_3.9h_2o$ Composites

The samples of PANI and $Fe(NO_3)_3.9H_2O$ composites were prepared by adding 10, 20, 30, 40 and 50 weight percentage of $Fe(NO_3)_3.9H_2O$ to 0.2 M aniline hydrochloride (Aldrich) solution in distilled water before oxidizing with vigorous stirring for 2 hours in order to keep the $Fe(NO_3)_3.9H_2O$ powder suspended in the solution. Following this procedure, five different PANI/ $Fe(NO_3)_3.9H_2O$ composites with different weight percentage 10%, 20%, 30%, 40% and 50 weight % of $Fe(NO_3)_3.9H_2O$ were prepared and named as FN1, FN2, FN3, FN4 and FN5 respectively.

2.3 Analytical Techniques

The samples were characterized by X-ray diffraction (XRD), Fourier Transform Infrared Spectroscopy (FTIR) Scanning Electron Microscope (SEM). DC conductivity measurements were also made. X-ray diffraction studies of the samples were performed by using Rigaku Table-Top X-ray diffractometer. FTIR analysis was done by using Shimadzu IR affinity- 1 8000 FTIR spectrometer by mixing the powder sample with dry KBr. SEM was done using Microtrac Semtrac Mini SM-300. DC conductivity measurements were made by using Keithley 6517B electrometer.

III. RESULTS AND DISCUSSION

3.1 XRD analysis

The XRD patterns of the pure PANI and PANI/$Fe(NO_3)_3.9H_2O$ composites, synthesized by doping during polymerization method are shown in Fig.1. XRD pattern of polyaniline has broad band at a value of 2θ about 25 degrees. Perusal of the figure shows that XRD pattern of all the composites are similar and all are amorphous in nature. Present studies indicate hardly any effect of Fe^{3+} on the crystallinity of PANI/iron nitrate composites. This result is in agreement with those reported in the literature [11].

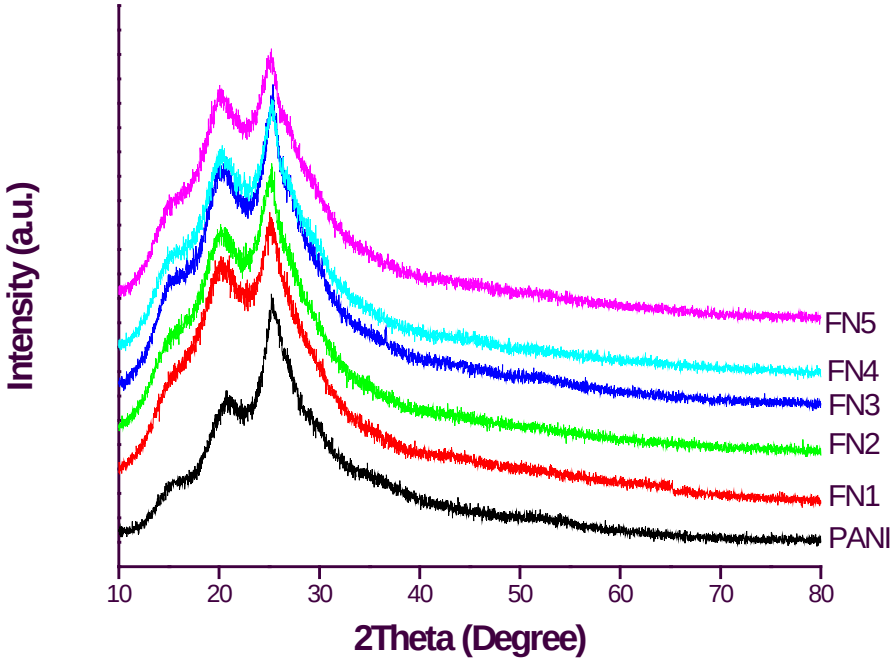

Fig.1 XRD patterns of PANI and PANI/ $Fe(NO_3)_3.9H_2O$ composites

3.2 FTIR Analysis

FTIR spectra of PANI, PANI/ $Fe(NO_3)_3.9H_2O$ composites has been shown by Fig. 2. The FTIR spectrum of PANI shows characteristic vibrations in the region of 1000-1500 cm^{-1}. Characteristic bands of PANI have been shown by 520 cm^{-1}, 815 cm^{-1}, 1163 cm^{-1}, 1317 cm^{-1}, 1495 cm^{-1} and 1589 cm^{-1}. The bands at 520 and 815 cm^{-1} are due to C-H out of plane bending vibration and para-disubstituted aromatic rings, respectively [12]. The C-N stretching vibration has been shown by a band at 1317 cm^{-1} [8]. In plane bending vibration in C-H occurs at 1163 cm^{-1} [13]. The presence of bands in the range of 1450-1600 cm^{-1} are attributed to non- symmetric C_6 ring stretching modes [12].

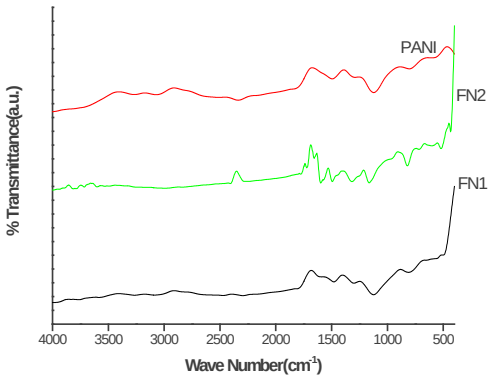

Fig.2 FTIR spectra of (a) PANI and PANI/ $Fe(NO_3)_3.9H_2O$ composites

The higher frequency vibration at 1589 cm^{-1} has a major contribution from the quinoid rings, while the lower frequency mode at 1495 cm^{-1} shows the presence of benzenoid ring units. The broad band at 2400-2750 cm^{-1} is due to aromatic C-H stretching vibrations while the band at 2950-3300 cm^{-1} is due to N-H stretching of aromatic amines [13].

3.3 Scanning Electron Microscopy (SEM)

SEM images of composites show the presence of $Fe(NO_3)_3.9H_2O$ particles in PANI matrix. In the micrographs of pure PANI, relatively bigger size particles are observed (Fig. 3). While SEM of the composite with 30 wt% shows the interaction between particles in the composite. The structures with bigger sized particles such as that seen for the pure PANI could not be seen in Fig. 4 of the composite (30 wt %). SEM of PANI/ $Fe(NO_3)_3.9H_2O$ composites shows the presence of micro crystallites which are uniformly distributed as seen in Fig. 4. The particle size comes out to be in micrometer range (» 3 µm).

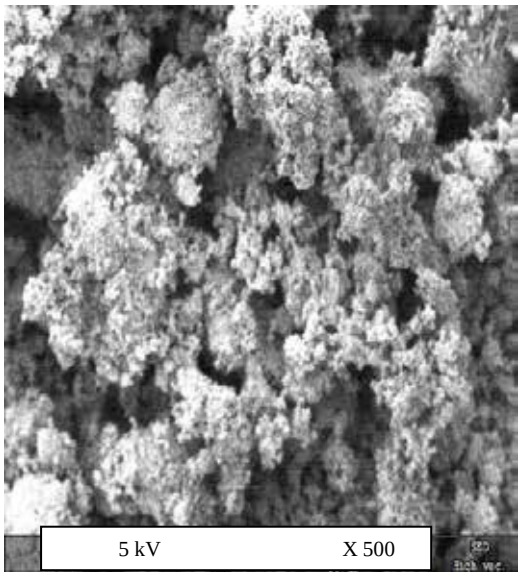

Fig. 3 - SEM micrographs of Pure PANI

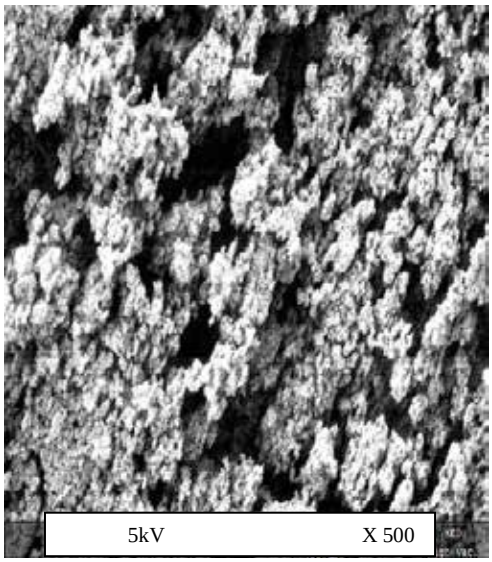

Fig. 4 - SEM micrographs of $Fe(NO_3)_3.9H_2O$ (30 wt %)

3.3 DC Conductivity

Current (I) - Voltage (V) characteristics of PANI and its composites with $Fe(NO_3)_3.9H_2O$ (20 wt %) at various temperatures is shown in Fig. 5. The current increases non-linearly with applied voltage in the composites. From the measured I-V characteristics of these samples, the values of dc electrical conductivities (σ) have been estimated at different temperatures at 0.5 V:

$$\sigma = \frac{I X L}{V X A} \quad \ldots (1)$$

where I is the current, L is the thickness, V is the voltage and A is the area of cross section of the sample. The dc conductivity decreases when doped with $Fe(NO_3)_3.9H_2O$ and also conductivity decreases with increasing content of $Fe(NO_3)_3.9H_2O$ in PANI/ $Fe(NO_3)_3.9H_2O$ composites as mentioned in Table 1. This decrease in conductivity by the addition of semiconducting $Fe(NO_3)_3.9H_2O$ may be due to the blocking of charge carriers, to hop between favorable sites which in turn lower the overall conductivity of composite. This type of result was

also reported in other paper[14]. As shown in Fig. 6, dc electrical conductivity increases with increase in temperature. This may be due to increase in free charges with increase in temperature.

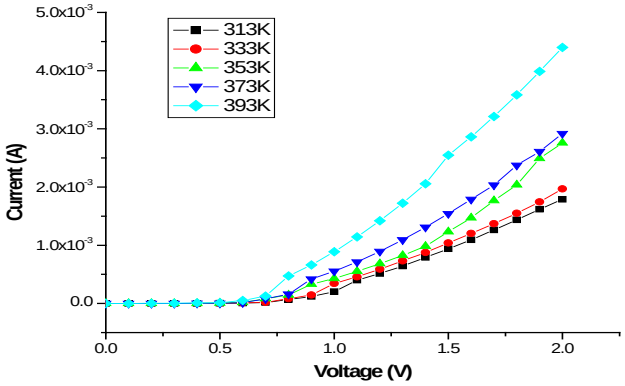

Fig. 5 - I-V characteristic of PANI / $Fe(NO_3)_3.9H_2O$ 20 wt% at various temperatures

Table 1: DC conductivity of PANI(inset) and PANI/ $Fe(NO_3)_3.9H_2O$ composites at 0.5V at various temperatures

TEMP.	Conductivity ($x10^{-5}$) Scm^{-1}				
	PANI	FN2	FN3	FN4	FN5
313	58.8	1.61	0.71	0.14	0.12
333	69.7	2.75	1.17	0.64	0.20
353	78.1	3.42	1.65	1.08	0.26
373	84	4.42	3.73	2.27	0.27
393	86.8	7.06	5.29	2.84	0.37

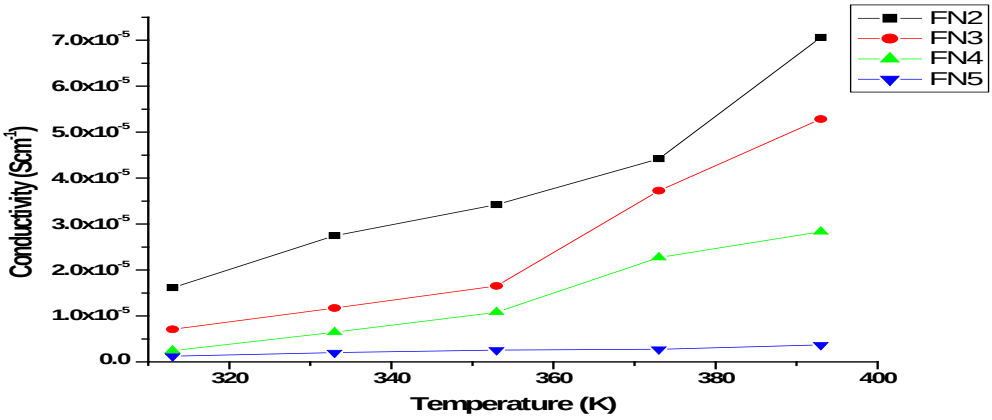

Fig.6 - Conductivity of PANI/ $Fe(NO_3)_3.9H_2O$ composites vs Temp.

The models for thermally activated and Mott's variable range hopping (VRH) is given by Equation (2)

$$\sigma(T) = \sigma_0 \exp\left[-\left(\frac{T_0}{T}\right)^{\gamma}\right] \quad \ldots\ldots(2)$$

where σ_0 is the high temperature limit of conductivity, T_0 is the Mott's characteristics temperature associated with the degree of localization of the electronic wave function. The exponent $\gamma = 1/(1+d)$ determines the dimensionality of the conducting medium [15]. The possible values of γ are 1/4, 1/3 and 1/2 for three, two and one-dimensional systems respectively. Conductivity varies with various values of the exponent (e.g. $T^{-1/4}$, $T^{-1/3}$, $T^{-1/2}$ and T^{-1}) which have been reported to interpret the data. The values of $\ln\sigma_0$ obtained from the intercept is obtained from the above mentioned plots and shown in Table 2. The plot of $\ln\sigma$ (T) vs. $T^{(-1/4)}$ is a straight line as shown in Fig. 7 and indicates that three dimensional (3D) charge transport occurs in all the samples

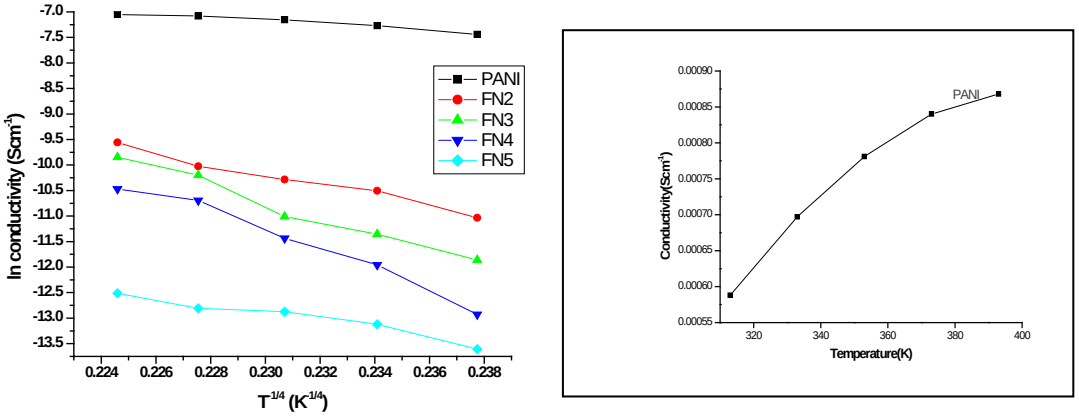

Fig. 7 - Graph between ln (σ_{dc}) vs $T^{-1/4}$ of PANI and PANI/$Fe(NO_3)_3$.$9H_2O$ composites

Table 2- The values of $\ln\sigma_0$ and T_0

Sample	$\ln\sigma_0$ (S/cm)	T_0 (10^6) K
PANI	-0.5964	0.661
FN2	6.469	27.6
FN3	30.108	984
FN4	33.319	1390
FN5	-2.391	4.42

IV. CONCLUSION

PANI and PANI/ $Fe(NO_3)_3.9H_2O$ composites were synthesized by means of the oxidative polymerization of aniline hydrochloride in presence of different wt% of $Fe(NO_3)_3.9H_2O$ with ammonium persulphate. Amorphous nature of the prepared composites has been ascertained by X-ray diffraction pattern. The FTIR results confirm the presence of PANI in the composites. In composites of PANI/ $Fe(NO_3)_3.9H_2O$, there exists small shifting in frequencies of the bands as observed in PANI. SEM also confirms the presence of $Fe(NO_3)_3.9H_2O$ in the composites of PANI/ $Fe(NO_3)_3.9H_2O$. The temperature dependence of the DC conductivity of PANI/ $Fe(NO_3)_3.9H_2O$, as measured in temperature range (313 to 393 K), has been investigated. DC electrical conductivity of PANI and PANI/ $Fe(NO_3)_3.9H_2O$ composites increases with increase of temperature but DC conductivity decreases with increasing content of $Fe(NO_3)_3.9H_2O$ in the composites. At higher temperatures, dc conductivity increases because of hopping of polarons from one localized states to another localized states. As future actions, this work opens new perspectives for the use of PANI/ $Fe(NO_3)_3.9H_2O$ composites as suitable electronics devices. It is thought that such composites may find important technological applications.

V. ACKNOWLEDGMENT

Authors are thankful to University Grants Commission (UGC), New Delhi for granting major research project no. 41-888/2012 (SR) and Department of Science and echnology (DST-FIST) for providing financial support.

REFERENCES

[1] K. Anuar, S. Murali, A. Fariz and H.N.M. Mahmud Ekramul, Conducting polymer/clay composites: preparation and characterization, Materials Science, 10, 2004, 255-258.

[2] A. Kassim, Z. Bte Basar, H.N.M. Ekramul Mahmud, Effects of preparation temperature on the conductivity of polypyrrole conducting polymer, Journal of Chemical Sciences, 114(2), 2002, 155–162.

[3] S.L. Patil, S.G. Pawar, M.A. Chougule, B.T. Raut, P.R. Godse, S. Sen and V.B. Patil, Structural, morphological, optical and electrical properties of PANi-ZnO nanocomposites, International Journal of Polymeric Materials, 61, 2012, 809–820.

[4] J.C. Chiang and A.G. Macdiarmid, 'Polyaniline': Protonic acid doping of the emeraldine form to the metallic regime, Synthetic Metals, 13(1), 1986, 193-205.

[5] J. Stejskal, I. Sapurina, M. Trchova and E.N. Konyushenko, Oxidation of aniline: Polyaniline granules, nanotubes and oligoaniline microspheres, Macromolecules, 41, 2008, 3530-3536.

[6] T. Yamauchi, S. Tansuriyavong, K. Doi, K. Oshima, M. Shimomura, N. Tsubokawa, S. Miyauchi, & J. F. V. Vincent, Preparation of composite materials of polypyrrole and electroactive polymer gel using for actuating system, Synthetic Metals, 152, 2005, 45-48.

[7] C.W. Lin, B. J.Hwang and C. R. Lee, Methanol sensors- based on conductive polymer composites from polypyrrole- poly(vinyl alcohol), Materials Chemistry and Physics, 55, 1998 , 139-144.

[8] K. A. Noh, D. W. Kim, C. S. Jin, K. H. Shin , J. H. Kim and J. M. Ko, Synthesis and pseudo-capacitance of chemically-prepared polypyrrole powder, Journal of Power Sources, 124, 2003, 593-595.

[9] C. Y. Lee, H. M . Kim, J. W.Park, Y. S. Gal, J. I. Jin and J. Joo, AC electrical properties of conjugated polymers and theoretical high-frequency behavior of multilayer films, Synthetic Metals, 117, 2001, 109-113.

[10] G. N. Marija, T. S. Jadranka, G. A. Bowmaker, R. P. Cooney , C. Thompson and P. A. Kilmartin, The antioxidant activity of conducting polymers in biomedical applications, Current Appl Phys., 4, 2004, 347-350.

[11] J. P. Pouget, M. E. Jozefowicz, A. J. Epstein, X. Tang and G. MacDiarmid, X-ray structure of polyaniline, Macromolecules, 41, 1991, 723–789.

[12] S.A. Chen, K.R.Chung, C.L. Chao and H.T. Lee, White light omission from electroluminescence diode with polyaniline as the emitting layer, Synthetic Metals, 82, 1996, 207-210.

[13] G. Raman and G. Aharon, Organic- inorganic hybrid materials based on polyaniline/ TiO_2 nanocomposites for ascorbic acid fuel cell systems, Nanotechnology, 19 , 2008, 435709-435713.

[14] K. Majid, S. Awasthi and M.L. Singla, Low temperature sensing capability of polyaniline and Mn_3O_4 composite as NTC material, Sensors and Actuators: A ,135, 2007, 113-118.

[15] V. Shaktawat , N. Jain, R. Saxena, N. S. Saxena, K. Sharma and T. P. Sharma, Temperature dependence of electrical conduction in pure and doped polypyrrole, Polymer Bulletin, 57, 2006, 535-543.

BIOGRAPHICAL NOTES

Ms. Smriti Sharma is presently pursuing Ph. D. in Physics from Department of Applied Physics, Guru Jambheshwar University of Science and Technology, Hisar-125001, Haryana, India.

Dr. Sneh Lata Goyal is working as a Professor in Physics, Department of Applied Physics, Guru Jambheshwar University of Science and Technology, Hisar-125001, Haryana, India.

Ms. Deepika Jain is working as a Project Fellow in UGC Major Research Project with Prof. Sneh Lata Goyal, Department of Applied Physics, Guru Jambheshwar University of Science and Technology, Hisar-125001, Haryana, India.

Dr. Nawal Kishore is Ex. Professor in Physics, Department of Applied Physics, Guru Jambheshwar University of Science and Technology, Hisar- 125001, Haryana, India.

OPTIMIZED DESIGN OF AN INTEGRATED CONVERTER FOR DUAL MODE ELECTRIC VEHICLE APPLICATION

[1]B.Navya sree , [2]Dr. P. Udaya Bhaskar, [3]G. Kamalaker

[1]Assistant Professor, [2]Professor & Head, [3]Assistant Professor,
Department of EEE, BIET, Hyderabad, (India)

ABSTRACT

A new integrated circuit for motor drives with dual mode control for EV/HEV applications is proposed. The proposed integrated circuit allows the permanent magnet synchronous motor to operate in motor mode or acts as boost inductors of the boost converter, and thereby boosting the output torque coupled to the same transmission system or dc-link voltage of the inverter connected to the output of the integrated circuit. Moreover, a new control technique for the proposed integrated circuit under boost converter mode is proposed to increase the efficiency. The proposed control technique is to use interleaved control to significantly reduce the current ripple and thereby reducing the losses and thermal stress under heavy-load condition. In contrast, single phase control is used for not invoking additional switching and conduction losses under light-load condition. In this paper we can connect more number of batteries. Which are bi directional and these are used for different types of applications by reducing the switches which are used for the required operation. In this paper we may get the output voltage is increased up to 3 times(90v to 270v),only 9 switches are used for the operation of inverting, bidirectional power flow for three sources. When used a conventional existing converter it may use 12 switches for the same operations and efficiency will improve high compared to other methods.

Key Words: EV/HEV, ICE, SMPS, DCM, CCM, PWM

I INTRODUCTION

A hybrid electric vehicle (HEV) is a type of hybrid vehicle and electric vehicle which combines a conventional internal combustion engine (ICE)propulsion system with an electric propulsion system. The most common form of HEV is the hybrid electric car, although hybrid electric trucks (pickups and tractors) and buses also exist.

Modern HEVs make use of efficiency-improving technologies such as regenerative braking, which converts the vehicle's kinetic energy into electric energy to charge the battery, rather than wasting it as heat energy as conventional brakes do Many HEVs reduce idle emissions by shutting down the ICE at idle and restarting it when needed; this is known as a start-stop system

With the advancement of power electronics, micro processors and digital electronics, typical electric drive systems now a day are becoming more compact, efficient, cheaper and versatile. The voltage and current applied to the motor can be changed at will by employing power electronic converters.AC motor is no longer limited to application where only AC source is available, however, it can also be used when the power source available.

A new integrated circuit for motor drives with dual mode control for EV/HEV applications is proposed. The proposed integrated circuit allows the permanent magnet synchronous motor to operate in motor mode or acts as boost inductors of the boost converter, and thereby boosting the output torque coupled to the same transmission system or dc-link voltage of the inverter connected to the output of the integrated circuit. In motor mode, the proposed integrated circuit acts as an inverter and it becomes a boost-type boost converter, while using the motor windings as the boost inductors to boost the converter output voltage. Moreover, a new control technique for the proposed integrated circuit under boost converter mode is proposed to increase the efficiency. The proposed control technique is to use interleaved control to significantly reduce the current ripple and thereby reducing the losses and thermal stress under heavy-load condition. In contrast, single phase control is used for not invoking additional switching and conduction losses under light-load condition. Experimental results derived from digital-controlled 3-kW inverter/converter using digital signal processing show the voltage boost ratio can go up to 600W to 3 kW. And the efficiency is 93.83% under full-load condition while keeping the motor temperature at the atmosphere level. [1] In this we can connect more number of batteries. these batteries are bi directional and these are used for different types of applications. In this paper am reducing the switches which are used for the required operation.

II EXISTING METHODS

The method is interleaved method. It is also called 2phase method. In this method we use 2 inductors 2 switches the operation and simulation results are shown in below.

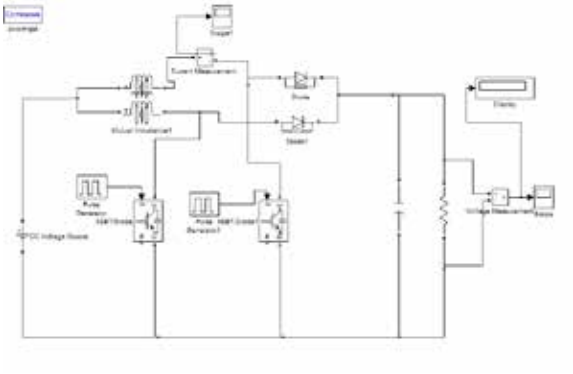

Figure 1 Interleaved Diagram

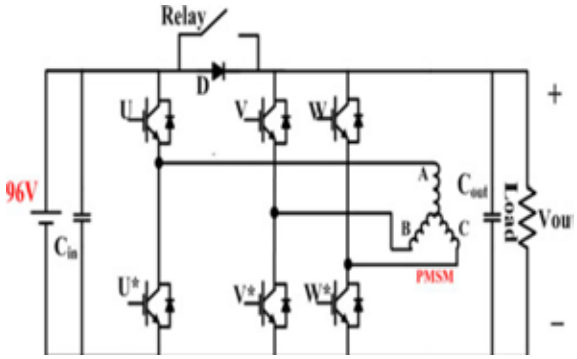

Figure 2 Integrated Circuit

For 50% of duty ratio the output voltage we have 55.37.the output voltage compared to normal boost converter is increased in this method [2]. And another method is integrated inverter/converter method in this method the boost converter and inverter are placed in one circuit only. By this it reduces the size and the cost of the equipment.

Based upon the interleaved control idea, a boost-control technique using motor windings as boost inductors for the proposed integrated circuit will be proposed. Under light load, the integrated circuit acts as a single-phase boost converter for not invoking additional switching and conduction losses, and functions as the two-phase interleaved boost converter under heavy load to significantly reduce the current ripple and thereby reducing the losses and thermal stress [3]-[4]. Therefore, the control technique for the proposed integrated circuit under boost converter mode can increase the efficiency. Detailed operation of interleaved method and boost converter are shown below.

2.1 Interleaved Operation

The interleaved boost converters consists of several identical boost converters connected in parallel and controlled by the interleaved method which has the same switching frequency and phase shift. Ripple cancellation both in the input-output voltage and current waveforms, reduced current peak value, and high ripple frequency are some of the benefits of interleaving operation in converters. Moreover, increased efficiency and high reliability can be achieved. Also, by high frequency, the size and losses of the magnetic components can be reduced. These interleaved boost converters are distinguished similar with conventional converters by critical operation mode, discontinuous conduction mode (DCM), and continuous conduction mode (CCM).

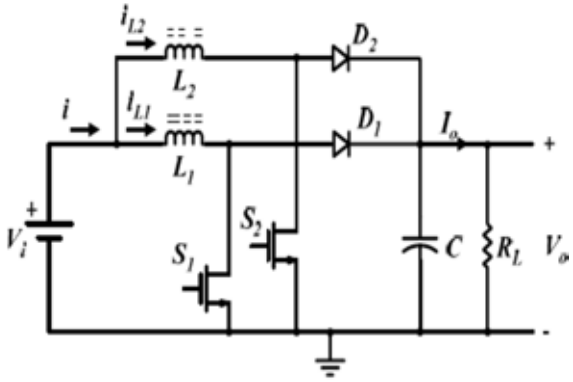

Figure 3 Two-phase interleaved boost converter

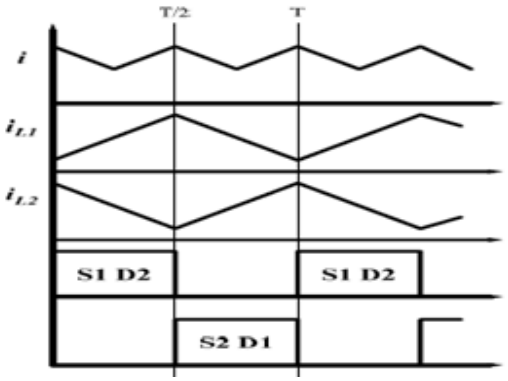

Figure 4 Ideal waveforms of the currents in the inductors L1 and L2 for interleaved boost converter operating at CCM.

These methods are primarily used in the design of inductors for switching-mode power supplies (SMPS) [5]. In this paper, core geometry approach used to select magnetic core. For interleaved operation two identical boost converter parallel connected and operated with 180° phase shifted. Designed inductor will used for both phases.

2.2 Integrated Circuit Method

Solution of gain equation for the boost converter**:**

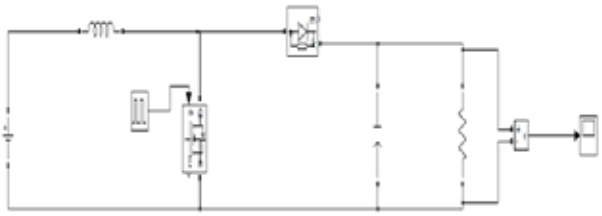

Normal boost converter

CASE 1: When the switch is in ON position

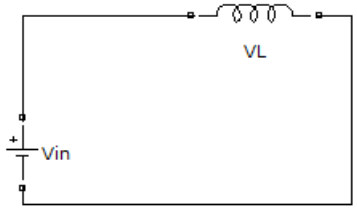

$$V_{in} = V_L$$

CASE 2: When the switch is in OFF position

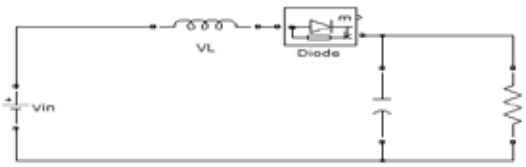

$$V_L = V_{in} - V_o$$

$$V_{in} = V_L + V_o$$

As we know Duty ratio

$$D = \frac{T_{ON}}{T_{ON} + T_{OFF}}$$

$$D = \frac{T_{ON}}{TS} \qquad T_{ON} = DT_S \qquad T_{OFF} = (1 - D) \times T_S$$

Average voltage across inductor =0

$$\frac{V_{in} \times D \times T_S + (V_{in} - V_o) \times (1 - D) T_S}{T_S} = 0$$

$$V_{in} D + (V_{in} - V_0)(1 - D) = 0$$

$$V_{in} - V_0(1 - D) = 0$$

The final gain equation is $\frac{V_0}{V_{in}} = \frac{1}{1 - D}$

In Parallel hybrid electric vehicle (HEV) and electric vehicle (EV) system as shown in Fig. 5 the converter is used for boosting the battery voltage to rated dc bus for an inverter to drive motor. In the multi motor drive system the system will use two or more motors to boost torque, especially under low speed and high-torque region as shown in Fig. 6. For such applications, two or more inverters/ converters are required. Fig. 7 shows the application of the proposed integrated circuit for motor drives with dual-mode control for EV/HEV applications. As shown in Fig. 7, the proposed integrated circuit allows the permanent magnet synchronous motor.

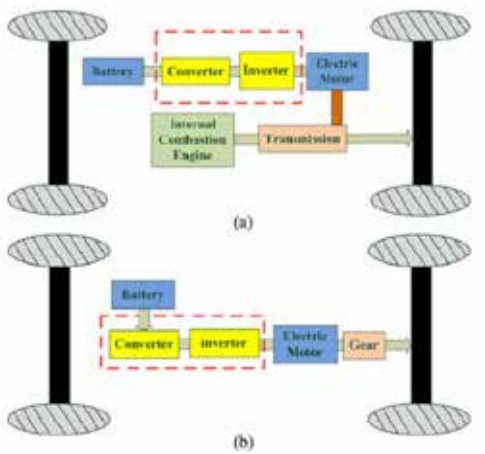

Figure 5 HEV and EV system. (a) Parallel HEV drive train. (b) EV drive train

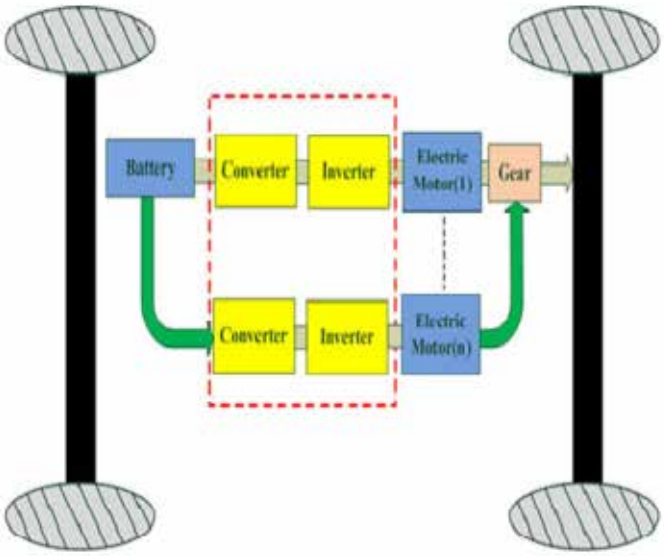

Figure 6 Conventional multi motor drive system of EV/HEV.

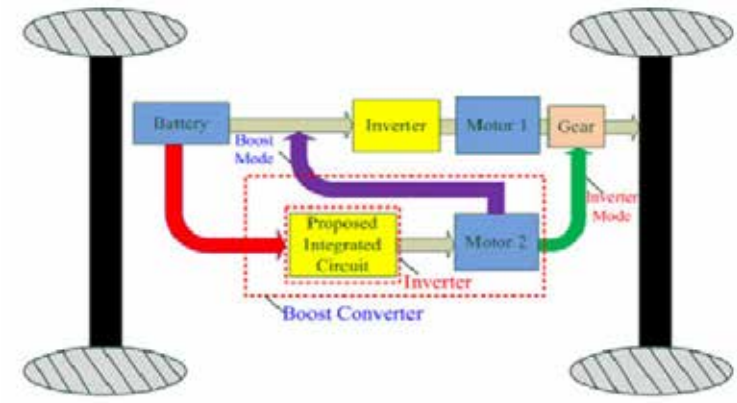

Figure 7 Proposed integrated inverter/converter for the multi motor drive system of EV/HEV.

(PMSM) to operate in motor mode or acts as boost inductors of the boost converter, and thereby, boosting the output torque coupled to the same transmission system or dc-link voltage of an inverter connected to the output of the integrated circuit.

The integrated circuit presented in this paper can act as an inverter and a boost converter depending on the operation mode[9]. For the integrated circuit, it not only can reduce the volume and weight but also boost torque and dc-link voltage for motor/converter modes, respectively. Moreover, a new control technique for the proposed integrated circuit under boost converter mode is proposed to increase the efficiency.

Based upon the interleaved control idea, a boost-control technique using motor windings as boost inductors for the proposed integrated circuit will be proposed.

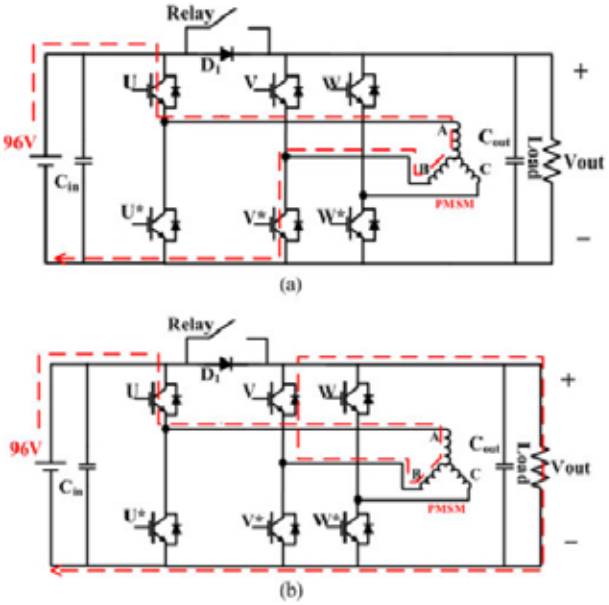

Figure 8 Single-phase boost mode. (a) Charge path for inductor. (b) Discharge path for inductor.

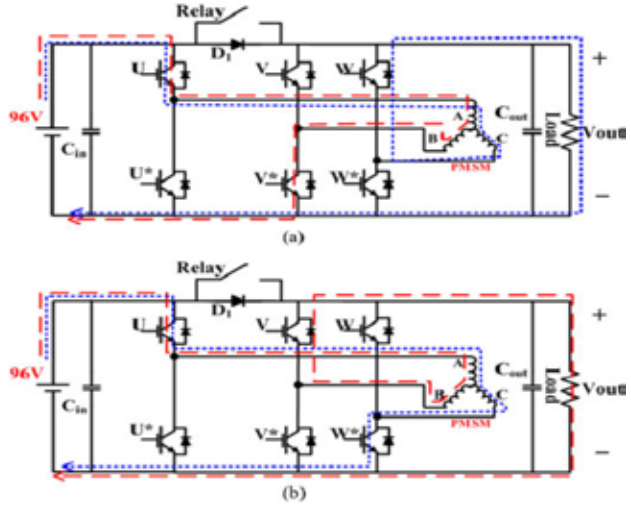

Figure 9 Proposed interleaved boost mode. (a) Phase B: Charge; Phase C: Discharge. (b) Phase B: Discharge; Phase C: Charge.

Therefore, the proposed control technique for the proposed integrated circuit under boost converter mode can increase the efficiency. Fig above shown the integrated circuit for dual-mode control. In that fig Cin and Cout can stabilize the voltage when input and output voltages are disturbed by source and load, respectively. Diode (D) is used for preventing output voltage impact on the input side. When the integrated circuit is operated in inverter (Motor) mode, relay will be turned ON and six power devices are controlled by pulse width modulation (PWM) control signals. When the proposed integrated circuit is operated in the converter mode, relay is turned OFF. And a single-phase or interleaved control method will be applied to control of the power devices depending upon the load conditions. Figs. 8 and 9 show the single-phase and two-phase interleaved boost converters. In the above Fig 8 the single-phase boost converter uses power switch V*, stator winding "A" and winding "B" to boost the output voltage. In Fig. 9 two-phase interleaved boost converter uses power switches V * and W*, stator winding "A" winding "B" and winding "C" to boost the output voltage and reduce the current ripple.

III MODELLING AND CONTROLLER DESIGN UNDER BOOST MODE

This section will introduce the model of boost converter and derive the transfer function of the voltage controller. Fig. 10 shows the non ideal equivalent circuit of the boost converter, it considers non ideal condition of components: inductor winding resistance R_L, collector-emitter saturation voltage V_{CE}, diode forward voltage drop V_D, and equivalent series resistance of capacitor Resr. Analysis of the boost converter by using the state-space averaging method, small-signal ac equivalent circuit can be derived, as shown in Fig. 11. By Fig. 11, the transfer function of the voltage controller can be derived, at the bottom of the next page.

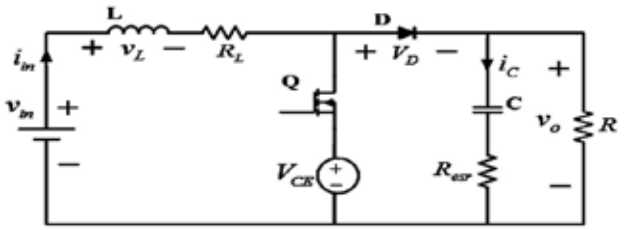

Figure 10 Equivalent circuit of the boost converter.

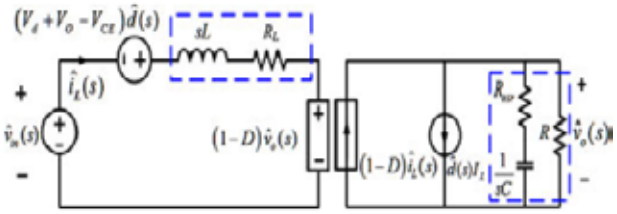

Figure 11 Small-signal equivalent circuit

$$G_{vd}(s)=\frac{\overrightarrow{V_o(s)}}{\overrightarrow{d(s)}}=\frac{s^2\times L\times C\times(R+R_{esr})+s[L+C\times R_L(R+R_{esr})+(1-D)^2C\times R.\times R_{esr}]+[(1-D)^2.R+R_L]}{-s^2\times C.\times R\times R_{esr}\times L\times I_L+s\{C\times R\times R_{esr}[(V_d+V_o-V_{CE})(1-D)-R_LI_L]-R_LI_L\}+R[(V_d+V_o-V_{CE})(1-D)-R_LI_L]}$$

Fig. 12 shows the block diagram of voltage loop, using a proportional-integral (PI) controller for the compensator. In this paper, the switching frequency is 20 kHz and voltage loop bandwidth will be less than 2 kHz. And the phase margin should be more than 45° to enhance the noise immunity.

$$C(s)=\frac{0.0248387s+13.073}{s}$$

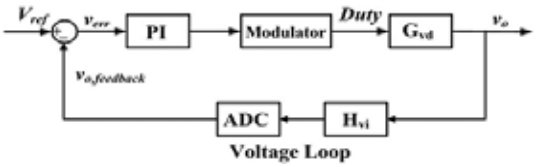

Figure 12 Block diagram of voltage loop.

IV SIMULATION RESULTS

CASE 1: Interleaved boost mode: B phase discharges the power until the C phase charges, after c is charged this phase will send the power to the load in that time B is going to charge. Fig 13 and Fig.14 shows the block diagram and output results of the two phase mode operation.

CASE 2: Single phase to two phase interleaved mode: In this mode of operation the both single phase and two phase operation is performed. From single phase to two phase conversion is performed in this case, the below figures shows the circuit and output results. In this circuit contains switch,

this is used to phase conversion.

CASE 3: Two phase interleaved to single phase mode: In this mode also same operation is performed as case3. But the phase conversion is from two phase to single phase.

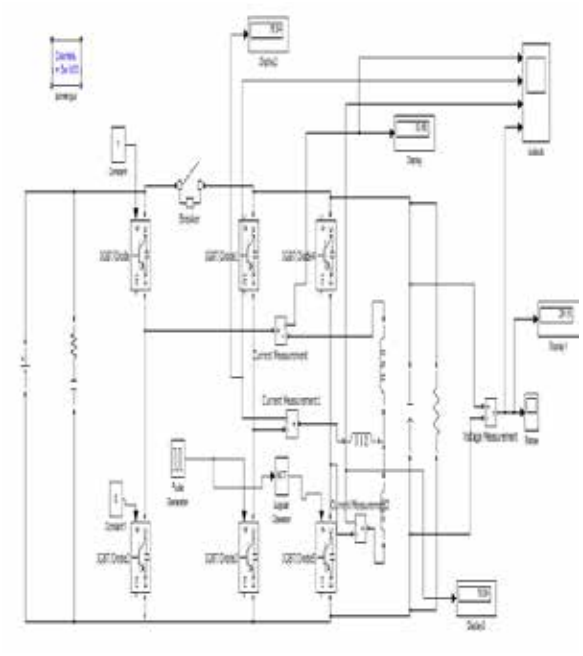

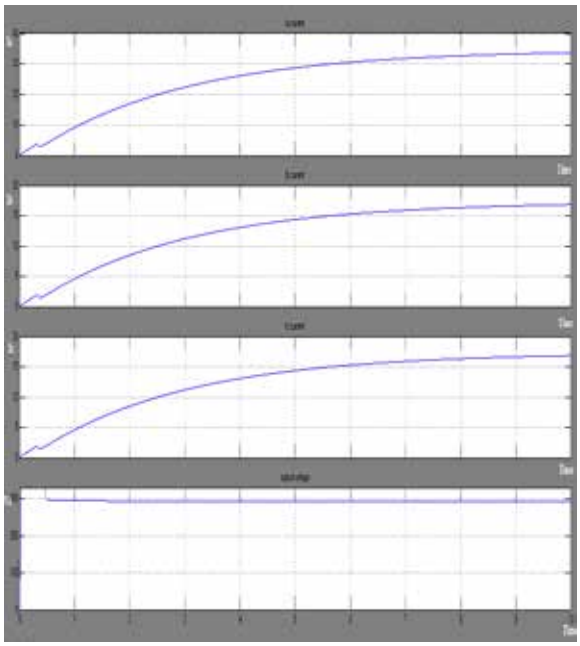

Figure 13 interleaved boost mode **Figure 14 output results of interleaved boost mode**

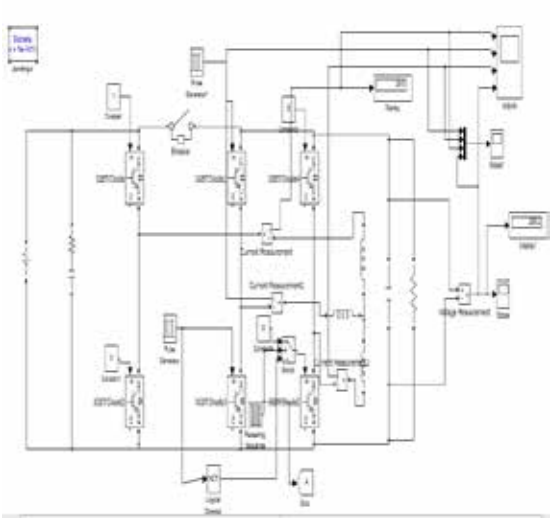

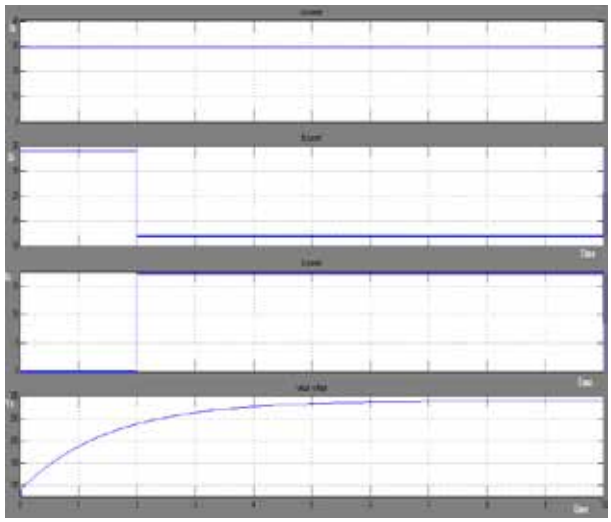

Figure 15 single phase to two phase interleaved mode. **Figure 16 output results**

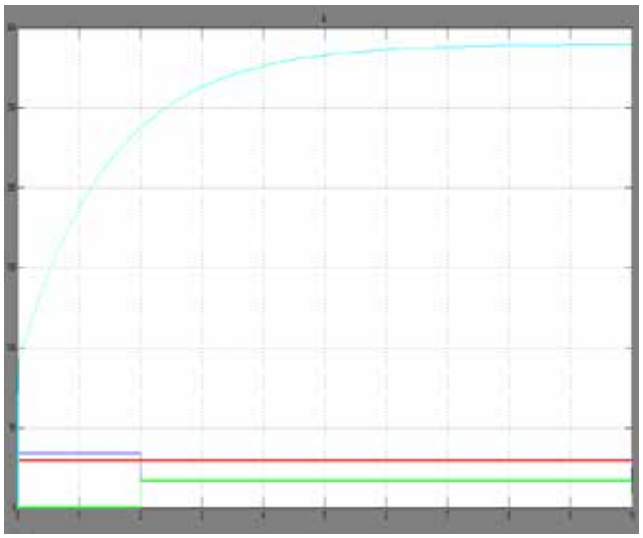

Figure 17 combined output results

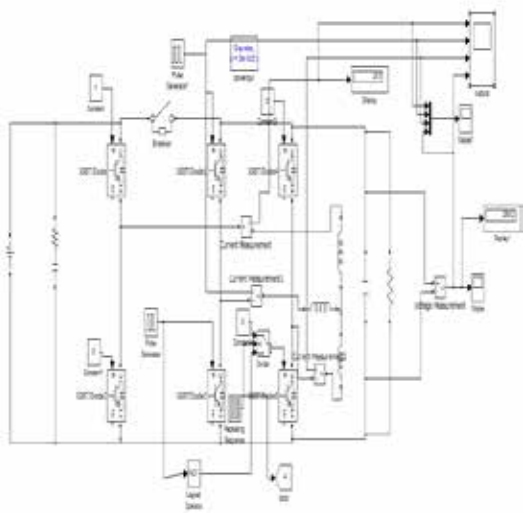

Figure 18 Two Phase interleaved to single phase mode

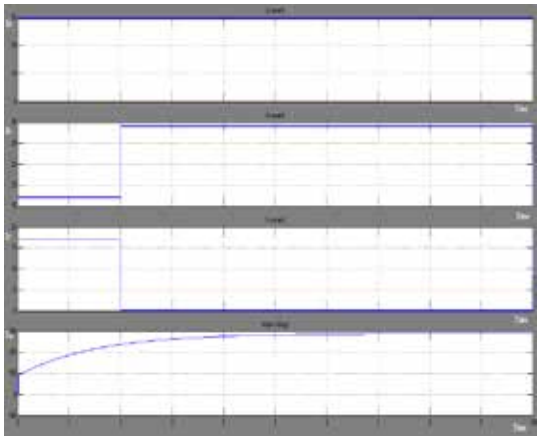

Figure 19 output results of two phase interleaved to single phase mode

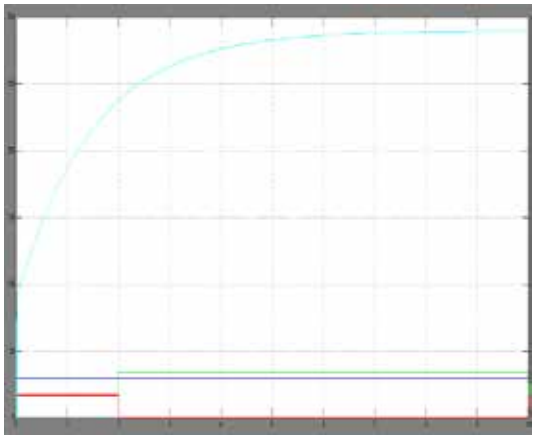

Figure 20 combined results of two phases interleaved to single phase mode

Table 1 CALCULATION FOR RIPPLE CONTENT MEASURE

Normal boost converter			
Duty ratio	Higher point of ripple in current	Lower point	Total ripple content(subtract from higher to lower)
50	3.4	0	3.4
40	3.6	0	3.6
60	-	-	-
Interleaved Boost Converter			
50	3.7	3.4	0.3
40	2.6	3.2	0.6
60	4.1	4.5	0.4

From normal boost converter ripple content is for 50% duty ratio ripple is 3.45.for 40% also same ripple content, for 60% no ripple is appear. In interleaved boost converter the ripple content is reduced compared to normal boost converter. for 50%,the ripple content is 0.3,for 60% it is 1,and for 40% the current ripple content

measured is 0.6.But in new integrated converter topology no ripple content is observed, if appear it will be very small and neglected quantity But In this only converter operation is explained and in this method it uses many switches for connecting of bidirectional batteries. And the output voltage is 288v.So in proposed method we used to make many change for better efficiency and less switches and for low losses.

V PROPOSED CIRCUIT AND CONTROL TECHNIQUE

In this circuit we are using bidirectional batteries as multiple batteries. These are because of when we are using one battery, it causes discontinue of supply when the charged battery is complete .and also when one of the battery is not working also vehicle works because of other batteries, for this batteries it required more number of switches, but am reducing switches. By this same results are getting, and by this circuit complexity reduced, cost of the circuit also decreases. And in integrated circuit the inverter operation is not explain. In this extension automatically inversion operation is performing after the converter operation. By this it is proved that efficiency improved and current ripples are reduced and the cost also less for this circuit.

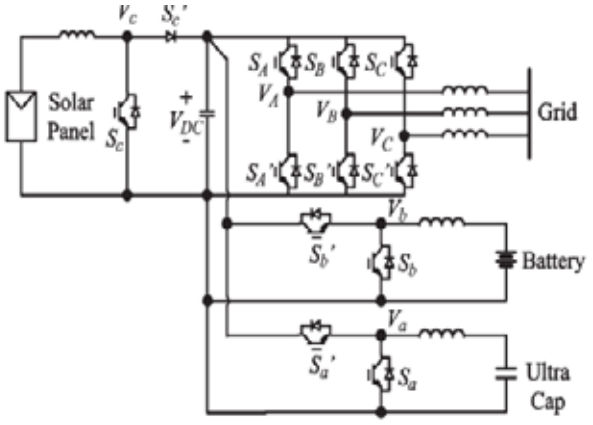

Figure 21more switches connected integrated circuit

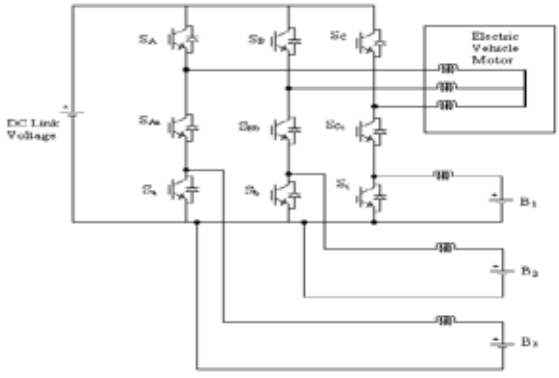

Figure 22 integrated less switches circuit

Table 2 switching states and output voltages of figure 21

S_A	S_A	S_a	S_a	V_A	V_a
ON	OFF	ON	OFF	V_{DC}	V_{DC}
ON	OFF	OFF	ON	V_{DC}	0
OFF	ON	OFF	ON	0	0
OFF	ON	ON	OFF	0	V_{DC}

Table 3 switching states and output voltages of figure 22

S_A	S_{Aa}	S_a	V_A	V_a
ON	ON	OFF	V_{DC}	V_{DC}
ON	OFF	ON	V_{DC}	0
OFF	ON	ON	0	0

Fig.21 shows integrated 6 switch circuit here 11 controllable switches are used, in which 6 switches are for integrated circuit and 4 switches for 2 batteries.1 for supply, When 3 batteries connected it uses 2 more batteries extra.Table3,4, Shows The Switches Operation, Means On Or Off Operation Of Switches.

The further development is made by integrating the above circuit by reducing the number of switches to 9 instead of 12 as shown in fig. In that upper 6 switches $\{S_A, S_B, S_C, S_{Aa}, S_{Bb}, S_{Cc}\}$ are used for inversion and lower 6 switches $\{S_a, S_b, Sc, S_{Aa}, S_{Bb}, S_{Cc}\}$ are for conversion. In that switches the switches in the middle $\{S_{Aa}, S_{Bb}, S_{Cc}\}$ are common for both inversion and conversion processes.

Operation:

A control circuit is designed which creates a reference signal for AC and DC. This reference is made ripple free using a PI controller. In closed loop circuits we use PI controller for better operation. with these reference signals the triggering pulses are generated using PWM technique which helps in switching operation. 3 batteries are connected, each battery voltage is 30v.these will help to supply power to load when more power required for the vehicle. When one battery is not working also the other 2 batteries give the supply to load. From this no interruptions accrue in the vehicle. And for upper switches a reference AC voltage also supplied to the circuit, for better operation.

Table 4 Parameter values of circuit

V_{in}	$175V_{dc}$
Battery voltage	30
Inductor value	5mh
RC	1ohm,2200μf
RL	13ohm,1mh

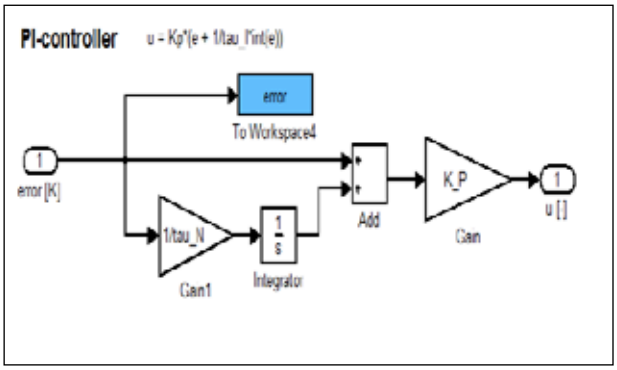

Figure 23 PI Controller

The definition of proportional feedback control is still

$u = K_p e$

where

e = is the "error"

K_P = Proportional gain

The definition of the integral feedback is

$u = K_I \int e \times dt$

where K_I is the integration gain factor.

In the PI controller we have a combination of P and I control, i.e.: $u = K_p e + K_I \int e \times dt$

$$u = K_p e + \frac{1}{t_I} \int e \times dt$$

$$u = K_P \left[e + \frac{1}{t_N} \int e \times dt \right]$$

Where, τ_I = "Integration time" [s]

τ_N = "Reset time" [s]

The combination of proportional and integral terms is important to increase the speed of the response and also to eliminate the steady state error. The PID controller block is reduced to P and I blocks only as shown in figure 24

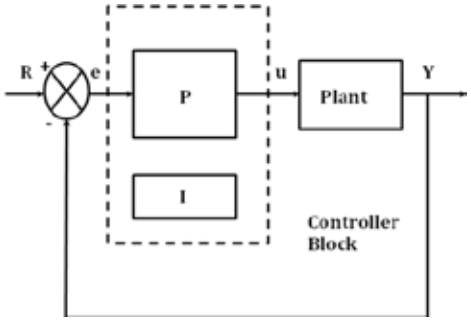

Figure 24 Proportional Integral (PI) Controller block diagram

The proportional and integral terms is given by:

$$u(t) = K_P \times e(t) + K_I \int e(t) \times dt$$

PWM Technique:

Pulse-width modulation (PWM),or pulse-duration modulation (PDM), is a modulation technique that controls the width of the pulse, formally the pulse duration, based on modulator signal information. Although this modulation technique can be used to encode information for transmission, its main use is to allow the control of the power supplied to electrical devices, especially to inertial loads such as motors. In addition, PWM is one of the two principal algorithms used in photovoltaic solar battery chargers, the other being MPPT. the two basic approaches used to generate the PWM signals for multilevel inverters are:

· Sub harmonic or Sub-Oscillation carrier based PWM-modulating waveform comparison with offset triangular carriers.

· Space Vector PWM-space vector modulation based on a rotating vector in multilevel space.

These are the extensions of traditional two level control strategies to several levels. The two main advantages of PWM inverters in comparison to square-wave inverters are

- control over output voltage magnitude
- Reduction in magnitudes of unwanted harmonic voltages.

Good quality output voltage in SPWM requires the modulation index (m) to be less than or equal to 1.0. For m>1 (over-modulation), the fundamental voltage magnitude increases but at the cost of decreased quality of output waveform. The maximum fundamental voltage that the SPWM inverter can output (without resorting to over-modulation) is only 78.5% of the fundamental voltage output by square-wave inverter.

The merits and demerits of these two PWM techniques are compared under comparable circuit conditions on the basis of factors like (i) quality of output voltage (ii) obtainable magnitude of output voltage (iii) ease of control etc. The peak obtainable output voltage from the given input dc voltage is one important figure of merit for the inverter.

Fig. 25 shows generation of reference and carriers signal for SHPWM technique, which is used to control the switches of TBMCSL H- bridges inverter.

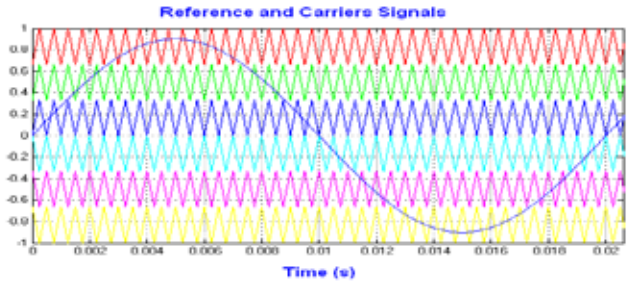

Figure 25 Reference and carriers signals for SHPWM technique.

VI EXPERIMENT RESULTS AND DISCUSSIONS

Experiment results of proposed circuit are given below. In this source voltage is 89.5v.In the above circuit we have 9 switches instead of 12 switches, the operation is explained in previous chapter .Error free reference signals are generated by the control circuit and by using this, pulses are generated by pwm technique.

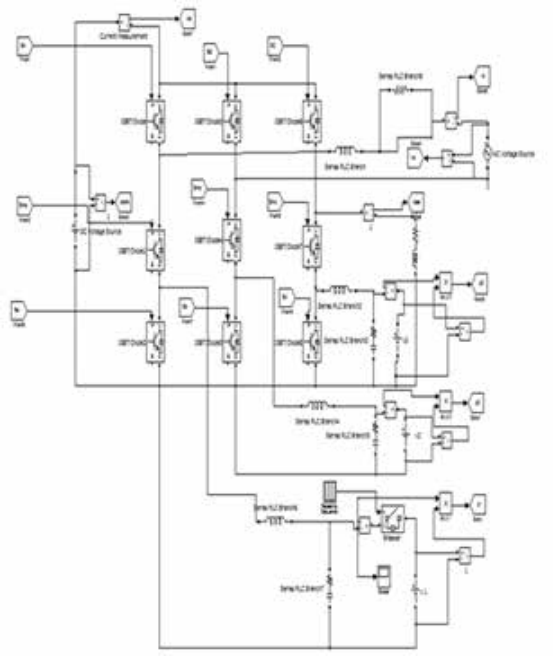

Figure 26 proposed extension circuit

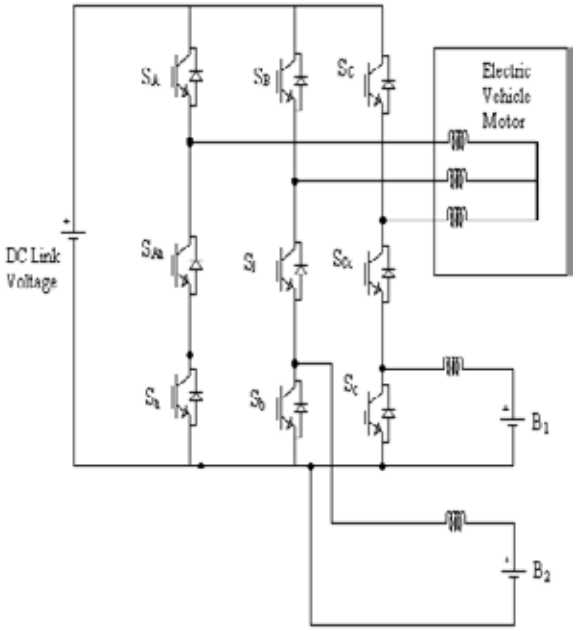

Figure 27 absence of one battery

In this circuit no load is connected means we can connect any type of load to this circuit. And it gives both AC And DC output, so we can connect both type of loads and we can use it for AC and DC type of applications For example in car we use many applications, in that some are AC And some are DC. And the use of bidirectional batteries are when the charged power is completed in the vehicle, the bidirectional batteries supplies the power to the vehicle.

In the above 26 figure we have 3 batteries .Actually In the proposed concept if one battery not working also the other batteries will supply the power to load, the fig.27 shows absence of one battery but basically in the circuit we placed one breaker to connect the battery or disconnect the battery, and also the repeating sequence values will decide the battery to what time it should ON, and what time it should OFF. These Will Show the Results.

Table 5 Output values

	For 2 switches	For 3 switches
Source voltage V_s	89.5v	89.5v
I_s	2amp	2amp
DC link	175v	175v
Power in battery1(P_1)	100w	100w
P_2	154w	154w
P_3	203w	0
I_{load}	4amp	4amp

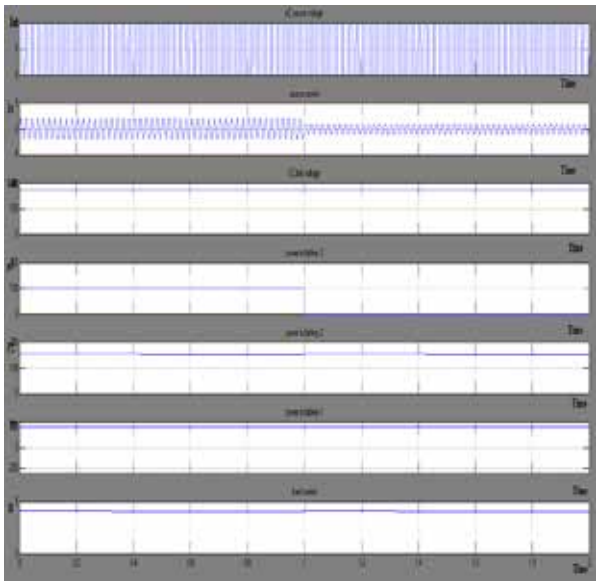

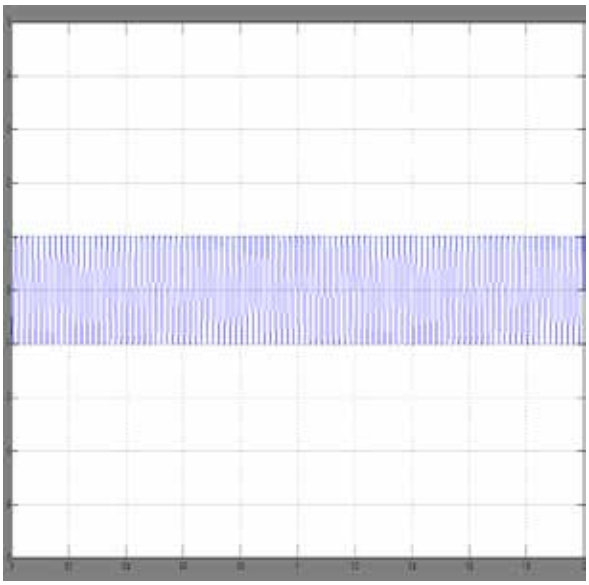

Figure 28 Simulation results of extension circuit Figure 29 Simulation result of AC reference

In the above results it shows source voltage, source current, DC link voltage, powers flowing in 3 bidirectional batteries, load current. The below fig shows the control circuit of the circuit, in this reference voltage for AC, DC are generated. In battery -3upto time 1sec it is ON, so the power in that battery is appear. But after that it is OFF, so the battery power is zero. But the link voltage is not zero, and the load current also not zero. It means the other remaining 2 batteries will supply the power to load, so it is not zero in that time.

The Figure 30 shows the control circuit and the reference of AC voltage. In that first we fix one value. DC link voltage and the fixed value both are compared and this result given to the PI controller to rectify the errors. After that some additions, multiplications, divisions are performed to get efficient reference voltage. The reference which created by the control circuit is given to the PWM circuit to generate the triggering pulses for the switches in main circuit. In PWM circuit the triggering pulses are created for 9 switches. These are generated according to the logical gates for better operation. After that the switches in main circuit are operated based on these logical gates and operated as inverter and converter in only one circuit. S_A, S_B, S_C Switches are used for inversion and S_{ma}, S_{mb}, S_{mc} are used for both inversion and conversion and $S_a S_b S_c$ switches are used for conversion in main circuit.

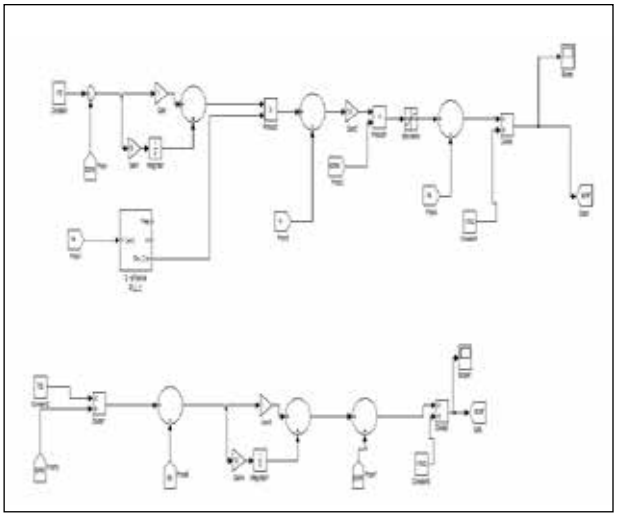

Figure 30 control circuit

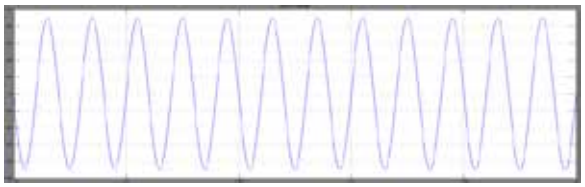

Figure 29 source voltage

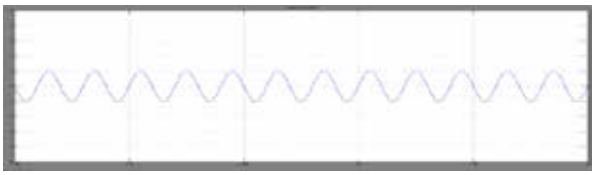

Figure 30 source current

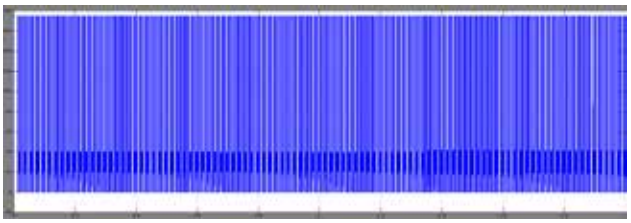

Figure 31 load voltage

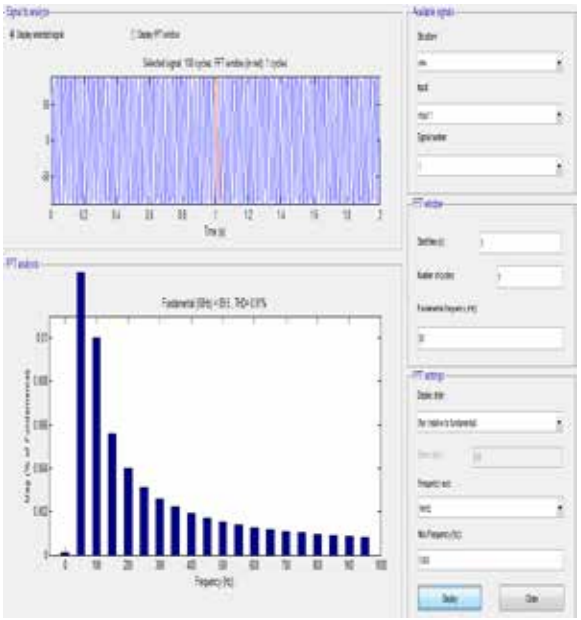

Figure 32 FFT analysis

And also from FFT analysis the THD is 0.01% for AC.

The middle switches in the circuit are operated based on XOR gate. When one switch from upper case or 1 switches from lower case should be in ON position, in that position the power flows in the circuit. When one switch or 3 switches in one phase leg is ON it won't work. Means it is in OFF position.

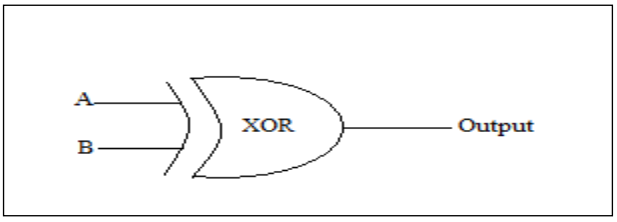

Figure 33 XOR gate block diagram and truth table

Table 6 XOR gate truth table

A	B	OUT

0	0	0
0	1	1
1	0	1
1	1	0

VII CONCLUSION

From the above it is concluded that when charged power is completed in the vehicle, the alternate multiple batteries are supply the power to vehicle. When 3 bidirectional batteries are connected to the vehicle, these will supplies the power to the vehicle without interruption. If any battery is not responding also the other batteries will supplies power to load, the switches also less used in this circuit. By this circuit complexity, cost and ripple content are decreases. And conversion and inversion operation performed in only one circuit. And also it gives good efficiency with these changes

REFRENCES

[1] Yen-shin lai, senior member, ieee, wei-ting lee, yong-kai lin, member, ieee, and jian-feng tsai, “Integrated Inverter/Converter Circuit And Control Technique Of Motor Drives With Dual-Mode Control For Ev/Hev Applications”, ieee transactions on power electronics, vol. 29, no. 3, march 2013.

[2] X. D. Xue, member, ieee, k. W. E. Cheng, senior member, ieee, j. K. Lin, z. Zhang,k. F. Luk, t. W. Ng, and n. C. Cheung, senior member, ieee. “Optimal Control Method Of Motoring Operation For Srm Drives In Electric Vehicles” ieee transactions on vehicular technology, vol. 59, no. 3, march 2010.

[3] Dipl. El. -ing. Andrea vezzini, pro$ dr: konrad reichert department of electrical machines, swiss federal institute of technology, switzerland physikstrasse 3, ch-8092 zurich, “Power Electronics Layout In A Hybrid Electric Or Electric Vehicle Drive System”, 1996 ieee.

[4] Ali emadi, senior member, ieee, young joo lee, student member, ieee, and kaushik rajashekara, fellow, ieee, “Power Electronics And Motor Drives In Electric,Hybrid Electric, And Plug-In Hybrid Electric Vehicles”, ieee transactions on industrial electronics, vol. 55, no. 6, june 2008.

[5] K. T. Chau, senior member, ieee, c. C. Chan, fellow, ieee, and chunhua liu, student member, ieee, “Overview Of Permanent-Magnet Brushless Drives For Electric And Hybrid Electric Vehicles”, ieee transactions on industrial electronics, vol. 55, no. 6, june 2008.

[6] Shuai lu, student member, ieee, keith a. Corzine, senior member, ieee, and mehdi ferdowsi, member, ieee, “A New Battery/Ultracapacitor Energy Storage System Design And Its Motor Drive Integration For Hybrid Electric Vehicles”, ieee transactions on vehicular technology, vol. 56, no. 4, july 2007.

[7] Omar hegazy, member, ieee, joeri van mierlo, member, ieee, and philippe lataire, “Analysis, Modeling, And Implementation Of A Multidevice Interleaved Dc/Dc Converter For Fuel Cell Hybrid Electric Vehicles”, ieee transactions on power electronics, vol. 27, no. 11, november 2012.

[8] Wei qian, honnyong cha, member, ieee, fang zheng peng, fellow, ieee,and leon m. Tolbert, senior member, ieee, “55-Kw Variable 3x Dc-Dc Converter For Plug-In Hybrid Electric Vehicles”, Ieee Transactions On Power Electronics”, vol. 27, no. 4, april 2012.

[9] Murat yilmaz, member, ieee, and philip t. Krein, fellow, ieee, “Review Of Battery Charger Topologies, Charging Power Levels, And Infrastructure For Plug-In Electric And Hybrid Vehicles”, ieee transactions on power electronics, vol. 28, no. 5, may 2013

[10] Yungtaek jang, senior member, ieee, and milan m. Jovanovic´, fellow, ieee, "Interleaved Boost Converter With Intrinsic Voltage-Doubler Characteristic For Universal-Line Pfc Front End", ieee transactions on power electronics, vol. 22, no. 4, july 2007.

[11] Mehrdad ehsani, fellow ieee, yimin gao, and john m. Miller, fellow ieee, "Hybrid Electric Vehicles:Architecture And Motor Drives", 2007 ieee 95, no. 4, april 2007 | proceedings of the ieee.

[12] Huang-jen chiu, member, ieee, and li-wei lin," A Bidirectional Dc–Dc Converter For Fuel Cell Electric Vehicle Driving System", ieee transactions on power electronics, vol. 21, no. 4, july 2006.

[13] Nobuyoshi mutoh, senior member, ieee, mikiharu nakanishi, masaki kanesaki, and joji nakashima, "Emi Noise Control Methods Suitable For Electricvehicle Drive Systems", ieee transactions on electromagnetic compatibility, vol. 47, no. 4, november 2005.

[14] Antonio affanni, alberto bellini, member, ieee, giovanni franceschini, paolo guglielmi, and carla tassoni, senior member, ieee, battery choice and management for new-generation electric vehicles, ieee transactions on industrial electronics, vol. 52, no. 5, october 2005.

[15] Shuanghong wang, qionghua zhan, zhiyuan ma, and libing zhou, implementation of a 50-kw four-phase switched reluctance motor drive system for hybrid electric vehicle, ieee transactions on magnetics, vol. 41, no. 1, january 2005.

[16] Richard saeks, fellow, ieee, chadwick j. Cox, james neidhoefer, paul r. Mays, and john j. Murray, senior member, ieee, adaptive control of a hybrid electric vehicle,ieee transactions on intelligent transportation systems, vol. 3, no. 4, december 2002.

[17] Robert b. Inderka, marcus menne, member, ieee, and rik w. A. A. De doncker, fellow, ieee, control of switched reluctance drives for electric vehicle applications, ieee transactions on industrial electronics, vol. 49, no. 1, february 2002.

[18] Woosuk sung, jincheol shin, and yu-seok jeong, member, ieee, energy-efficient and robust control for high-performance induction motor drive with an application in electric vehicles, ieee transactions on vehicular technology, vol. 61, no. 8, october 2012.

[19] Konstantinos i. Laskaris, member, ieee, and antonios g. Kladas, member, ieee, internal permanent magnet motor design for electric vehicle driveieee transactions on industrial electronics, vol. 57, no. 1, january 2010.